THE *IN VITRO* ANTIMYCOBACTERIAL ACTIVITIES OF EXTRACTS AND ISOLATED COMPOUNDS FROM SELECTED MEDICINAL PLANTS AGAINST *MYCOBACTERIUM SMEGMATIS*

By

KOMA POTSISO LETAU

[redacted]

A RESEARCH DISSERTATION

Submitted in fulfilment of the requirements of the degree of

MASTER OF SCIENCE

In

MICROBIOLOGY

In the

FACULTY OF SCIENCE AND AGRICULTURE

(School of molecular and life sciences)

At the

UNIVERSITY OF LIMPOPO

Supervisor: Prof P Masoko

2022

Declaration

I, Potsiso Letau Koma, declare that the dissertation hereby submitted to the University of Limpopo for the degree of Master of Science in Microbiology has not been submitted by me for the degree at this or any other University, and this is my own work in design and in execution and that all the material contained herein has been duly acknowledged.

……. ……..

Signature Date

Dedication

I dedicate this work to my mother, Koma Mante, and my grandmother, Letau; my son, Neo, and my siblings, Phethego and Mpho; lastly, to everyone who made this work possible.

Acknowledgements

I wish to extend my sincere gratitude to:

- The Almighty God for providing me with excellent health, courage, and strength to carry out this project.
- My supervisor Prof P Masoko, for his supervision of my study, support, encouragement, guidance, patience, and interest in all my wellbeing.
- Ms. T Ramakgadi for her assistance with NMR analysis.
- Prof O Mazimba from Botswana International University of Science and Technology for assistance with the structural elucidation of the isolated compounds.
- Dr M Matotoka for assistance with anti-inflammatory and antibiofilm activities.
- The Department of Biochemistry, Microbiology, and Biotechnology, and the colleagues in the Department.
- My family and my partner for their prayers, support, and encouragement.
- The University of Limpopo for giving me an opportunity to do a Master's degree.

TABLE OF CONTENTS

Declaration i

Dedication ii

Acknowledgements iii

LIST OF ABBREVIATIONS xi

LIST OF FIGURES xiii

LIST OF TABLES xix

CONFERENCE PRESENTATIONS xxi

ABSTRACT xxii

CHAPTER 1 1

1. INTRODUCTION 1

1.2 References 2

CHAPTER 2 4

2. LITERATURE REVIEW 4

2.1. Medicinal plants 4

2.2. Metabolites of plants 4

2.3. Plants secondary metabolites 5

2.3.1. Phenolic compounds 5

2.3.2. Alkaloids 6

2.3.3. Flavonoids 7

2.3.4. Terpenes 7

2.3.5. Tannins 8

2.3.6. Phlobatannin 9

2.3.7. Quinones 9

2.3.8. Saponins 10

2.3.9. Cardiac glycosides 11

2.4. Biological activities of medicinal plants 12

2.4.1. Antioxidant activity 12
2.4.2. Antimicrobial activity 14
2.4.3. Anti-inflammatory activity 15
2.4.4. Antibiofilm activity 16
2.5. Separation, purification, and isolation of compounds 16
2.6. Structure elucidation of compounds 17
2.7. Bacteria for clinical significance 18
2.7.1. *Mycobacterium smegmatis* 18
2.8. Selected medicinal plants for this study 18
2.8.1. *Rhoicissus tridentata* Wild and Drum. 18
2.8.2. *Rosmarinus officinalis* L. 19
2.8.3. *Ximenia caffra* Sond. 20
2.8.4. *Zanthoxylum capense* (Thunb) Hary 20
2.8.5. *Ziziphus mucronata* Willd 21
2.9. Aims and objectives 22
2.9.1. Aim 22
2.9.2. Objectives 22
2.10. References 23
CHAPTER 3 35
3. Extraction and preliminary phytochemical analysis **..... 35**
3.1. Introduction 35
3.2. Method and materials 36
3.2.1. Collection of plant material and extraction 36
3.2.2. Phytochemical analysis 37
3.2.2.1. Qualitative phytochemical analysis 37
3.2.3. Screening of major phytochemicals 37
3.2.3.1. Saponins 37

3.2.3.2. Terpenes 37
3.2.3.3. Phlobatannin 38
3.2.3.4. Tannins 38
3.2.3.5. Cardiac glycosides 38
3.2.3.6. Flavonoids 38
3.2.3.7. Steroids 38
3.2.3.8. Alkaloids 39
3.2.4. Quantitative phytochemical analysis 39
3.2.4.1. Total phenolic content 39
3.2.4.2. Total tannin content 40
3.2.4.3. Total flavonoid content 40
3.3. Results 41
3.3.1. Preliminary extraction 41
3.3.2. Phytochemical analysis 41
3.3.3. Screening of major phytochemicals 44
3.3.4. Standard curves used for quantification of phyto-constituents 44
3.4. Discussion 47
3.5. Conclusion 50
3.6. References 51
CHAPTER 4 55
4. Antioxidant activity **..... 55**
4.1. Introduction 55
4.2. Method and materials 56
4.2.1. Qualitative antioxidant activity on TLC plates 56
4.2.2. Quantitative antioxidant activity assays 57
4.2.2.1. DPPH free radical scavenging activity assay 57
4.2.2.2. Ferric reducing antioxidant power (FRAP) assay 57

4.2.3. The egg albumin denaturation inhibition assay 58
4.3. Results 59
4.3.1. Qualitative antioxidant assay on TLC plates 59
4.3.2. Quantitative antioxidant activity 59
4.3.2.1. DPPH free radical scavenging activity assay 59
4.3.2.2. Ferric Reducing Antioxidant Power (FRAP) assay 62
4.3.3. The egg albumin denaturation inhibition assay 63
4.4. Discussion 64
4.5. Conclusion 67
4.6. References 68
CHAPTER 5 ..... **72**
5. Antimycobacterial screening and cytotoxic effects 72
5.1. Introduction 72
5.2. Method and materials 74
5.2.1. Qualitative antibacterial activity 74
5.2.1.1. Bioautographic assay 74
5.2.1. Quantitative antibacterial activity assay 75
5.2.2.1. Serial broth dilution assay 75
5.2.2.2. The antibacterial interaction effects 76
5.2.2. Antibiofilm activity 76
5.2.3. Cell viability assay 77
5.2.4. Statistical analysis 78
5.3. Results 78
5.3.1. Bioautography assay 78
5.3.2. Quantitative antimicrobial assay 79
5.3.2.1. Serial broth dilution assay 79
5.3.2.2. The antibacterial interaction effects 81

5.3.3. Antibiofilm activity 82
5.3.4. Cell viability assay 83
5.4. Discussion 84
5.5. Conclusion 88
5.6. References 89
CHAPTER 6 95
6. Isolation and purification of antioxidant and antimycobacterial compounds **..... 95**
6.1. Introduction 95
6.2. Method and materials 97
6.2.1. Serial exhaustive extraction 97
6.2.2. Phytochemical analysis 97
6.2.3. Antioxidant activity on TLC 97
6.2.4. Bioautography assay 97
6.2.5. Serial broth micro-dilution assay 97
6.2.6. Isolation of antioxidant and antibacterial compounds 98
6.2.6.1. First open column chromatography 98
6.2.6.2. Second open column chromatography 99
6.2.6.3. Preparative Thin Layer chromatography 100
6.3. Results 100
6.3.1. Serial exhaustive extraction: The quantity of the plant material extracted from *R. officinalis* 100
6.3.2. Phytochemical analysis on TLC 101
6.3.3. DPPH Thin Layer Chromatography assay 103
6.3.4. Bioautography assay 104
6.3.5. Serial broth micro-dilution assay 105
6.3.6. Isolation of bioactive compounds from dichloromethane extracts 106
6.3.6.1. First open column chromatography 106

6.3.6.2. Second open column chromatography 112
6.3.6.3. Preparative Thin Layer Chromatography (TLC) 119
6.4. Discussion 121
6.5. Conclusions 124
6.6. References 124
CHAPTER 7 126
7.1. Introduction 126
7.2. Method and materials 127
7.2.1. Structural elucidation of isolated compound 127
7.3. Results 127
7.3.1. NMR analysis of compound 1 127
7.3.2. Spectroscopic data for compound 1 129
7.3.3. The structure of compound 1 129
7.3.4. NMR analysis for compound 2 130
7.3.5. Spectroscopic data for compound 2 132
7.3.6. The structure of compound 2 133
7.3.7. NMR analysis of compound 3 133
7.3.8. Spectroscopic data for compound 3 and 4 134
7.3.9. The structure of compound 3 136
7.3.10. The analysis of compound 4 using NMR 136
7.3.11. The structure of compound 4 138
7.4. Discussion 138
7.5. Conclusion 139
7.6. References 139
CHAPTER 8 142
8.Biological activity of the isolated compounds **..... 142**

8.1. Introduction 142
8.2. Method and materials 142
8.2.1. Phytochemical analysis of the isolated compounds 142
8.2.2. Antibacterial activity 143
8.2.2.1. Bioautography 143
8.2.2.2. Broth micro-dilution assay 143
8.3. Results 143
8.3.1. Phytochemical analysis of the isolated compound 143
8.3.2. Biological activity of the isolated compounds 144
8.3.2.1. Bioautography 144
8.3.2.2. Broth micro-dilution assay 144
8.4. Discussion 145
8.5. Conclusion 145
8.6. References 146
CHAPTER 9 148
9. General discussions, conclusions, and recommendations **148**
9.1. General discussion 148
9.2. Conclusions and recommendations 149
9.3. References 150

LIST OF ABBREVIATIONS

^{13}C - Carbon-13

^{1}H - Hydrogen-1

ABTS - 2,2′-azino-bis-3-ethylbenzthiazoline-6-sulphonic acid

A - Acetone

BEA - Benzene: Ethanol: Ammonium hydroxide

CEF - Chloroform: Ethyl acetate: Formic acid

D - Dichloromethane

DMSO - Dimethyl sulfoxide

DPPH - 2,2-diphenyl-1-picrylhydrazyl

EMW - Ethyl acetate: Methanol: Water

FBS - Foetal Bovine Serum

FIC - Fractional Inhibitory Concentration

FRAP - Ferric Reduction Antioxidant Potential

GAE - Gallic acid equivalence

H - n-Hexane

INT - p-iodonitrotetrazolium violet

M - Methanol

MIC - Minimum Inhibitory Concentration

MMT - 3-(4,5-dimethylthiazol-2-yl)-2,5-diphenyltetrazolium bromide

QE - Quercetin equivalence

R_f - Retardation factor

RO - *Rosmarinus officinalis*

ROS - Reactive Oxygen Species

RT - *Rhoicissus tridentata*

TB - Tuberculosis

TLC - Thin Layer chromatography

UV - Ultraviolet

W - Water

WHO - World Health Organisation

XC - *Ximenia caffra*

ZC - *Zanthoxylum capense*

ZM - *Ziziphus muronata*

LIST OF FIGURES

CHAPTER 2

Figure 2.1: Figure 2. 1: General structure of phenolic compounds (Granato *et al*., 2016). 6

Figure 2.2: Structure of an alkaloid (Roaa, 2020). 6

Figure 2.3: The general structure of flavonoid molecule (Vuolo *et al*., 2019)..... 7

Figure 2.4: Different classification of terpenes by the number of isoprene present in the structure (Prado-Audelo *et al*., 2021). 8

Figure 2. 5: Structure of (A) hydrolysable and (B) condensed tannins (Das *et al*., 2020). 9

Figure 2. 6: Structure of phlobatannin (Kamarudin *et al*., 2019). 9

Figure 2. 7: Chemical structures of representative quinones, quinone and hypericin (Ferdes, 2018)..... 10

Figure 2. 8: The general structure of Quilaic acid, a saponin (Böttcher and Drusch, 2017). 11

Figure 2. 9: Structures features and classification of cardiac glycosides (Ayogu and Odoh, 2020)..... 12

Figure 2. 10: Structure of DPPH (Sarkar, 2018). 13

Figure 2. 11: Picture of *R. tridentata* Wild and Drum (Mdletshe, 2018). 19

Figure 2. 12: A picture of *R. officinalis* plant in full blossom (Lešnik *et al*., 2020). 20

Figure 2. 13: Picture of *X. caffra* Sond. Var. caffra (Tlaamela, 2019). 20

Figure 2. 14: Picture of *Z. capense* (Thunb) Hary (Sunday, 2017). 21

Figure 2. 15: Different plant parts of *Ziziphus mucronata* (stem bark, 1A), (Leaves, thorns, green and ripe fruits, 1B &1C), (Leaves and flower, 1D) (Mongalo *et al*., 2020)..... 21

CHAPTER 3

Figure 3. 1: The mass of *Z. capense*, *R. tridentata*, *R. officinalis*, *X. caffra* and *Z. mucronata* extracted from 1 g of powdered leaf materials with 10 mL of different solvents (n-hexane, dichloromethane, acetone, methanol, and water)..... 41

Figure 3. 2: Chromatograms attained after running TLC plates loaded with different plant extracts in three different mobile phases (EMW, CEF,

and BEA) and visualised under ultraviolet light at 254 nm. The visualised compounds in which the plants were extracted with n-hexane (H), dichloromethane (D), acetone (A), methanol (M), and water (W). 42

Figure 3. 3: Chromatograms attained after running TLC plates loaded with different plant extracts in three different mobile phases (EMW, CEF, and BEA) and visualised under ultraviolet light at 365 nm. The visualised compounds in which the plants were extracted with n-hexane (H), dichloromethane (D), acetone (A), methanol (M), and water (W). 43

Figure 3. 4: Chromatograms attained after running TLC plates loaded with different plant extracts in three different mobile phases (EMW, CEF, and BEA) and sprayed with vanillin-sulphuric acid. The visualised compounds in which the plants were extracted with n-hexane (H), dichloromethane (D), acetone (A), methanol (M), and water (W). . 43

Figure 3. 5: Garlic acid standard curve for determination of total phenolic content. 45

Figure 3. 6: Garlic acid standard curve for determination of total tannin content. 45

Figure 3. 7: The quercetin standard curve used for determination of total flavonoid content. 46

CHAPTER 4

Figure 4. 1: Chromatograms attained after running TLC plates loaded with different plant extracts in three different mobile phases (EMW, CEF, and BEA) and sprayed with 0.2% DPPH. The visualised compounds of different plants which were extracted with: n-hexane (H), dichloromethane (D), acetone (A), methanol (M), and water (W). . 59

Figure 4. 2: The DPPH free radical scavenging activity of: A (*Z. capense*), B (*X. caffra*), C (*Z. mucronata*), D (*R. officinalis*) and E (*R. tridentata*) compared with L-ascorbic acid as the standard in percentage inhibition. The results are expressed as mean of the triplicates ± standard deviation. 61

Figure 4. 3: Graphs showing the ferric reducing power activity of: A (*Z. capense*), B (*X. caffra*), C (*Z. mucronata*), D (*R. officinalis*) and E (*R. tridentata*) compared with L-ascorbic acid as the standard at 700 nm. The results are expressed as mean of the triplicates ± standard deviation. 63

Figure 4. 4: The evaluation of the anti-inflammatory activity of plants acetone extracts using egg albumin denaturation inhibition assay. The results were analysed using one-way ANOVA, followed by Dunett's multiple comparison test. 64

CHAPTER 5

Figure 5. 1: Bioautograms attained after running TLC plates loaded with different plant extracts in three different mobile phases (EMW, CEF, and BEA) and sprayed with *Mycobacterium smegmatis* for overnight. Then visualised by spraying with 2 mg/mL of INT. Different plants extracts were extracted with: hexane (H), dichloromethane (D), acetone (A), methanol (M), and water (W). 79

Figure 5. 2: The antibiofilm activity of the plant extracts against *M. smegmatis*. Results were analysed using two-way ANOVA, followed by Tukey multiple comparison post-hoc test. 83

Figure 5. 3: The cytotoxicity effects of *Z. capense*, *Z. muconata*, *X. caffra*, *R. officinalis*, and *R. tridentata* using acetone extracts on THP-1 cells. Results were analysed using two-way ANOVA, followed by Tukey multiple comparison post hoc test. 84

CHAPTER 6

Figure 6. 1: The chromatograms obtained using extracts from serial exhaustive extraction of *R. officinalis* leaves using different solvents and developed in EMW, CEF, and BEA solvent systems and visualised at 254 nm (A) and 365 nm (B). 102

Figure 6. 2: The chromatograms obtained using extracts from serial exhaustive extraction of *R. officinalis* leaves using different solvents and developed in EMW, CEF, and BEA solvent systems and sprayed with vanillin sulphuric acid reagent.....103

Figure 6. 3: Chromatograms of *R. officinalis* extracts developed in EMW, CEF, and BEA mobile systems and sprayed with 0.2% DPPH dissolved in methanol.....104
Figure 6. 4: The chromatograms showing antibacterial activity of *R. officinalis* plant extracts developed in EMW, CEF, and BEA and sprayed with *M. smegmatis*. 105
Figure 6. 5: The chromatograms of different fractions obtained from first open column chromatography of *R. officinalis* developed in EMW, CEF, and BEA mobile systems and visualised at 254 nm (A) and 365 nm (B) using ultraviolet light. 108
Figure 6. 6: The chromatograms of different fractions obtained from first open column chromatography of *R. officinalis* developed in EMW, CEF, and BEA mobile systems and sprayed with vanillin-sulphuric acid reagent. 109
Figure 6. 7: The chromatograms of different fractions obtained from first open column chromatography of *R. officinalis* developed in EMW, CEF, and BEA mobile systems and sprayed with 0.2% DPPH.....110
Figure 6. 8: The bioautograms of different fractions obtained from first open column chromatography of *R. officinalis* developed in EMW, CEF, and BEA mobile systems against *M. smegmatis*. 111
Figure 6. 9: Chromatograms obtained after developing the TLC plates in 100% n-hexane, 50% n-hexane: 50% ethyl acetate, and 100% ethyl acetate, then visualised at 254 nm (A), 365 nm (B) and further spayed with vanillin sulphuric acid reagent (C).....113
Figure 6. 10: Chromatograms of combined chosen *R. officinalis* fractions obtained after developing the TLC plates in 70% n-hexane in ethyl acetate, 80% n-hexane in ethyl acetate, and 90% n-hexane in ethyl acetate mobile systems then visualised at 254 nm (A), 365 (B), and further sprayed with vanillin-sulphuric acid reagent (C). 114
Figure 6. 11: Chromatograms of *R. officinalis* fractions obtained from second open column chromatography then developed in 80% n-hexane: 20% ethyl acetate and visualised at 254 nm. 115

Figure 6. 12: Chromatograms of *R. officinalis* fractions obtained from second open column chromatography then developed in 80% n-hexane: 20% ethyl acetate and visualised at 365 nm. 116
Figure 6. 13: Chromatograms of *R. officinalis* fractions obtained from second open column chromatography then developed in 80% n-hexane: 20% ethyl acetate and sprayed with vanillin-sulphuric acid reagent.....117
Figure 6. 14: Phytochemical analysis of the grouped fractions developed in 80% hexane: 20% ethyl acetate then visualised under UV light at 254 nm (A) and 365 nm (B) and sprayed with vanillin sulphuric acid reagent (C). 118
Figure 6. 15: Bioautogram showing antibacterial activity of groups 1-4 against *M. smegmatis*. 119
Figure 6. 16: Diagram showing summary of the isolation process.....120

CHAPTER 7

Figure 7. 1: ^{1}H NMR spectrum of isolated compound 1.....128
Figure 7. 2: ^{13}C NMR spectrum of isolated compound 1. 128
Figure 7. 3: COSY NMR spectrum of isolated compound 1.....128
Figure 7. 4: Structure of compound 1. 130
Figure 7. 5: ^{1}H NMR spectrum of isolated compound 2.....130
Figure 7. 6: ^{13}C NMR spectrum of compound 2.....131
Figure 7. 7: DEPT 135 NMR spectrum of isolated compound 2. 131
Figure 7. 8: COSY NMR spectrum of compound 2.....131
Figure 7. 9: HSQC NMR spectrum of compound 2.....132
Figure 7. 10: HMBC NMR spectrum of compound 2. 132
Figure 7. 11: Structure of compound 2. 133
Figure 7. 12: ^{1}H NMR spectrum of isolated compound 3.....134
Figure 7. 13: ^{13}C NMR spectrum of isolated compound 3. 134
Figure 7. 14: Structure of compound 3. 136
Figure 7. 15: ^{1}H NMR spectrum of isolated compound 4.....136
Figure 7. 16: ^{13}C NMR spectrum of isolated compound 4. 137
Figure 7. 17: DEPT 135 NMR spectrum of isolated compound 4. 137
Figure 7. 18: HSQC NMR spectrum of isolated compound 4. 137
Figure 7. 19: Structure of compound 4. 138

CHAPTER 8

Figure 8. 1: Phytochemical analysis of isolated compounds developed in 80% n-hexane: 20% ethyl acetate, visualised at 254 nm (A) and 365 nm (B), and then sprayed with vanillin-sulphuric acid reagent (C). 143

Figure 8. 2: The antibacterial activity of the four isolated compounds against *M. smegmatis* developed in EMW, CEF, and BEA. 144

LIST OF TABLES

CHAPTER 3

Table 3. 1: Phytoconstituents of *Z. capense*, *R. tridentata*, *R. officinalis*, *X. caffra* and *Z. mucronata* leaf extracts. 44

Table 3. 2: Total phenolic, tannin and flavonoid content of *Z. capense*, *R. tridentata*, *R. officinalis*, *X. caffra* and *Z. mucronata* extracts. Data was analysed and recorded as mean ± standard deviation. 46

CHAPTER 5

Table 5. 1: The MIC values of selected plant extracts in mg/mL against *M. smegmatis*. 80

Table 5. 2: Total activity of the selected plant extracts (mL/g). 80

Table 5. 3: The fractional inhibitory Concentration (FIC) of selected plants using n-hexane extracts. 81

Table 5. 4: The fractional inhibitory Concentration (FIC) of selected plants using acetone extracts. 82

CHAPTER 6

Table 6. 1: Solvent systems used in the first column. 98

Table 6. 2: Mobile phases used to determine the eluent for second open column chromatography. 99

Table 6. 3: Non-polar systems for determination of the eluent for second open column chromatography. 99

Table 6. 4: Masses (g) extracted from *R. officinalis*. 101

Table 6. 5: The MIC values obtained from serial exhaustive extraction extracts against *Mycobacterium smegmatis*. 105

Table 6. 6: Extracted fraction masses (g) obtained from a combination of dichloromethane extracts using solvents of varying polarities. 106

Table 6. 7: MIC (mg/mL) value of *R. officinalis* fractions from first open column chromatography against *Mycobacterium smegmatis*. 111

CHAPTER 7

Table 7. 1: The summary of ^{1}H and ^{13}C spectroscopic data for compound 1. ..129

Table 7. 2: The summary of ^{1}H and ^{13}C spectroscopic data for compound 2. ..132

Table 7. 3: The summary of ^{1}H and ^{13}C spectroscopic data for compounds 3 and 4, and the one from literature. 134

CHAPTER 8

Table 8. 1: MIC values of the isolated compounds against *Mycobacterium smegmatis*. 145

CONFERENCE PRESENTATIONS

1. Potsiso L. Koma, Peter. Masoko. “Extraction, preliminary phytochemical screening, total phenolic content and antioxidant activity of five selected medicinal plants.” Presented during the 11th Faculty of Science and Agriculture Postgraduate Research Day held at Bolivia Lodge, Polokwane, Limpopo, South Africa, October 2021.
2. Potsiso L. Koma, Peter. Masoko. “Evaluation of phytochemicals, antioxidant, antimicrobial activity, and cytotoxic effects of five selected medicinal plants.” Presented during the 24th Indigenous Plant Use Forum, July 2022.
3. Potsiso L. Koma, Peter. Masoko. “Antimycobacterial evaluation and preliminary phytochemical investigation of selected medicinal plants traditionally used in Limpopo province, South Africa.” Presented during the 12th Faculty of Science and Agriculture Postgraduate Research Day held at Bolivia Lodge, Polokwane, Limpopo, South Africa, September 2022.
4. Potsiso L. Koma, Peter. Masoko. “Antimycobacterial evaluation and preliminary phytochemical investigation of selected medicinal plants traditionally used in Limpopo province, South Africa.” Presented during the 2nd African Traditional and Natural Product Medicine Conference held at Protea Hotel, the Ranch Resort, Polokwane, Limpopo, South Africa, October 2022.

ABSTRACT

Mycobacterium tuberculosis is an intracellular facultative microorganism that belongs to the *M. tuberculosis* complex and causes tuberculosis (TB) in human beings. TB is a global pandemic which poses a health security as the leading cause of death. This study aimed to determine the antioxidant activity, antibacterial activity, synergistic and cytotoxic effects, isolate and characterise bioactive compounds of five selected medicinal plants (*Zanthoxylum capense*, Ziziphus *mucronata, Rosmarinus officinalis*, *Ximenia caffra* and *Rhoicissus tridentata*). The leaves of the plants were collected, dried, and extracted using solvents of varying polarities (n-hexane, dichloromethane, acetone, methanol, and water). Methanol extracted the highest mass for *Z. capense*, Z. *mucronata* and *R. tridentata* while water extracted the highest mass for *R. officinalis* and *X. caffra*. Preliminary screening of major-phytoconstituents was determined using standard chemical methods and all plants lacked alkaloids. Qualitative phytochemical composition, antioxidant and antimycobacterial activity were determined using Thin Layer Chromatography (TLC). The quantity of phytochemicals and antioxidants was determined using colorimetric assay, while the quantitative antimicrobial activity and synergistic effects of the hexane and acetone extracts were determined using microbroth dilution assay. The anti-inflammatory activity was determined using egg albumin denaturation inhibition assay and the antibiofilm activity was also analysed. Cell viability was determined using the [3-(4,5-dimethylthiazol-2-yl)-2,5-diphenyltetrazolium bromide] MMT reduction assay. On preliminary screening, the different colours indicated the presence of different compounds. The quantity of phytochemicals showed that *R. tridentata* had the highest total phenolic and tannin content from its water extracts while the highest total flavonoid content was from the methanol extract of *R. officinalis*. Qualitative antioxidant activity analysis using 2,2-diphenyl-1-picrylhydrazyl (DPPH) assay, where the yellow bands against the purple indicated the presence of antioxidant compounds, showed that antioxidant compounds were present in all plants except for *Z. capense*. It also had the lowest quantified antioxidant compounds. Qualitative antibacterial activity showed that *R. officinalis* and *Z. mucronate* had inhibited the growth of *M. smegmatis* from all extracts except their water extracts. *R. officinalis* had the highest antibacterial activity as compared to all plants and a synergistic outcome was observed when the n-hexane extracts *R. officinalis* and *Z. capense* were combined. All the plants were able to inhibit

protein denaturation, even though *Z. capense* had poor anti-inflammatory activity with percentage inhibition of 42%. The plant extracts had a concentration dependent biofilm activity against *M. smegmatis*. Cell viability assay revealed that acetone extracts of *R. tridentata* had the highest percentage cell viability while *Z. mucronata* and *Z. capense* had the lowest percentage cell viability. Isolation of bioactive compounds was done using bioassay guided fractionation and the structure of the compounds was characterised using nuclear magnetic resonance spectroscopy. The isolated compounds were 2 chromones with (compound 1 is 5-hydroxyl-2-methyl-7-(propan-2βol)-chromone and compound 2 as 7-acetonyl-5-hydroxy-2-methylchromone) and β-sitosterol compounds. All compounds had antibacterial activity against *M. smegmatis*, compound 4 had the lowest minimum inhibitory concentration (MIC) of 0.125 mg/mL. The study demonstrated that selected medicinal plants have different phytochemicals that are responsible for antioxidant, antibacterial, anti-inflammatory and antibiofilm activities. Further studies are recommended on *Mycobacterium tuberculosis* and *in vivo* studies.

CHAPTER 1

1. INTRODUCTION

TB is a continuously infectious bacterial disease that is caused by *Mycobacterium tuberculosis* complex. It usually affects the respiratory system, and it can further affect other body parts inducing extrapulmonary and pulmonary TB (Obakiro *et al*., 2020). Approximately eight million new cases and two million deaths occur worldwide because of TB. Care, prevention methods and the degree at which it spreads is a major concern to individuals and the World Health Organisation (WHO) (Ankomah, 2020). *Mycobacterium tuberculosis* has developed and become resistant to the current available drugs to treat TB. *M. tuberculosis* is resistant to the first- and second-line TB drugs, narrated as multidrug resistant (MDR) and extensively drug resistant (XDR) (Poro *et al*., 2021; Ekundayo *et al*., 2020).

Antibiotic resistance occurs naturally, but misusing and taking an excessive dose of the drugs have caused several resistance problems. The rise of multidrug resistance (MDR) pathogens is usually caused by the continuous selective pressure, and the development of new strategies by bacteria to survive newly developed antibiotics. Furthermore, the incorrect and inappropriate use of antibiotics has increased the common occurrence of resistant bacteria (Ferdes, 2018). Since there is an increase in antibiotic resistance by pathogens, the public health of the world is threatened. There are numerous mechanisms used by bacterial cells to inactivate antibiotics, which includes antibiotics chemical alteration, exporting of the antibiotics, and bacteria changing their binding molecules (Saboora *et al*., 2019).

Plants are the main sources of traditional medicine and have been used for thousands of years as remedies by human beings (Roy, 2017). Recently, there is a rising attention of drug discovery from medicinal plants compared to synthetic drugs which are regarded as unsafe to humans. The therapeutic value of the medicinal plants exists within its secondary metabolites. The secondary metabolites play a significant role in the development of new drugs because of their effectiveness, less side effects and relatively low cost compared to synthetic drugs (Rohini and Padmini, 2016; Shazhni *et al*., 2016).

Natural herbs have been used as medicines by all cultures for many years and have been a source for developing synthetic drugs. Drugs developed from herbal plants are quite important for human health and welfare (Rana *et al*., 2021). The WHO is also hopeful that medicinal plants would be the best source for obtaining new drugs (Manandhar *et al*., 2019). The use of plants for therapeutic purposes includes anti-tumour, anti-viral, anti-inflammatory, and anti-malarial activities (Roy, 2017).

Medicinal plants are referred to as plants that have therapeutic properties or a beneficial pharmacological effect on the human or animal body (Sunday *et al*., 2021). Various environmental factors such as climate, altitude, rainfall, and other conditions may affect the growth of plants, which in turn affects the quality of herbal ingredients present in a particular species even when it is produced in the same country. These conditions may produce major variations in the bioactive compounds present in the plants (Santhi and Sengottuvel, 2016).

1.2 References

Ankomah, R. 2020. Antimycobacterial activities of selected medicinal plants extracts in the management of *Mycobacterium tuberculosis* H37Rv and *Mycobacterium bovis*. *Transatlantic Journal of Multidisciplinary Research*, **2**(4): 67–85.

Ekundayo, E.O., Kalu, U.O. and Enya, E. 2020. *In vitro* inhibitory activity of extracts of some medicinal plants against *Mycobacterium smegmatis*. *Nigerian Journal of Microbiology*, **34**(1): 5044–5052.

Ferdes, M. 2018. Antimicrobial compounds from plants. *Fighting Antimicrobial Resistance. IAPC-OBP, Zagreb*, 243–271.

Obakiro, S.B., Kiprop, A., Kowino, I., Kigondu, E., Odero, M.P., Omara, T. and Bunalema, L. 2020. Ethnobotany, ethnopharmacology, and phytochemistry of traditional medicinal plants used in the management of symptoms of tuberculosis in East Africa: a systematic review. *Tropical Medicine and Health*, **48**(1): 1–21.

Manandhar, S., Luitel, S. and Dahal, R.K. 2019. *In vitro* antimicrobial activity of some medicinal plants against human pathogenic bacteria. *Journal of Tropical Medicine*, 1–5.

Poro, K.E., Hoekou, Y., Pissang, P., Kpabi, I., Novidzro, K.M., Dagnra, A.Y., Tchacondo, T. and Batawila, K. 2021. *In vitro* antimycobacterial activity of selected medicinal plants against *Mycobacterium tuberculosis*. *International Journal of Current Microbiology and Applied Sciences*, **10**(02): 3201–3208.

Rana, A., Negi, P.B. and Sahoo, N.G. 2021. Phytochemical screening and characterization of bioactive compounds from *Juniperus squamata* root extract. *Materials Today: Proceedings*, **48**(3): 672–675.

Rohini, M.V. and Padmini, E. 2016. Preliminary phytochemical screening of selected medicinal plants of polyherbal formulation. *Journal of Pharmacognosy and Phytochemistry*, **5**(5): 277.

Roy, A. 2017. A review on the alkaloids an important therapeutic compound from plants. *International Journal of Plant Biotechnology*, **3**(2): 1–9.

Saboora, A., Sajjadi, S.T., Mohammadi, P. and Fallahi, Z. 2019. Antibacterial activity of different composition of aglycone and glycosidic saponins from tuber of *Cyclamen coum* Miller. *Industrial Crops and Products*, **140**: 111662.

Santhi, K. and Sengottuvel, R. 2016. Qualitative and quantitative phytochemical analysis of *Moringa concanensis* Nimmo. *International Journal of Current Microbiology and Applied Sciences*, **5**(1): 633–640.

Shazhni, J.A., Renu, A. and Murugan, M. 2016. Phytochemical screening and *in vitro* antimicrobial activity of ornamental plant *Anthurium* and *Raeanum*. *Journal of Pharmaceutical Sciences and Research*, **8**(7): 668.

Sunday, E.A., Nnedimma, N.C., Peter, W.G. and Orlando, G.B. 2021. Screening for pharmacological compounds and antioxidant activity of *Hedychium coronarium* J. Koenig. *Asian Journal of Research in Botany*, 34-47.

CHAPTER 2

2. LITERATURE REVIEW

2.1. Medicinal plants

Medicinal plants are defined as plants which consist of different compounds with therapeutic properties, or precursors of chemo-pharmaceutical synthesis (Jain *et al*., 2019). Plant chemistry is the main therapeutic use of herbs. Knowing the chemical composition of a plant leads one to understand its possible medical use (Hussein and El-Anssary, 2019). For thousands of years, people used plants as a source of food and for medical purposes. (Masoko and Masiphephethu, 2019). Medicinal plants have been used to treat TB related symptoms in endemic countries and they serve as the potential source for the development of new drugs (Ekundayo *et al*., 2020).

Medicinal plants are the major store of biological active compounds with curative properties that have been reported and used by different people to treat various diseases (Aye *et al*., 2019). Almost 80% of the population in developing countries depends on traditional medicine as primary healthcare and this is because traditional medicine is easily accessible and affordable (Tuyiringire *et al*., 2020).

2.2. Metabolites of plants

The presence of bioactive compounds significantly varies according to agroclimatic conditions (Dhull *et al*., 2016). Plants produce primary metabolites which perform various metabolic activities such as growth and development of the plants (Singh and Sharma, 2020). Secondary metabolites are also produced and used as defenders against invading pathogens (Masoko and Masiphephethu, 2019). Secondary metabolites are chemical compounds produced by the cells of plants through metabolic pathways derived from primary metabolic pathways (Hussein and El-Anssary, 2019). The secondary metabolites form the basis for many commercial pharmaceutical drugs and herbal remedies derived from medicinal plants. The different chemical constituents in medicinal plants possess biological activities that can improve human health through pharmaceuticals and food industries (Li *et al*., 2020).

2.3. Plants secondary metabolites

The massive and versatile pharmacological effects of medicinal plants depend on their phytochemical constituents, which are primary and secondary metabolites. Secondary metabolites contain biological effects, which supply the scientific base for using herbaceous plants for traditional medicine during ancient times. Secondary metabolites are described as antibiotic, antiviral and antifungal (Hussein and El-Anssary, 2019).

Plants contain various types of secondary metabolites such as phenolic compounds, tannins, alkaloids, and flavonoids. They were found *in vitro* to have antimicrobial properties (Manandhar *et al*., 2019). Plants secondary metabolites are not used as therapeutic agents only, but also as starting materials to synthesise new drugs or pharmacologically as models of active compounds (Tanveer *et al*., 2017).

2.3.1. Phenolic compounds

Phenolic compounds are one of the largest groups of plants secondary constituents. Their hydroxyl group is attached to a benzene ring, making them aromatic alcohols. The simplest form of phenols contains an aromatic ring in which a hydrogen is replaced by a hydroxyl group (Figure 2.1) (Pengelly and Bone, 2020). Phenolic compounds consist of several subgroups such as lignans, phenylpropanoids, flavonoids and condensed tannins (flavonoids polymers) (Shitan, 2016).

Phenolic compounds have promising antioxidant properties, with their ability being directly associated with the type of solvent used for extraction, with the origin of the plant, growing conditions of the plant, time for harvesting, and storage conditions. Phenolic extracts derived from plant species are among the highest studied topics in the scientific community, usually the *in vitro* studies (Martins *et al*., 2016). They are referred to as antioxidants because they donate an electron or hydrogen atom to free radicals, thus causing the chain for oxidation reaction to break. Their antioxidant effects or activity depends on the position and number of hydroxyl groups (Albuquerque *et al*., 2021; Cianciosi *et al*., 2018).

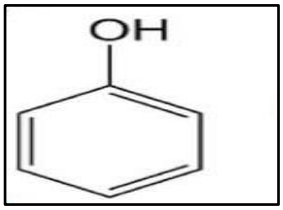

Figure 2. 1: General structure of phenolic compounds (Granato *et al*., 2016).

2.3.2. Alkaloids

Alkaloids are heterocyclic compounds derived from amino acids, consisting of one or more nitrogen atoms in its structure. Alkaloids form part of the largest group of plant secondary metabolites. The saturation of nitrogen atoms (from primary to quaternary) is what characterises them. Alkaloids are poorly soluble in water when they have a free base, but are usually soluble organic solvents (Rosalis *et al*., 2020). Most alkaloids have complex cyclic structures (Figure 2.2) (Cheng *et al*., 2020). There are different types of alkaloids, and their differentiation is based on their chemical structure, biological activity, biosynthesis pathway and occurrence into heterocyclic and nonheterocyclic alkaloids. They are often referred to as proto-alkaloids or biological amines (Bribi, 2018; Kukula-Koch and Widelski, 2017).

Alkaloids possess therapeutic properties and according to their biosynthetic precursor and heterocyclic ring system, the compounds are classified into a numerous number of categories, which include the indoles, piperidines, tropanes, purines, pyrrolizidines, imidazole, quinolozidine, isoquinoline and pyrrolidine alkaloids (Dey *et al*., 2020). They contain antibacterial activities where they inhibit transcription, the production of toxins, etc. (Raji *et al*., 2019). Alkaloids prevent the rise of various chronic diseases through free radical scavenging or by binding with the catalyst of oxidative reaction. The major source of alkaloid is flowering plants, i.e. Angiosperm (Roy, 2017).

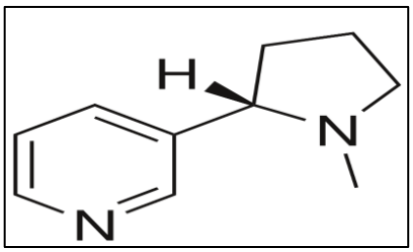

Figure 2. 2: Structure of an alkaloid (Roaa, 2020).

2.3.3. Flavonoids

Flavonoids are a group of polyphenolic compounds. Flavonoids have medicinal properties and have played a major role in medicinal treatment since ancient times to date. They are the dominant antioxidants that are water-soluble and free radical scavengers preventing oxidative cell damage (Jain *et al*., 2019). They are usually the most available phenolic compounds consisting of fifteen carbon atoms (C6-C3-C6), which are made up of two benzene rings (A and B) linked by the heterocyclic pyrane ring (C) (Figure 2.3). Flavonoids are divided into six different subgroups in which the C ring is responsible for their variation, namely: anthocyanins, flavonols, isoflavonoids, flavones, flavonones and flavanols (Albuquerque *et al*., 2021; Cong-Cong *et al*., 2017). The A ring of flavonoids is derived from the acetate pathway while the B ring is derived from shikimate pathway (Vuolo *et al*., 2019). Flavonoids have antibacterial activity through the inhibition of enzymes, and they interfere with metabolism (Raji *et al*., 2019).

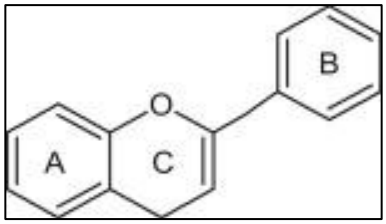

Figure 2. 3: The general structure of flavonoid molecule (Vuolo *et al*., 2019).

2.3.4. Terpenes

Terpenes are one of the largest and various classes of secondary metabolites linked by their biosynthetic source glycolytic intermediates. Terpenes play a major role in defence in plants as toxins and play a role in humans' diet by protecting against diseases such as cancer (Jamwal *et al*., 2018). Terpenes contains the five carbon cyclic isoprene units that are assembled to each other (many isoprene units) in different ways. Terpenes are classified based on organisation and the number of isoprene units they have. An isoprene unit is a gaseous hydrocarbon that contains the molecular formula C_5H_8 as the building block of terpenoids (Cox-Georgian *et al*., 2019).

Terpenes are the simplest form of hydrocarbons and the modified class of terpenes with different functional groups and oxidised methyl groups removed or moved at different positions are called terpenoids. Depending on carbon units, terpenoids are

further classified into monoterpenes, sesquiterpenes, diterpenes, sesterpenes and triterpenes (Figure 2.4) (Kiran *et al*., 2022).

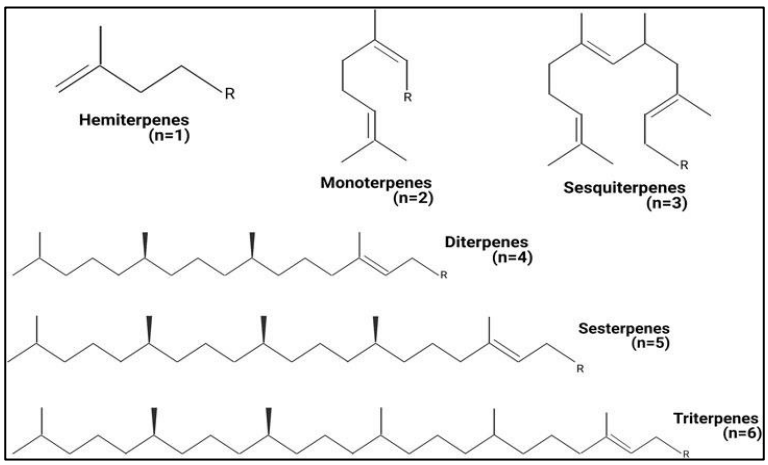

Figure 2. 4: Different classification of terpenes by the number of isoprenes present in the structure (Prado-Audelo *et al*., 2021).

2.3.5. Tannins

Tannins are referred to as the most plenty plants secondary metabolites, usually ranging from 5% to 10% dry weight on tree leaves (Jamwal *et al*., 2018). They occur naturally as water soluble polyphenolic compounds and can precipitate alkaloids, gelatin, and other proteins obtained from aqueous solutions *(*de Hoyos-Martínez *et al*., 2019). Tannins have antibacterial activity through which they inhibit bacterial enzymes or remove the required substrate for microbial growth or interrupt metabolism (Raji *et al*., 2019).

Tannins are divided into two main types: the condensed and hydrolysable tannins (Figure 2.5). The hydrolysable tannins are produced from various phenolic acid molecules such as gallic acid and hexahyroxydiphenic acid molecules, which are bound together by ester bonds to central glucose molecule (Hussein and El-Anssary, 2019). Condensed tannins (proanthocyanidins) are polymers of three-ring flavonols joined through carbon-carbon bonds. The monomers of condensed tannins are divided into procyanidins and prodelfinidins (Adamczyk *et al*., 2017). The are other two recently discovered tannins known as complex tannins and phlorotannins. Phlorotannins are found in brown algae and consist of phloroglucinol units (1,3,5-trihydroxybenzene). Traditional tannin is also known as complex tannins. The

traditional tannins are characterised by the presence of monomeric units of condensed and hydrolysable tannins (de Hoyos-Martínez *et al*., 2019).

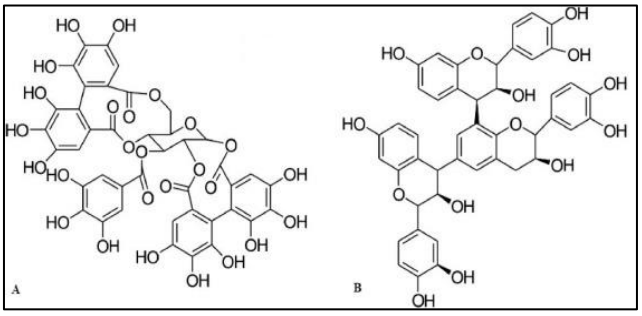

Figure 2. 5: Structure of (A) hydrolysable and (B) condensed tannins (Das *et al*., 2020).

2.3.6. Phlobatannin

Phlobatannin, also known as phlobaphene, is one of the most common condensed tannins, meaning it is not hydrolysable. It is an oligomer or polymer consisting of flavan-3-ol nucleic acid (Figure 2.6) (Kamarudin *et al*., 2019).

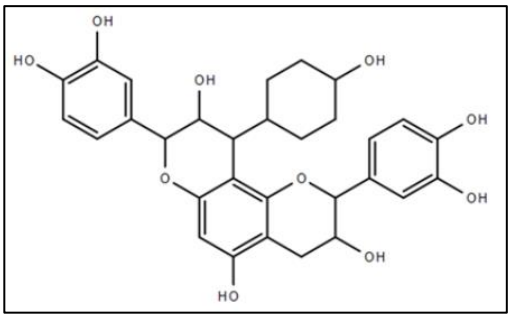

Figure 2. 6: Structure of phlobatannin (Kamarudin *et al*., 2019).

2.3.7. Quinones

Quinones are organic compounds derived from aromatic compounds and are found in natural processes of bio-metabolism, such as plastoquinone for photosynthesis and ubiquinone for respiration (Yan *et al*., 2020). The aromatic rings of quinones consist of two ketone substitutions, which are further divided into four different classes based on the number of benzene rings within the structure. The four different classes are benzoquinones, naphtoquinones, phenanthrenequinones, and anthraquinones. The structure of quinones makes them to be very reactive. They are colourful compounds playing a huge role in the browning reactions of fruits and vegetables. They are also the intermediates during the synthesis of melanin in the skin (Figure 2.7) (Ferdes, 2018).

Quinones have various biological activities, such as antibacterial, antioxidant, antitumor and anti-HIV activities. Quinones biological activities are related to the redox properties of the carbonyl functionality of quinones (Patel *et al*., 2021; Song *et al*., 2021; Ferdes, 2018).

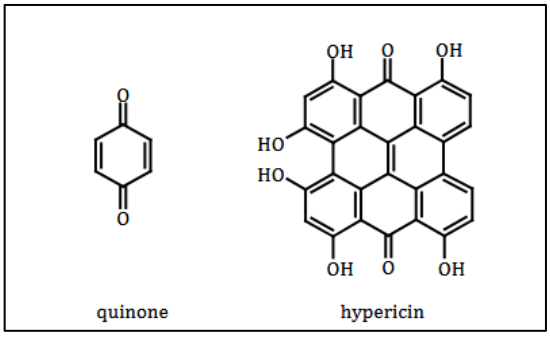

Figure 2. 7: Chemical structures of representative quinones, quinone and hypericin (Ferdes, 2018).

2.3.8. Saponins

Saponins are secondary metabolites that are scattered along the kingdom of plants and act as a chemical barrier or a shield in the plant defence system from pathogens. Saponins are found in plant tissues that are mostly vulnerable to fungal or bacterial attack (Ravi and Manasvi, 2016). They are characterised by their chemical agent properties because they are water-soluble and form a foam when dissolved. Saponins are divided into two groups, namely, steroidal saponins and triterpenoid saponins. They are potential compounds that act synergistically with antibiotics (Tagousop *et al*., 2018).

Saponins are natural compounds that consists of a sugar (glycon) and a non-sugar part (aglycon) connected by a glycosidic linkage. The aglycone part is also called sapoginins, which may be either steroidal or a triterpenoid and attached to one or more glycone moieties that may be hexoses and pentoses (Figure 2.8) (Khan *et al*., 2018). Saponins have biological activities such as antibacterial activity (Raji *et al*., 2019), anti-inflammatory, antifungal, and antiviral activity, based on their chemical structures (Dong *et al*., 2020).

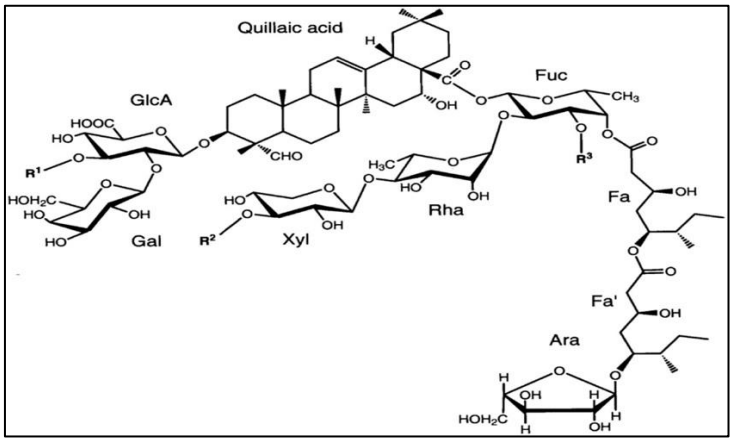

Figure 2. 8: The general structure of Quilaic acid, a saponin (Böttcher and Drusch, 2017).

2.3.9. Cardiac glycosides

Cardiac glycosides are regarded as chemical compounds used for the poisoning of livestock and to treat heart failure. Cardiac glycosides consist of drug-like molecules that are used for numerous investigations, and they play a huge role in drug development (Morsy, 2017). In most plants, cardiac glycosides are found in an inactive form and are activated by hydrolysis enzymes (Ferdes, 2018).

Cardiac glycosides as natural compounds are used to treat various cardiac conditions and they are recognised as potential antitumor compounds. Cardiac glycosides consist of an unsaturated lactone moiety at C17 on a steroid nucleus and a sugar moiety attached to C3. The nature of the lactone moiety characterises two subgroups, the cardenolides (five-membered α,β-unsaturated butyrolactone ring) and the bufadienolides (six-membered α,β-γ,δ-unsaturated 2-pyrone ring) (Figure 2.9) (Ayogu and Odoh, 2020; Schneider *et al*., 2017). Their activity is related to the lactone ring, while sugar residues are a determinant for toxicodynamic and toxicokinetic of each substance (Botelho *et al*., 2019).

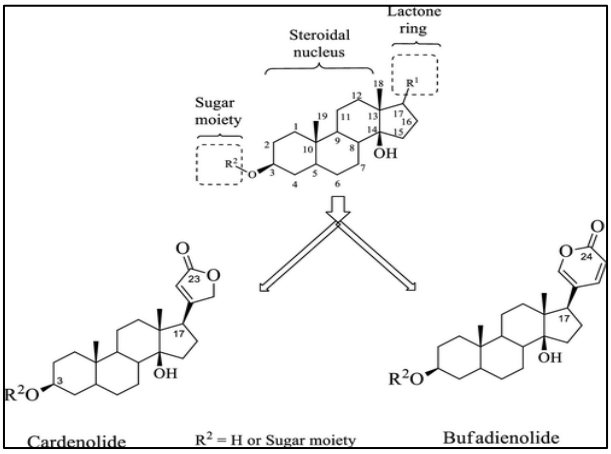

Figure 2. 9: Structures features and classification of cardiac glycosides (Ayogu and Odoh, 2020).

2.4. Biological activities of medicinal plants

2.4.1. Antioxidant activity

Reactive oxygen species (ROS) are the greatest source of a primary catalyst, which initiates the oxidation process *in vivo* and *in vitro* and the production of oxidative stress. Oxidative stress is produced when the reactive forms of oxygen are produced faster than they should be produced and neutralised by antioxidant mechanisms and/or when the antioxidant defence decreases (Dalimunthe *et al*., 2018). Respiratory infections such as *Mycobacterium tuberculosis* cause an increase in oxidative stress and inflammation in the lungs. Additionally, TB is also associated with an increased risk of developing a chronic obstructive pulmonary disease (Dua *et al*., 2019).

Free radicals are the major substances for biological activities and are produced in different parts of the body using oxygen. Free radicals affect people in their daily lives from different environmental resources like tobacco, drugs, alcohol, smoke, barbecued food, pesticides, harmful chemicals, and pollutants in the air (Islam *et al*., 2018). The uncontrolled production of oxygen free radicals in biological systems lead to cellular damages, and results in cell death (Behbahani *et al*., 2017). Antioxidants are defined as compounds that can inhibit or delay the oxidation of other molecules by its inhibition or propagation of an oxidising chain reactions. Antioxidant compounds trap the free radicals, which can be either phenolic acids, polyphenols or even flavonoids that can scavenge free radicals (Arina and Harisun, 2019).

Antioxidant activity is among the wide range of biological and pharmacological activities exhibited by medicinal plants (Sunday *et al*., 2021). Antioxidants, both from natural and synthetic sources, have proved to be highly effective in controlling the production of free radicals to prevent its undesirable effects and prevent the human body from reactive oxygen species (Arina and Harisun, 2019; Martins *et al*., 2016). The balance between oxidation and antioxidants in living organisms is maintained by exogeneous antioxidants (Sevindik, 2019).

Antioxidants can inhibit free radical reactivity through several mechanisms, including the donation of hydrogen, and radical scavenging. Antioxidants occur naturally and through synthetic chemical processes. DPPH assay is simple and one of the most widely used methods. The current methods used for determining antioxidant activity are based on the spectrophotometric determination through hydrogen atom transfer and single electron transfer mechanisms. These assays include 2,2-azino-bis(3-ethylbenzothiazoline-6-sulfonic acid (ABTS) assay, 2,2-diphenyl-1-(2,4,6-trinitrophenyl) hydrazyl (DPPH) radical scavenging activity, and ferric reducing antioxidant potential (FRAP) assay. It is based on the reduction of the violet DPPH radical by the antioxidant via a hydrogen atom transfer mechanism to cause a change in the colour to a stable pale-yellow DPPH molecules (Figure 2.10) (Sirivibulkovit *et al*., 2018).

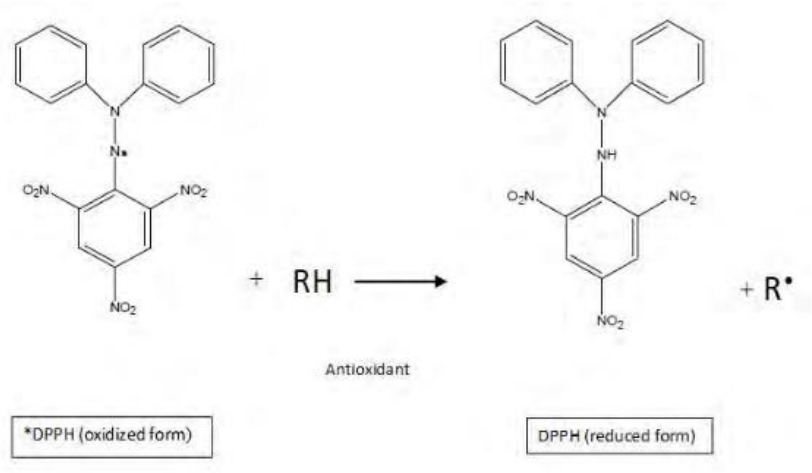

Here, * DPPH = 1, 1-diphenyl-2-picrylhydrazyl

Figure 2. 10: Structure of DPPH (Sarkar, 2018).

2.4.2. Antimicrobial activity

Infectious diseases are the major cause of morbidity and reduced mortality mostly in developing countries. A wide range of synthetic and semi-synthetic antibacterial agents are available to control microorganisms (Wang *et al*., 2017). However, the rise of the multidrug resistant (MDR) strain in pathogenic bacteria has become a public health threat as there are fewer, or even sometimes no effective antimicrobial agents available for the infection caused by pathogenic bacteria (Manandhar *et al*., 2019). Available antibiotics cause various negative drug reactions like hypersensitivity and immunosuppression. The development of negative side effects, and the constant development of resistance by bacteria resulted in a continuous need to develop new antimicrobial agents that are effective against microorganisms and less harmful to hosts. As such, the development of alternative antimicrobial agents is a great motivation to pharmaceutical industries (Manandhar *et al*., 2019; Bouyahya *et al*., 2016; Stankovic *et al*., 2016).

Testing of antimicrobials is used for drug discovery, epidemiology, and prediction of therapeutic outcome. The discovery of new antibiotics is entirely an important objective. Natural products are still one of the major sources for drug discovery (Balouiri *et al*., 2016). Identifying pants with antimicrobial activity from screening and further investigation is usually the first choice in antimicrobial studies (Anyanwu and Okoye, 2017). Othman *et al*., (2019) reported on *Salvadora persica* L. or miswak chewing sticks aqueous extracts, which have antimicrobial properties against seven microbial species such as *Streptococcus mutans*, *Streptococcus faecalis*, *Streptococcus pyogenes*, *Lactobacillus acidophilus*, *Pseudomonas aeruginosa*, *Staphylococcus aureus*, and *Candida albicans*.

There are different bioassays used to test antimicrobial activity, the well diffusion, disk-diffusion, and broth or agar dilution methods. The lowest concentration of an antimicrobial agent that completely inhibits the growth of the organism in micro-dilution wells or tubes as detected is known as the MIC. The MIC value is determined by performing dilution methods, to estimate the concentration of the tested antimicrobial agent in the agar or broth medium (Chouhan *et al*., 2017). Direct bioautography is the most applied method for testing antimicrobial activity. The developed TLC plate is dipped into or sprayed with a microbial suspension. For growth detection or

visualisation of the plates, tetrazolium salts are used to form a formazan colour through the dehydrogenase of the cells (Balouiri *et al*., 2016).

2.4.3. Anti-inflammatory activity

TB has a gap in understanding the complex interaction between bacterial virulence and host resistance, and the immune correlates responsible for ridding the body of TB infection. Mycobacteria increase and evade the bactericidal host immune response by surviving and proliferating within the macrophages (Gupta *et al*., 2016). The determinants of the TB clinical presentation are described to involve a complex relationship between the mycobacterium and the host immune responses. Successful host response against *M. tuberculosis* requires the production of pro-inflammatory cytokines, including interferon- gamma and tumour necrosis factor alpha. *Mycobacterium tuberculosis* infection is known to cause inflammation and lung tissue damage in high-risk populations (Mesquita *et al*., 2016).

Inflammation usually occurs when infectious microorganisms such as bacteria, viruses or fungi invade the body, reside tissues and/or circulate in the blood. Inflammation may also happen in response to processes such as tissue injury, cell death, cancer, ischemia, and degeneration. Mostly, both the innate immune response as well as the adaptive immune response are involved in the formation of inflammation. The adaptive immune systems involve the activity of more specialised cells, such as B and T cells, which are responsible for eliminating invading pathogens and cancer cells by producing specific receptors and antibodies (Azab *et al*., 2016). The innate immune system is the foremost defence mechanism against invading microorganisms and cancer cells, involving the activity of various cells, including macrophages, mast cells and dendritic cells. (Muefong and Sutherland, 2020).

Inflammation is characterised by the protective response of the immune system that involves the recognition of highly conserved pathogenic structures or endogenous non-infectious molecules by pathogen-recognition receptors (Ginwala *et al*., 2019). At the tissue level, inflammation is characterised by redness, swelling, heat, pain, and loss of tissue function, which result from local immune, vascular, and inflammatory cell responses to infection or injury (Chen *et al*., 2018; Serhan, 2017). When the inflammatory response is not regulated, it results in an increase in the concentration of inflammatory mediators, which might lead to the occurrence of several chronic

diseases, namely, rheumatoid arthritis, coronary diseases, and cancer, among others (Leyva-López *et al*., 2016). The discovery of new therapeutic agents to treat inflammation are required and plants are believed to be the promising agents since they produce curative secondary metabolites (Nunes *et al*., 2020).

2.4.4. Antibiofilm activity

Mycobacterium tuberculosis are difficult to be cleared from the human body and their resistant strains reactivate *in vivo*, this leads to TB recurring. Its wall consists of a specific lipid-peptidoglycan complex and in biofilms is enclosed in a lipid extracellular matrix, including the mycolic acids that are involved in cell wall synthesis (Wang *et al*., 2019).

A biofilm is a community of microorganisms held together by self-produced polymer matrix consisting of polysaccharides, secreted proteins, and extracellular DNAs. Biofilm formation is one of the survival mechanisms by microorganisms (Muhammad *et al*., 2020). The development of biofilms initiates with the adhesion of the bacteria, followed by attachment to the surface, sessile growth, matrix synthesis, and dispersal. Intercellular communication occurs through a quorum-sensing phenomenon. Different molecules from the bacterial cell wall called adhesins mediate the initial attachment of bacteria to the surfaces. Once attached to the surface, sessile bacteria initiate the synthesis of an extracellular matrix, usually composed of glycopeptides, DNA, and other molecules (Sharma *et al*., 2019; Esteban and García-Coca, 2018).

Biofilm related infections are continuous, resistant to most antibiotics, and unmanageable by the host immunity (Padhi *et al*., 2016). Biofilms prevent the diffusion of antibiotics, thus making cells within the biofilm to be resistant to antibiotic. Since antibiotics target active cells, tolerance to antibiotics is also increased because of their low metabolic activity of cells within the biofilm. As such, there is a need for the development of new antibiofilm strategies that will interfere with the cells within the biofilm (Schilcher and Horswill, 2020).

2.5. Separation, purification, and isolation of compounds

Column chromatography is a chromatographic technique used to separate compounds based on the distribution coefficients of the components in the stationary phase and mobile phase (Wen *et al*., 2019). It is used to obtain pure natural compounds from a mixture of different compounds. The adsorption column

chromatography is mostly used to separate natural products during the first stage of separation. This is because it is simple, has high capacity, and the cost-effective adsorbents, such as silica gel and macroporous resins are used (Zhang *et al*., 2018).

TLC and column chromatography have been used to isolate and purify many bioactive compounds. Column chromatography and TLC are still being employed because of their convenience and availability in several stationary phases (Altemimi *et al*., 2017). The separation is based on the differences between the adsorption affinities of the natural products for the surface of the adsorbents. The selection of the stationary phase as well as the mobile phase is important to achieve a good separation of natural products, it increases the chances of recovering the compounds of interest and prevents the irreversible adsorption of target compounds onto the adsorbents. Silica has the best value for separating phytochemicals. Compounds are kept by the silica gel in hydrogen bonds and dipole–dipole interactions. As such, the polar natural compounds are kept longer on the silica gel column than nonpolar compounds (Zhang *et al*., 2018).

Preparative TLC is a separation method that does not require a lot of instruments. Preparative TLC is not good for separating a large number of samples, it can only separate small samples. Compounds separate based on their polarity and bonding strength between silicon atoms of the TLC plate and the organic molecule as the mobile phase progresses along the length of the silica plate. The separated compounds are visualised under a fluorescent light, and the individual bands are collected (Mahato *et al*., 2019).

2.6. Structure elucidation of compounds

Data obtained from the UV-visible, Nuclear Magnetic Resonance (NMR), Infrared (IR), and mass spectroscopy are usually used to determine the structure of compounds. The spectroscopy principle is based on the passing of electromagnetic radiation trough an organic molecule that absorbs some light. Spectroscopy is based on the passing of electromagnetic radiation trough an organic molecule that absorbs light. A spectrum is produced by measuring the amount of electromagnetic radiation absorbed. The spectra are specific to certain bonds in a molecule. The structure of the organic molecule is identified depending on the spectra (Altemimi *et al*., 2017).

NMR is related to the magnetic properties of the nucleus of hydrogen atoms, protons, carbon molecule, and an isotope of the carbon. NMR spectroscopy provides the difference between the various magnetic nuclei, thus giving a clear picture of what the positions of these nuclei are in the molecule. It demonstrates which atoms are present in neighbouring groups, so that one can conclude how many atoms are present in each of these environments (Mahato *et al*., 2019).

Mass spectrometry (MS) is a powerful analytical tool with many applications in the pharmaceutical and biomedical field. It is used to determine the molecular weight of a molecule, where the molecular formula can also be predicted. It is based on the conversion of the sample into an ionised state, with or without fragmentation, which are then identified by their mass-to-charge ratio (Baghel *et al*., 2017).

Preparative or semi preparative TLC, liquid chromatography, and column chromatography have been used to isolate individual phenols, and their structures are determined using NMR (Altemimi *et al*., 2017).

2.7. Bacteria for clinical significance

2.7.1. *Mycobacterium smegmatis*

Mycobacterium smegmatis is an environmental, non-pathogenic *Mycobacterium* that is widely used as a model organism to study mycobacterial metabolism and pathogenicity (Goethe *et al.*, 2020; Yamada *et al.*, 2018). It is used to investigate TB because its biochemical properties and genetic information are closely related to *Mycobacterium tuberculosis. M. smegmatis* is rapidly growing, and is usually found in soil, water and plants (Ranjitha *et al*., 2020).

2.8. Selected medicinal plants for this study

The selection of the medicinal plants that were studied was based on the information from literature about plants with ethnopharmacological properties. The selected plants are: *Rhoicissus tridentata* Wild and Drum; *Rosmarinus officinalis* L.; *Ximenia caffra* Sond; *Zanthoxylum capense* (Thunb) Hary; and *Ziziphus mucronata* Willd.

2.8.1. *Rhoicissus tridentata* Wild and Drum

Rhoicissus tridentata (L.f) Wild & Drumm. subsp. *cuneifolia* (Eckl. & Zehr.), N.R. Urton in the Vitaceae family is commonly known as wild grape (English), *isinwazi* (IsiZulu), and *umnxeba* (isiXhosa). Species from *Rhoicissus* genus contain several secondary metabolites (alkaloids, terpenoids and flavonoids), which have biological effects such

as anti-inflammatory, anti-cancer and antioxidant activities (Figure 2.11) (Dube *et al.*, 2021). Tubers, leaves, and stem (wood) are used in the treatment of TB-related diseases or their symptoms (Sharifi-Rad *et al*., 2020). *Rhoicissus tridentata* is used traditionally by crushing and taking it orally with warm water to treat TB-related symptoms (Semenya and Maroyi, 2019).

Figure 2. 11: Picture of *R. tridentata* Wild and Drum (Mdletshe, 2018).

2.8.2. *Rosmarinus officinalis* L.

Rosemary is an aromatic herb used mostly for cooking and has various bioactivities, such as anti-inflammatory and antioxidant activity. Phenolics like carnosic acid, carnosol, and rosmarinic acid are responsible for the bioactivities (Moreira *et al*., 2019). *Rosmarinus officinalis*, L. is an evergreen shrub with needle-like leaves (Satyal *et al.*, 2017), with curved edges and tiny pink, white, blue or purple flowers (Figure 2.12) (Lešnik *et al*., 2020).

Rosmarinus officinalis, L. originates from the Mediterranean region and it is an aromatic plant from the family Lamiaceae. It is usually used as an antioxidant. Extracts from *Rosemarinus officinalis* L. have been used to treat diseases because of their ability to prevent damage to the liver, treat Alzheimer's disease and also reduce the growth of new blood cells. (Nieto *et al*., 2018). Traditional healers used to boil *Rosmarinus officinalis* (Lamiaceae family) for 5 minutes. The extract is taken orally for chest pain, cough, and fever (Semenya and Maroyi, 2019).

Figure 2. 12: A picture of *R. officinalis* plant in full blossom (Lešnik *et al*., 2020).

2.8.3. *Ximenia caffra* Sond.

Ximenia caffra Sond is a member of Ximeniaceae family, formally known as Olacaceae, which is called the sour plum in English. It is divided into two varieties, *X. caffra* Sond. var. *caffra* (their leaves are hairy till mature) and *X. caffra* Sond. var. *natalensis* Sond (which has hairless leaves and branches) (Chingwaru *et al*., 2020). *X. caffra* Sond. var. *natalensis* leaves occur in tuffs, grey-green or oblong blue, and are hairless, folded upwards along the midrib. It has clustered green-whitish flowers on the axils of spines (Figure 2.13) (Tlaamela, 2019). Its leaves or roots are used to treat constipation, leprosy, and stomach pains (Masuku *et al*., 2020).

Figure 2. 13: Picture of *X. caffra* Sond. Var. caffra (Tlaamela, 2019).

2.8.4. *Zanthoxylum capense* (Thunb) Hary

Zanthoxylum capense belongs to the family Rutaceae. It contains shrubs and trees, but mostly dioecious. Species of *Zanthoxylum* are characterised by sharp thorns on their trunk and branches. Its leaves alternate, unevenly compound, with four to eight pairs of leaflets. The leaves are characterised by a citrus smell (Sunday, 2017). It has noticeable citrus-scented leaves and fruits. The fruits are round capsules with a

diameter of 5 mm (Figure 2.14). It usually grows in the eastern region of Southern Africa and is used to treat ailments such as cough (Komape, 2019).

Figure 2. 14: Picture of *Z. capense* (Thunb) Hary (Sunday, 2017).

2.8.5. *Ziziphus mucronata* Willd

Ziziphus mucronate Willd belongs to the family Rhamnaceae. It appears as spiny shrubs or trees and is mostly found in the Malayan arid region, Africa, Australia, America, and the subcontinent of South Asia (Payus *et al*., 2020). Its leaves, roots and bark are used to treat TB-related infections and their symptoms. Its bark and roots are also used medicinally for the treatment of various ailments, including rheumatism, gastrointestinal complaints, and snake bites. The root infusions are used for treating gonorrhoea, diarrhoea, and dysentery (Olajuyigbe and Afolayan, 2011). The bark is used for body pains, cough, respiratory infections, and chest problems (Sharifi-Rad *et al*., 2020). Mongalo *et al*. (2020) also reported that it is used to treat respiratory or chest complaints (Figure 2.15).

Figure 2.15: Different plant parts of *Ziziphus mucronata* (stem bark, 1A), (Leaves, thorns, green and ripe fruits, 1B &1C), (Leaves and flower, 1D) (Mongalo *et al*., 2020).

2.9. Aims and objectives

2.9.1. Aim

The aim of the study was to isolate and characterise antimycobacterial and antioxidant compounds of the leaf extracts and determine synergistic effects.

2.9.2. Objectives

The objectives of the study were to:

i. analyse chemical profile of the plant extracts using TLC;
ii. determine the presence of major phytochemical groups using standard chemical methods;
iii. quantify major phytochemicals using standard chemical methods;
iv. determine antioxidant activity of plant extracts using 2,2-diphenyl-1-picrylhydrazyl (DPPH) assay and ferric reducing power assay;
v. analyse the antimycobacterial activity of plant extracts using bioautographic assay and serial microdilution assay;
vi. perform synergistic/antagonistic study of the plant extracts;
vii. determine the anti-inflammatory and antibiofilm activities;
viii. investigate the cytotoxicity effects of the plant extracts on THP-1 cells using cell viability assay,
ix. isolate bioactive compounds and analyse the structure using NMR and mass spectrometry.

2.10. References

Adamczyk, B., Simon, J., Kitunen, V., Adamczyk, S. and Smolander, A. 2017. Tannins and their complex interaction with different organic nitrogen compounds and enzymes: old paradigms versus recent advances. *Chemistry Open*, **6**(5): 610.

Albuquerque, B.R., Heleno, S.A., Oliveira, M.B.P., Barros, L. and Ferreira, I.C. 2021. Phenolic compounds: current industrial applications, limitations, and future challenges. *Food and Function*, **12**(1): 14-29.

Altemimi, A., Lakhssassi, N., Baharlouei, A., Watson, D.G. and Lightfoot, D.A. 2017. Phytochemicals: extraction, isolation, and identification of bioactive compounds from plant extracts. *Plants*, **6**(4): 42.

Ankomah, R. 2020. Antimycobacterial activities of selected medicinal plants extracts in the management of *Mycobacterium tuberculosis* H37Rv and *Mycobacterium bovis*, **2**(4): 67-85.

Anyanwu, M.U. and Okoye, R.C. 2017. Antimicrobial activity of Nigerian medicinal plants. *Journal of Intercultural Ethnopharmacology*, **6**(2): 240.

Arina, M.I. and Harisun, Y. 2019. Effect of extraction temperatures on tannin content and antioxidant activity of *Quercus infectoria* (Manjakani). *Biocatalysis and Agricultural Biotechnology*, **19**: 101104.

Aye, M.M., Aung, H.T., Sein, M.M. and Armijos, C. 2019. A review on the phytochemistry, medicinal properties and pharmacological activities of 15 selected Myanmar medicinal plants. *Molecules*, **24**(2): 293.

Ayogu, J.I. and Odoh, A.S. 2020. Prospects and therapeutic applications of cardiac glycosides in cancer remediation. *ACS Combinatorial Science*, **22**(11): 543-553.

Azab, A., Nassar, A. and Azab, A.N. 2016. Anti-inflammatory activity of natural products. *Molecules*, **21**(10): 1321.

Baghel, U.S., Singh, A., Singh, D. and Sinha, M. 2017. Application of mass spectroscopy in pharmaceutical and biomedical analysis. *Spectroscopic Analyses: Developments and Applications*, **105**.

Balouiri, M., Sadiki, M. and Ibnsouda, S.K. 2016. Methods for *in vitro* evaluating antimicrobial activity: a review. *Journal of Pharmaceutical Analysis*, **6**(2): 71-79.

Behbahani, B.A., Shahidi, F., Yazdi, F.T., Mortazavi, S.A. and Mohebbi, M. 2017. Antioxidant activity and antimicrobial effect of tarragon (*Artemisia dracunculus*) extract and chemical composition of its essential oil. *Journal of Food Measurement and Characterization*, **11**(2): 847-863.

Botelho, A.F.M., Pierezan, F., Soto-Blanco, B. and Melo, M.M. 2019. A review of cardiac glycosides: structure, toxicokinetics, clinical signs, diagnosis, and antineoplastic potential. *Toxicon*, **158**: 63-68.

Böttcher, S. and Drusch, S. 2017. Saponins—self-assembly and behaviour at aqueous interfaces. *Advances in Colloid and Interface Science*, **243**: 105-113.

Bouyahya, A., Abrini, J., El-Baabou, A., Bakri, Y. and Dakka, N. 2016. Determination of phenol content and antibacterial activity of five medicinal plants ethanolic extracts from North-West of Morocco. *Journal of Plant Pathology and Microbiology*, **7**(342): 2.

Bribi, N. 2018. Pharmacological activity of alkaloids: a review. *Asian Journal of Botany*, **1**(1): 6.

Cheng, C., Li, Z., Zhao, X., Liao, C., Quan, J., Bode, A.M., Cao, Y. and Luo, X. 2020. Natural alkaloid and polyphenol compounds targeting lipid metabolism: treatment implications in metabolic diseases. *European Journal of Pharmacology*, **870**: 172922.

Chen, L., Deng, H., Cui, H., Fang, J., Zuo, Z., Deng, J., Li, Y., Wang, X. and Zhao, L. 2018. Inflammatory responses and inflammation-associated diseases in organs. *Oncotarget*, **9**(6): 7204.

Chingwaru, C., Bagar, T. and Chingwaru, W. 2020. Aqueous extracts of *Flacourtia indica*, *Swartzia madagascariensis* and *Ximenia caffra* are strong antibacterial agents against *Shigella* spp., *Salmonella typhi* and *Escherichia coli* O157. *South African Journal of Botany*, **128**: 119-127.

Chouhan, S., Sharma, K. and Guleria, S. 2017. Antimicrobial activity of some essential oils—present status and future perspectives. *Medicines*, **4**(3):58.

Cianciosi, D., Forbes-Hernández, T.Y., Afrin, S., Gasparrini, M., Reboredo-Rodriguez, P., Manna, P.P., Zhang, J., Bravo Lamas, L., Martínez Flórez, S., Agudo Toyos, P. and Quiles, J.L. 2018. Phenolic compounds in honey and their associated health benefits: a review. *Molecules*, **23**(9): 2322.

Cong-Cong, X.U., Bing, W.A.N.G., Yi-Qiong, P.U., Jian-Sheng, T.A.O. and Zhang, T. 2017. Advances in extraction and analysis of phenolic compounds from plant materials. *Chinese Journal of Natural Medicines*, **15**(10): 721-731.

Cox-Georgian, D., Ramadoss, N., Dona, C. and Basu, C. 2019. Therapeutic and medicinal uses of terpenes. *Medicinal Plants,* **978**:333-359.

Dalimunthe, A., Hasibuan, P.A.Z., Silalahi, J., Sinaga, S.F. and Satria, D. 2018. Antioxidant activity of alkaloid compounds from *Litsea cubeba* Lour. *Oriental Journal of Chemistry*, **34**(2): 1149.

Das, A.K., Islam, M.N., Faruk, M.O., Ashaduzzaman, M. and Dungani, R. 2020. Review on tannins: Extraction processes, applications, and possibilities. *South African Journal of Botany*, **135**: 58-70.

de Hoyos-Martínez, P.L., Merle, J., Labidi, J. and Charrier–El Bouhtoury, F. 2019. Tannins extraction: A key point for their valorization and cleaner production. *Journal of Cleaner Production*, **206**: 1138-1155.

Dey, P., Kundu, A., Kumar, A., Gupta, M., Lee, B.M., Bhakta, T., Dash, S. and Kim, H.S. 2020. Analysis of alkaloids (indole alkaloids, isoquinoline alkaloids, tropane alkaloids). *Recent Advances in Natural Products Analysis*, **67**: 505-567.

Dhull, S.B., Kaur, P. and Purewal, S.S. 2016. Phytochemical analysis, phenolic compounds, condensed tannin content and antioxidant potential in Marwa (*Origanum majorana*) seed extracts. *Resource-Efficient Technologies*, **2**(4): 168-174.

Dong, S., Yang, X., Zhao, L., Zhang, F., Hou, Z. and Xue, P. 2020. Antibacterial activity and mechanism of action saponins from *Chenopodium quinoa* Willd. husks against foodborne pathogenic bacteria. *Industrial Crops and Products*, **149**: 112350.

Dua, K., Malyla, V., Singhvi, G., Wadhwa, R., Krishna, R.V., Shukla, S.D., Shastri, M.D., Chellappan, D.K., Maurya, P.K., Satija, S. and Mehta, M. 2019. Increasing complexity and interactions of oxidative stress in chronic respiratory diseases: an

emerging need for novel drug delivery systems. *Chemico-Biological Interactions*, **299**: 168-178.

Dube, N.P., Siwe-Noundou, X., Krause, R.W., Kemboi, D., Tembu, V.J. and Manicum, A.L. 2021. Review of the traditional uses, phytochemistry, and pharmacological activities of *Rhoicissus* species (Vitaceae). *Molecules*, **26**(8): 2306.

Ekundayo, E.O., Kalu, U.O. and Enya, E. 2020. *In vitro* inhibitory activity of extracts of some medicinal plants against *Mycobacterium smegmatis*. *Nigerian Journal of Microbiology*, **34**(1): 5044-5052.

Esteban, J. and García-Coca, M. 2018. Mycobacterium biofilms. *Frontiers in Microbiology*, **8**: 2651.

Ferdes, M. 2018. Antimicrobial compounds from plants. *Fighting Antimicrobial Resistance. IAPC-OBP, Zagreb*, 243-271.

Ginwala, R., Bhavsar, R., Chigbu, D.G.I., Jain, P. and Khan, Z.K. 2019. Potential role of flavonoids in treating chronic inflammatory diseases with a special focus on the anti-inflammatory activity of apigenin. *Antioxidants*, **8**(2): 35.

Goethe, E., Laarmann, K., Lührs, J., Jarek, M., Meens, J., Lewin, A. and Goethe, R. 2020. Critical role of Zur and SmtB in zinc homeostasis of *Mycobacterium smegmatis*. *MSystems*, **5**(2):1-19.

Gupta, N., Agrawal, B. and Kumar, R. 2016. Controlling inflammation: a superior way to control TB. *Immunotherapy*, **8**(10): 1157.

Granato, D., Santos, J.S., Maciel, L.G. and Nunes, D.S. 2016. Chemical perspective and criticism on selected analytical methods used to estimate the total content of phenolic compounds in food matrices. *TrAC Trends in Analytical Chemistry*, **80**: 266-279.

Hussein, R.A. and El-Anssary, A.A. 2019. Plants secondary metabolites: the key drivers of the pharmacological actions of medicinal plants. *Herbal Medicine*, **1**: 13.

Islam, M.S., Rahi, M.S., Koli, H.K., Jerin, I., Sajib, S.A., Hoque, K.M.F. and Reza, M.A. 2018. Evaluation of phytochemical, antioxidant, cytotoxicity, and *in vitro*

antibacterial activity of aqueous extract of *Ganoderma lucidum* cultivated in Bangladeshi habitat. *Malaya Journal of Biosciences*, **5**(1): 1-13.

Jain, C., Khatana, S. and Vijayvergia, R. 2019. Bioactivity of secondary metabolites of various plants: a review. *International Journal of Pharmaceutical Sciences and Research*, **10**(2): 494-498.

Jamwal, K., Bhattacharya, S. and Puri, S. 2018. Plant growth regulator mediated consequences of secondary metabolites in medicinal plants. *Journal of Applied Research on Medicinal and Aromatic Plants*, **9**: 26-38.

Kamarudin, N.A., Muhamad, N., Salleh, N.N.H.N. and Tan, S.C. 2021. Impact of solvent selection on phytochemical content, recovery of tannin, and antioxidant activity of *Quercus infectoria* galls. *Pharmacognosy Journal*, **13**(5).

Khan, M.I., Ahhmed, A., Shin, J.H., Baek, J.S., Kim, M.Y. and Kim, J.D. 2018. Green tea seed isolated saponins exerts antibacterial effects against various strains of gram positive and gram-negative bacteria, a comprehensive study *in vitro* and *in vivo*. *Evidence-Based Complementary and Alternative Medicine*, 1-12.

Kiran, G., Karthik, L., Thumma, G. and Vishnukirthi, A. 2022. Genome data mining, chemistry, and bioactivity of sesquiterpenes from actinobacteria. *Actinobacteria*,101-120.

Komape, N.P.M. 2019. *Microbiological and biochemical studies of traditional medicinal plants used in Limpopo Province for anti-Micobacterium tuberculosis activity*. (Doctoral dissertation, University of Limpopo).

Kukula-Koch, W.A. and Widelski, J. 2017. Alkaloids. *Pharmacognosy*, **3**:163-198.

Kumari, P., Kumari, C. and Singh, P.S. 2017. Phytochemical screening of selected medicinal plants for secondary metabolites. *International Journal of Life-Sciences Scientific Research*, **3**(4): 1151-1157.

Lešnik, S., Furlan, V. and Bren, U. 2021. Rosemary (*Rosmarinus officinalis* L.): extraction techniques, analytical methods, and health-promoting biological effects. *Phytochemistry Reviews*, **20**(6): 1273-1328.

Leyva-López, N., Gutierrez-Grijalva, E.P., Ambriz-Perez, D.L. and Heredia, J.B. 2016. Flavonoids as cytokine modulators: a possible therapy for inflammation-related diseases. *International Journal of Molecular Sciences*, **17**(6): 921.

Li, Y., Kong, D., Fu, Y., Sussman, M.R. and Wu, H. 2020. The effect of developmental and environmental factors on secondary metabolites in medicinal plants. *Plant Physiology and Biochemistry*, **148**: 80-89.

Mahato, N., Sinha, M., Sharma, K., Koteswararao, R. and Cho, M.H. 2019. Modern extraction and purification techniques for obtaining high purity food-grade bioactive compounds and value-added co-products from citrus wastes. *Foods*, **8**(11): 523.

Manandhar, S., Luitel, S. and Dahal, R.K. 2019. In vitro antimicrobial activity of some medicinal plants against human pathogenic bacteria. *Journal of Tropical Medicine*: 1-5.

Martins, N., Barros, L. and Ferreira, I.C. 2016. *In vivo* antioxidant activity of phenolic compounds: facts and gaps. *Trends in Food Science and Technology*, **48**: 1-12.

Masuku, N.P., Unuofin, J.O. and Lebelo, S.L. 2020. Phytochemical content, antioxidant activities and androgenic properties of four South African medicinal plants. *Journal of Herbmed Pharmacology*, **9**(3): 245-256.

Mdletshe, N.W. 2018. *Comparison of pharmalogical activity of Rhoicissus tomentosa and Rhoicissus tridentata for the treatment of elephantiasis in South Africa*. (Doctoral dissertation, University of the Free State).

Mesquita, E.D., Gil-Santana, L., Ramalho, D., Tonomura, E., Silva, E.C., Oliveira, M.M., Andrade, B.B. and Kritski, A. 2016. Associations between systemic inflammation, mycobacterial loads in sputum and radiological improvement after treatment initiation in pulmonary TB patients from Brazil: a prospective cohort study. *BMC Infectious Diseases*, **16**(1): 1-12.

Mongalo, N.I., Mashele, S.S. and Makhafola, T.J. 2020. *Ziziphus mucronata* Willd.(Rhamnaceae): It's botany, toxicity, phytochemistry and pharmacological activities. *Heliyon*, **6**(4).

Moreira, S.A., Alexandre, E.M., Pintado, M. and Saraiva, J.A. 2019. Effect of emergent non-thermal extraction technologies on bioactive individual compounds profile from different plant materials. *Food Research International*, **115**: 177-190.

Morsy, N. 2017. Cardiac glycosides in medicinal plants. Aromatic and medicinal plants–back to nature. *Intechopen*, 29-45.

Muefong, C.N. and Sutherland, J.S. 2020. Neutrophils in tuberculosis-associated inflammation and lung pathology. *Frontiers in Immunology*, **11**: 962.

Muhammad, M.H., Idris, A.L., Fan, X., Guo, Y., Yu, Y., Jin, X., Qiu, J., Guan, X. and Huang, T. 2020. Beyond risk: bacterial biofilms and their regulating approaches. *Frontiers in Microbiology*, **11**: 928.

Nieto, G., Ros, G. and Castillo, J. 2018. Antioxidant and antimicrobial properties of rosemary (*Rosmarinus officinalis*, L.): a Review. *Medicines*, **5**(3): 98.

Nunes, C.D.R., Barreto Arantes, M., Menezes de Faria Pereira, S., Leandro da Cruz, L., de Souza Passos, M., Pereira de Moraes, L., Vieira, I.J.C. and Barros de Oliveira, D., 2020. Plants as sources of anti-inflammatory agents. *Molecules*, **25**(16): 3726.

Odebiyi, O.O. and Sofowora, E.A. 1978. Phytochemical screening of Nigerian medicinal plants, part iii. *Lloydia Journal*, **41**: 234-246.

Obakiro, S.B., Kiprop, A., Kowino, I., Kigondu, E., Odero, M.P., Omara, T. and Bunalema, L. 2020. Ethnobotany, ethnopharmacology, and phytochemistry of traditional medicinal plants used in the management of symptoms of tuberculosis in East Africa: a systematic review. *Tropical Medicine and Health*, **48**(1): 1-21.

Olajuyigbe, O.O. and Afolayan, A.J. 2011. Phenolic content and antioxidant property of the bark extracts of *Ziziphus mucronata* Willd. subsp. *mucronata* Willd. *BMC Complementary and Alternative Medicine*, **11**(1): 1-8.

Othman, L., Sleiman, A. and Abdel-Massih, R.M. 2019. Antimicrobial activity of polyphenols and alkaloids in middle eastern plants. *Frontiers in Microbiology*, **10**: 911.

Padhi, A., Naik, S.K., Sengupta, S., Ganguli, G. and Sonawane, A. 2016. Expression of Mycobacterium tuberculosis NLPC/p60 family protein Rv0024 induce

biofilm formation and resistance against cell wall acting anti-tuberculosis drugs in *Mycobacterium smegmatis*. *Microbes and Infection*, **18**(4); 224-236.

Patel, O.P., Beteck, R.M. and Legoabe, L.J. 2021. Antimalarial application of quinones: a recent update. *European Journal of Medicinal Chemistry*, **210**: 113084.

Payus, C.M., Jikilim, C. and Sentian, J. 2020. Rainwater chemistry of acid precipitation occurrences due to long-range transboundary haze pollution and prolonged drought events during southwest monsoon season: climate change driven. *Heliyon*, **6**(9).

Pengelly, A. and Bone, K., 2020. *The constituents of medicinal plants: an introduction to the chemistry and therapeutics of herbal medicine*. 2nd ed. Routledge. London. United Kingdom, 184.

Poro, K.E., Hoekou, Y., Pissang, P., Kpabi, I., Novidzro, K.M., Dagnra, A.Y., Tchacondo, T. and Batawila, K. 2021. *In vitro* antimycobacterial activity of selected medicinal plants against *Mycobacterium tuberculosis*. *International Journal of Current Microbiology and Applied Sciences*, **10**(2): 3201-3208.

Prado-Audelo, D., Luisa, M., Cortés, H., Caballero-Florán, I.H., González-Torres, M., Escutia-Guadarrama, L., Bernal-Chávez, S.A., Giraldo-Gomez, D.M., Magaña, J.J. and Leyva-Gómez, G. 2021. Therapeutic applications of terpenes on inflammatory diseases. *Frontiers in Pharmacology*, **12**: 2114.

Raji, P., Samrot, A.V., Keerthana, D. and Karishma, S. 2019. Antibacterial activity of alkaloids, flavonoids, saponins and tannins mediated green synthesised silver nanoparticles against *Pseudomonas aeruginosa* and *Bacillus subtilis*. *Journal of Cluster Science*, **30**(4): 881-895.

Rana, A., Negi, P.B. and Sahoo, N.G. 2022. Phytochemical screening and characterization of bioactive compounds from *Juniperus squamata* root extract. *Materials Today: Proceedings*, **48**: 672-675.

Ranjitha, J., Rajan, A. and Shankar, V. 2020. Features of the biochemistry of *Mycobacterium smegmatis*, as a possible model for *Mycobacterium tuberculosis*. *Journal of Infection and Public Health*, **13**(9): 1255-1264.

Ravi, L. and Manasvi, V. 2016. Antibacterial and antioxidant activity of saponin from *Abutilon indicum* leaves. *Asian Journal of Pharmaceutical and Clinical Research*, 344-347.

Roaa, M.H. 2020. A review article: the importance of the major groups of plants secondary metabolism phenols, alkaloids, and terpenes. *International Journal for Research in Applied Sciences and Biotechnology*, **7**(5): 354-358.

Rohini, M.V. and Padmini, E. 2016. Preliminary phytochemical screening of selected medicinal plants of polyherbal formulation. *Journal of Pharmacognosy and Phytochemistry*, **5**(5): 277.

Rosales, P.F., Bordin, G.S., Gower, A.E. and Moura, S. 2020. Indole alkaloids: 2012 until now, highlighting the new chemical structures and biological activities. *Fitoterapia*, **143**: 104558.

Roy, A. 2017. A review on the alkaloids an important therapeutic compound from plants. *International Journal of Plant Biotechnology*, **3**(2): 1-9.

Saboora, A., Sajjadi, S.T., Mohammadi, P. and Fallahi, Z. 2019. Antibacterial activity of different composition of aglycone and glycosidic saponins from tuber of *Cyclamen coum* Miller. *Industrial Crops and Products*, **140**: 111662.

Santhi, K. and Sengottuvel, R. 2016. Qualitative and quantitative phytochemical analysis of *Moringa concanensis* Nimmo. *International Journal of Current Microbiology and Applied Sciences*, **5**(1): 633-640.

Sarkar, M. 2018. *Investigation of in-vitro antioxidant potential, brine shrimp lethality and Thrombolytic activity in Ficus mollis vahl leaves along with phytochemical screening*. (Honours dissertation, BRAC University).

Satyal, P., Jones, T.H., Lopez, E.M., McFeeters, R.L., Ali, N.A.A., Mansi, I., Al-Kaf, A.G. and Setzer, W.N. 2017. Chemotypic characterization and biological activity of *Rosmarinus officinalis*. *Foods*, **6**(3): 20.

Schilcher, K. and Horswill, A.R. 2020. Staphylococcal biofilm development: structure, regulation, and treatment strategies. *Microbiology and Molecular Biology Reviews*, **84**(3): e00026-19.

Schneider, N.F.Z., Cerella, C., Simões, C.M.O. and Diederich, M. 2017. Anticancer and immunogenic properties of cardiac glycosides. *Molecules*, **22**(11): 1932.

Semenya, S.S. and Maroyi, A. 2019. Ethnobotanical survey of plants used by Bapedi traditional healers to treat tuberculosis and its opportunistic infections in the Limpopo Province, South Africa. *South African Journal of Botany*, **122**: 401-421.

Serhan, C.N., 2017. Treating inflammation and infection in the 21st century: new hints from decoding resolution mediators and mechanisms. *The Federation of American Societies for Experimental Biology Journal*, **31**(4): 1273-1288.

Sevindik, M. 2019. Antioxidant and antimicrobial activity of *Cerrena unicolor*. *Mycopath*, **16**(1).

Sharifi-Rad, J., Salehi, B., Stojanović-Radić, Z.Z., Fokou, P.V.T., Sharifi-Rad, M., Mahady, G.B., Sharifi-Rad, M., Masjedi, M.R., Lawal, T.O., Ayatollahi, S.A. and Masjedi, J. 2020. Medicinal plants used in the treatment of tuberculosis-ethnobotanical and ethnopharmacological approaches. *Biotechnology Advances*, 107629.

Sharma, D., Misba, L. and Khan, A.U. 2019. Antibiotics versus biofilm: an emerging battleground in microbial communities. *Antimicrobial Resistance and Infection Control*, **8**(1): 1-10.

Shazhni, J.A., Renu, A. and Murugan, M. 2016. Phytochemical screening and *in vitro* antimicrobial activity of ornamental plant *Anthurium andraeanum*. *Journal of Pharmaceutical Sciences and Research*, **8**(7): 668.

Shitan, N. 2016. Secondary metabolites in plants: transport and self-tolerance mechanisms. *Bioscience, Biotechnology, and Biochemistry*, **80**(7): 1283-1293.

Singh, B. and Sharma, R.A. 2020. *Secondary metabolites of medicinal plants. 1st ed*. John Wiley & Sons. New York. United States, 6-47.

Song, S., Sun, X., Meng, L., Wu, Q., Wang, K. and Deng, Y. 2021. Antifungal activity of hypocrellin compounds and their synergistic effects with antimicrobial agents against *Candida albicans*. *Microbial Biotechnology*, **14**(2): 430-443.

Sirivibulkovit, K., Nouanthavong, S. and Sameenoi, Y. 2018. Based DPPH assay for antioxidant activity analysis. *Analytical Sciences*, **34**(7): 795-800.

Stanković, N., Mihajilov-Krstev, T., Zlatković, B., Stankov-Jovanović, V., Mitić, V., Jović, J., Čomić, L., Kocić, B. and Bernstein, N. 2016. Antibacterial and antioxidant activity of traditional medicinal plants from the Balkan Peninsula. *NJAS-Wageningen Journal of Life Sciences*, **78**: 21-28.

Sunday, B.O. 2017. *Phytochemical investigation and tissue culture studies on the South African knob trees, Zanthoxylum Capense* and *Senegalia Nigrescens.* (Doctoral dissertation, University of KwaZulu-Natal).

Sunday, E.A., Nnedimma, N.C., Peter, W.G. and Orlando, G.B. 2021. Screening for pharmacological compounds and antioxidant activity of *Hedychium coronarium* J. Koenig. *Asian Journal of Research in Botany*: 34-47.

Tagousop, C.N., Kengne, I.C., Ngnokam, D. and Voutquenne-Nazabadioko, L. 2018. Antimicrobial activities of saponins from *Melanthera elliptica* and their synergistic effects with antibiotics against pathogenic phenotypes. *Chemistry Central Journal*, **12**(1): 1-9.

Tanveer, A., Singh, N.D. and Khan, M.F. 2017. Phytochemical analysis, total phenolic content, antioxidant, and antidiabetic activity of *Sansevieria cylindrica* leaves extract. *Herb Med*, **3**(2): 6.

Tlaamela, D.M. 2019. *Ethnobotanical survey and biological activity of medicinal plants used against candida albicans in Aganang local municipality*. (Doctoral dissertation, University of Limpopo).

Tuyiringire, N., Deyno, S., Weisheit, A., Tolo, C.U., Tusubira, D., Munyampundu, J.P., Ogwang, P.E., Muvunyi, C.M. and Vander Heyden, Y. 2020. Three promising antimycobacterial medicinal plants reviewed as potential sources of drug hit candidates against multidrug-resistant tuberculosis. *Tuberculosis*, 101987.

Vuolo, M.M., Lima, V.S. and Junior, M.R.M. 2019. Phenolic compounds: structure, classification, and antioxidant power. *Bioactive Compounds*: 33-50.

Wang, C., Zhang, Q., Tang, X., An, Y., Li, S., Xu, H., Li, Y., Wang, X., Luan, W., Wang, Y. and Liu, M. 2019. Effects of CwlM on autolysis and biofilm formation in *Mycobacterium tuberculosis* and *Mycobacterium smegmatis*. *International Journal of Medical Microbiology*, **309**(1): 73-83.

Wang, L., Hu, C. and Shao, L. 2017. The antimicrobial activity of nanoparticles: present situation and prospects for the future. *International Journal of Nanomedicine*, **12**: 1227.

Wen, P., Hu, T.G., Linhardt, R.J., Liao, S.T., Wu, H. and Zou, Y.X. 2019. Mulberry: a review of bioactive compounds and advanced processing technology. *Trends in Food Science and Technology*, **83**: 138-158.

Yamada, H., Yamaguchi, M., Igarashi, Y., Chikamatsu, K., Aono, A., Murase, Y., Morishige, Y., Takaki, A., Chibana, H. and Mitarai, S. 2018. *Mycolicibacterium smegmatis*, basonym *Mycobacterium smegmatis*, expresses morphological phenotypes much more similar to *Escherichia coli* than *Mycobacterium tuberculosis* in quantitative structome analysis and CryoTEM examination. *Frontiers in Microbiology*, **9**: 1992.

Yan, L., Zhao, C., Sha, Y., Li, Z., Liu, T., Ling, M., Zhou, S. and Liang, C. 2020. Electrochemical redox behavior of organic quinone compounds in aqueous metal ion electrolytes. *Nano Energy*, **73**: 104766.

Zhang, Q.W., Lin, L.G. and Ye, W.C. 2018. Techniques for extraction and isolation of natural products: a comprehensive review. *Chinese Medicine*, **13**(1): 1-26.

CHAPTER 3

3. Extraction and preliminary phytochemical analysis

3.1. Introduction

The first step in the separation of desired natural products from the raw materials is known as extraction. There are different methods for extraction. They include distillation, solvent extraction; pressing and sublimation method. Solvent extraction is the most employed method. The solvent penetrates the solid matrix, the solute dissolves in the solvents, the solute is diffused out of the solid matrix and then the extracted solutes are collected (Zhang *et al*., 2018). Extraction depends on extraction factors like the extracting solvent, temperature for extracting, extraction time and extraction pH. The solvent used for extraction is the most important factor. Different solvents have been used for the extraction of medicinal plants. The selection of solvents is based on the chemical nature and polarity of antioxidant compounds to be extracted (Xu *et al*., 2017).

Phytochemicals are a large group of chemical compounds naturally occurring in plants, they play roles such as colour production, flavour, aroma, and texture (Barbieri *et al*., 2017). They are known to play a major role in the adaptation of plants, but they are also a good source of pharmaceuticals. Using plants and their extracts for drug discovery and preparation establishes the best foundation for modern therapeutic sciences and leads human beings to develop a good medical system (Jain *et al*., 2019). The phytochemical screening of medicinal plants is the major process towards identifying new sources for therapeutic and industrial important compounds. It is also employed in pharmaceutical and nutraceutical products of commercial importance (Kumari *et al*., 2017).

Preliminary phytochemical analysis outlines the occurrence of bioactive compounds such as alkaloids, glycosides, flavonoids, tannins, steroids carbohydrates, phenolic compounds, proteins, and amino acids. Several important phytochemicals such as alkaloids, flavonoids, tannins, saponins, and glycosides are responsible for the defence system of plants (Rana *et al*., 2021). Qualitative phytochemical screening helps with the understanding of a variety of chemical compounds produced by plants and the quantification of metabolites helps during the extraction, purification, and identification of plants bioactive compounds (Santhi and Sengottuvel, 2016).

TLC is an adsorption chromatography where samples are separated based on the interaction between a thin layer of adsorbent attached to the plate (Koparde *et al*., 2017). TLC is a cost effective and widely used separation method in analysing phytochemicals and natural products (Bräm and Wolfram, 2017). An examination of the developed TLC plates takes place under a light source or sprayed with chemical reagents to visualise and obtain separation profiles of the analytes (Cheng *et al*., 2018). Tests for secondary metabolites include Wagner's reagent (alkaloids), Shinoda test (flavonoids), Fehling's test (glycosides), 10% of lead acetate (tannins and polyphenols), shaken for extraction (saponins), Liebermann Burchard (steols), and Salkowski's reaction for terpenoids (Hassan *et al*., 2018). The aim of this chapter was to determine the presence of different phytochemicals from different plant extracts using TLC and standard chemical methods and further determine the quantity using Folin-Ciocalteau and aluminium chloride calorimetric assay.

3.2. Method and materials

3.2.1. Collection of plant material and extraction

Leaves of *Rhoisissus tridentata Wild and Drum, Rosmarinus officinalis* L*., Ximenia caffra* sond*, Zanthoxylum capense* (Thunb) Hary*, and Ziziphus mucronata* Wild were collected during winter (June 2021) at the Lowveld National Botanical Garden in Mbombela (Mpumalanga Province, South Africa) and deposited at Larry Leach Herbarium (University of Limpopo) for voucher specimen. Plant leaves were air-dried at an ambient temperature and ground to fine powder, and then stored in the dark inside airtight containers. One gram (1 g) of each ground leaf material was extracted with 10 mL of different solvents with varying polarities, including n-Hexane, dichloromethane, acetone, methanol, and water in different 50 mL centrifuge tubes. The tubes were shaken for 10 minutes in a shaking incubator (series 25: New Brunswick Scientific Co. Inc) at 200 rpm. The plant extracts were then filtered into labelled different pre-weighed vials and the filtrates were evaporated under a fan at room temperature. The mass of plant extracts' yield were measured and recorded.

3.2.2. Phytochemical analysis

3.2.2.1. Qualitative phytochemical analysis

The phytochemical profile of each plant extract was analysed using aluminium-backed TLC that was developed in ethyl acetate: methanol: water [EMW] (polar), chloroform: ethyl acetate: formic acid [CEF] (intermediate polarity: acidic), benzene: ethanol: ammonia hydroxide [BEA] (nonpolar/basic) eluent systems following the methods described by Kotzé and Eloff (2002). The plant extracts were reconstituted to a concentration of 10 mg/mL with acetone. About 10 µL of each reconstituted extract was loaded on 1 cm of the TLC plate and developed in the three mobile phases listed above. After running, the plates were air-dried at room temperature to get rid of the excess solvents on the plates. Separated compounds were visualised under an ultraviolet light at 254 nm and 365 nm. The plates were then sprayed with vanillin-sulphuric acid reagent [0.1 g of vanillin (Sigma ®): 28 mL concentrated sulphuric acid] and heated at 110 °C for 1-5 minutes for colour development. This was done to visualise the separated different compounds.

3.2.3. Screening of major phytochemicals

3.2.3.1. Saponins

The method described by Odebiyi and Sofowora (1978) was used to test for the presence of saponins in each ground plant material. Methodically, 1 g of the powdered leaf material was weighed and blended with 30 mL of tap water. The mixture was shaken vigorously and heated at 100 °C to observe the development of froth to draw interference.

3.2.3.2. Terpenes

The Salkowski test described by Odebiyi and Sofowora (1978) was used to test for the presence of terpenes. Exactly 0.5 g of the powdered leaf material was mixed with 2 mL chloroform, and then 3 mL of concentrated sulphuric acid (H_2SO_4) was added to form a layer. The presence of terpenes was observed with a colour change to a reddish-brown to link interference.

3.2.3.3. Phlobatannin

The method described by Borokini and Omotayo (2012) was used to test for the presence of phlobatannins. About 0.5 g of the powdered leaf material was mixed with 10 mL of distilled water, filtered and then the filtrate was boiled with 2 mL of 1% hydrochloric acid (HCl) solution. The formation of a red coloured precipitate indicated the presence of phlobatannin.

3.2.3.4. Tannins

The presence of tannins on each powdered plant material was tested using the method described by Borokini and Omotayo (2012). Exactly 0.5 g of the plant was weighed, mixed with 5 mL of distilled water, boiled at 100 °C and cooled to 25 °C. From the mixture, 1 mL was transferred to a clean vial and 3 drops of 1% ferric chloride were added to the solution. To draw interference, the sample was observed for colour change (either blue-black, brown-green, blue-green, or green).

3.2.3.5. Cardiac glycosides

To test for the presence of cardiac glycosides, the Keller-Killiani test described by Odebiyi and Sofowora (1978) was used. A powdered leaf extract (0.5 g) was mixed with 2 mL of glacial acetic acid containing 1 drop of 0.1% ferric chloride solution. Afterwards, 1 mL of concentrated sulphuric acid (H_2SO_4) was added to the mixture and the presence of cardiac glycosides was observed with colour change and a brown ring at the top point where the chemical and the plant were interacting.

3.2.3.6. Flavonoids

The presence of flavonoids was tested by weighing 0.5 g of the powdered leaf material and mixing the plant material with 5 mL of ammonia. Then, 1 mL of concentrated sulphuric acid was added. The sample was observed for colour change to draw interference (Borokini and Omotayo, 2012).

3.2.3.7. Steroids

The presence of steroids was tested using the method described by Borokini and Omotayo (2012), where 2 mL of acetic anhydride was added to 0.5 g of the different

powdered leaf material. Thereafter, 2 mL of concentrated sulphuric acid (H_2SO_4) was added. The presence of steroids was observed with a green or blue colour change to draw interference.

3.2.3.8. Alkaloids

To test for the presence of alkaloids of each plant material, a Drangendoff's reagent was used. Exactly 0.5 g of the powdered plants was extracted with 95% ethanol using a shaking incubator (series 25: New Brunswick Scientific Co. Inc) at 200 rpm. It was then filtered using the Whatman no. 1 filter paper and a Buchner funnel. Filtrates were then evaporated until they were dry using a vacuum evaporator [Buchi rotavaporator: R-144 (Labotec)]. The extract was dissolved in 5 mL of 1% hydrochloric acid and five drops of Drangendoff's reagent were added. The presence of alkaloids was marked by a change of colour to reddish-brown to draw interference (Odebiyi and Sofowora, 1978).

3.2.4. Quantitative phytochemical analysis

3.2.4.1. Total phenolic content

The total amount of condensed phenolics in each plant extract was determined using the Folin-Ciocalteu method of using a spectrophotometer, as described by Velioglu *et al*. (1998), with minor modifications (Humadi and Istudor, 2008). The extracted plant material was reconstituted to 10 mg/mL with acetone and reduced to a concentration of 5 mg/mL in a test tube. A micropipette was used to transfer 100 µL of 5 mg/mL into a new test tube. Then, 900 µL of distilled water was added to the test tube and 100 µL of Folin-Ciocalteu reagent was added. Standard solutions were prepared using gallic acid with different concentrations (1.25, 0.625, 0.313, 0.156, 0.078 mg/mL). The blank was prepared the same way without the addition of the extract; the plant extract was replaced with acetone. Thereafter, the reactions were stopped with the addition of 1 mL of 7% sodium carbonate solution and incubated in the dark at room temperature for 30 minutes. After incubating, the absorbance readings of the tests and standard solutions were determined using the ultraviolet or visible (UV/VIS) spectrophotometer (Thermo Scientific) against the blank at 550 nm. The total phenolic content was expressed as the milligram gallic acid equivalence/ gram of extract (mg of GAE/g extract), which was calculated using the standard formula obtained from the Gallic acid

standard curve ($y = 2.7011x + 0.0216$, $R^2 = 0.9984$). The experiment was performed in triplicates (Tambe and Bhambar, 2014).

3.2.4.2. Total tannin content

The total amount of condensed tannins in each plant extract was determined using the Folin-Ciocalteu method. Exactly 50 µL of 10 mg/mL plant extract was added into a volumetric flask containing 3.8 mL of distilled water. The Folin-Ciocalteu reagent (250 µL) was added, and the mixture was vortexed. Afterwards, 0.5 mL of 35% sodium carbonate (Na_2CO_3) solution was added to the mixture. The volume of the mixture was made to 10 mL through the addition of distilled water. The blank was prepared in the same way without adding an extract. Gallic acid (Sigma-Aldrich) was used to prepare standard solutions (1.000, 0.500, 0.250, 0.125, 0.0625 mg/mL), which were also prepared in the same way. All the samples were incubated in the dark at room temperature for 30 minutes. After incubation, the absorbance of the tests and standard solutions were measured against the blank at 725 nm. The total tannin content was expressed mg GAE/g extract, which was calculated using the formula obtained from the standard curve ($y = 1.4763x + 0.0026$, $R^2 = 0.9967$). The experiment was performed in triplicates (Tambe and Bhambar, 2014).

3.2.4.3. Total flavonoid content

The total flavonoid content of the selected plant materials was determined through the aluminium chloride colorimetric assay. Strictly, 100 µL of 10 mg/mL plant extract was added to 4.9 mL of distilled water in a test tube. Then, 300 µL of 5% sodium nitrite ($NaNO_2$) (dissolved in distilled water) was added to the mixture and incubated for five minutes at room temperature. After incubation, 300 µL of 10% aluminium chloride ($ALCl_3$) (dissolved in distilled water) was added to each reaction mixture and incubated at room temperature for 5 minutes. This was followed by the addition of 2 mL of 1 M sodium hydroxide (NaOH) in each tube. The different reaction mixtures were transferred to different volumetric flasks and made the volume of each flask up to 10 mL using distilled water. The preparation of standard solutions was done using Quercetin (Sigma-Aldrich). Several different concentrations (0.5, 0.25, 0.125, 0.0625, 0.0313 mg/mL) of quercetin were prepared in the same way as the extracts. The blank was also prepared in the same manner, but the extract was replaced with 100 µL of

distilled water and absorbance readings of the samples were measured at 510 nm using the UV/VIS spectrophotometer (Thermo scientific) against the blank. The total flavonoid content was expressed in milligram quercetin equivalence/gram of extract (mg QE/g extract) using the formula obtained from the standard curve ($y = 0.6371x + 0.0049, R^2 = 0.9972$). The experiment was performed in triplicates (Tambe and Bhambar, 2014).

3.3. Results

3.3.1. Preliminary extraction

Powdered leaf material (1 g) of *Zanthoxylum capense, Rhoicissus tridentata, Rosmarinus officinalis, Ximenia caffra* and *Ziziphus mucronata* were extracted with 10 mL of different solvents (hexane, dichloromethane, acetone, methanol, and water). Methanol was the best extractant for *Z. capense* (136 mg), *Z. mucronata* (136 mg), and *R. tridentata* (240 mg) (Figure 3.1). The best extractant for *R. officinalis* (140 mg) and *X. caffra* (220 mg) was water.

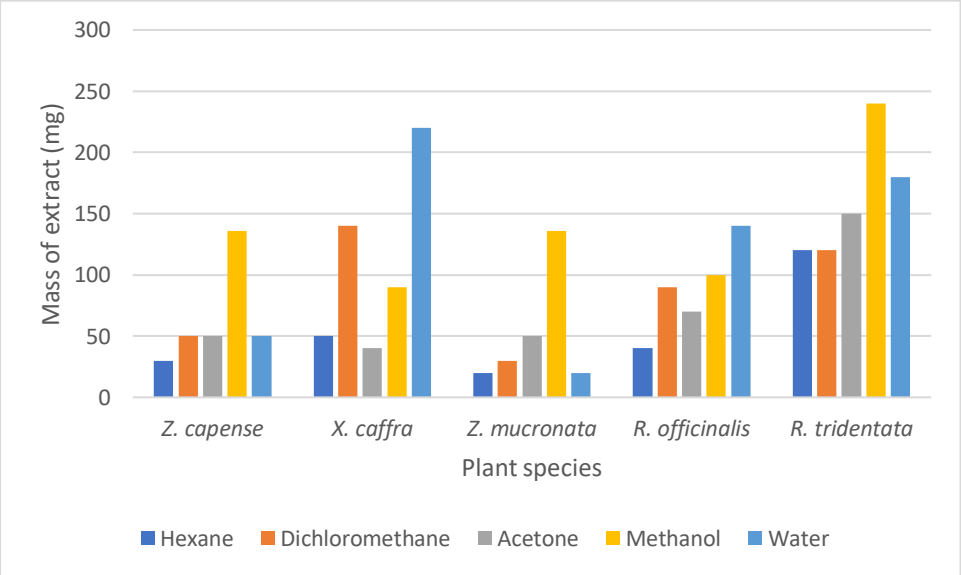

Figure 3. 1: The mass of *Z. capense*, *R. tridentata*, *R. officinalis*, *X. caffra* and *Z. mucronata* extracted from 1 g of powdered leaf materials with 10 mL of different solvents (n-hexane, dichloromethane, acetone, methanol, and water).

3.3.2. Phytochemical analysis

An analysis of phytochemicals in different extracts was carried out using TLC where the plant extracts of *Z. capense, R. tridentata, R. officinalis, X. caffra* and *Z. mucronata* extracted with n-hexane, dichloromethane, acetone, methanol, and water were loaded

on TLC plates and further developed in three mobile systems (EMW, CEF and BEA). The TLC plates separated the chemical constituents to create the phytochemical fingerprints of different extracts. The plates were visualised under an ultraviolet light at 254 nm (Figure 3.2) and 365 nm (Figure 3.3). Figure 3.2 shows that more bands were observed in a plate developed in EMW, while Figure 3.3 shows the different colours observed on the TLC plates, which represent the different chemical compounds present within the plant material. More compounds were observed in a plate developed in BEA. Non-fluorescing compounds or invisible bands of the different extracts were detected by spraying the TLC plates with vanillin-sulphuric acid reagent. Figure 3.4 shows that more bands were observed on a TLC plate developed in BEA, followed by the plate from CEF and plate from EMW had less bands. *R. officinalis* had more visualised bands as compared to all plants in BEA and had the least lands in EMW. In CEF, *R. tridentata* had less bands as compared to all plant species.

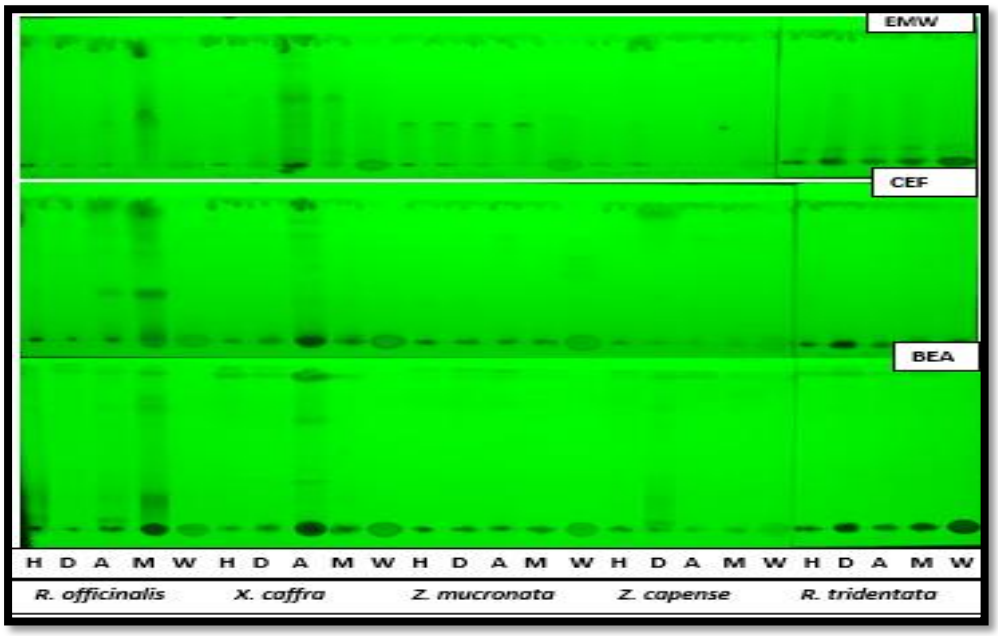

Figure 3. 2: Chromatograms attained after running TLC plates loaded with different plant extracts in three different mobile phases (EMW, CEF, and BEA) and visualised under an ultraviolet light at 254 nm. The visualised compounds in which the plants were extracted with n-hexane (H), dichloromethane (D), acetone (A), methanol (M), and water (W).

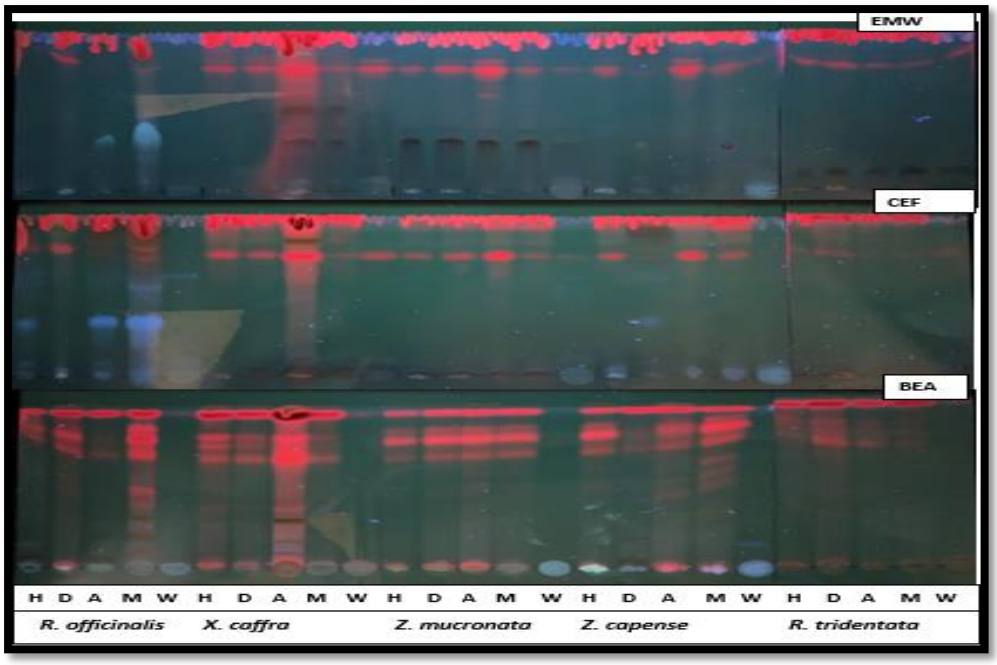

Figure 3. 3: Chromatograms attained after running TLC plates loaded with different plant extracts in three different mobile phases (EMW, CEF, and BEA) and visualised under an ultraviolet light at 365 nm. The visualised compounds in which the plants were extracted with n-hexane (H), dichloromethane (D), acetone (A), methanol (M), and water (W).

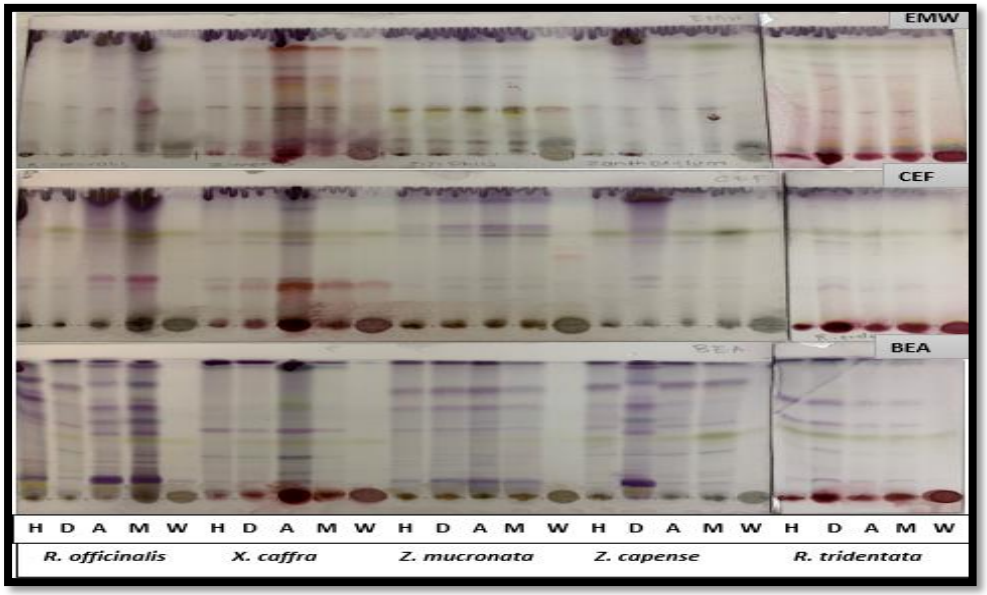

Figure 3. 4: Chromatograms attained after running TLC plates loaded with different plant extracts in three different mobile phases (EMW, CEF, and BEA) and sprayed with vanillin-sulphuric acid. The visualised compounds in which the plants were

extracted with n-hexane (H), dichloromethane (D), acetone (A), methanol (M), and water (W).

3.3.3. Screening of major phytochemicals

The screening of phytochemicals revealed that all plants species had terpenes, cardiac glycosides, and flavonoids, and lacked alkaloids. *Z. mucronate, R. officinalis* and *R. tridentata* had the highest variety of phyto-constituents compared to *X. caffra* and *Z. capense* which had the least variety (Table 3.1).

Table 3. 1: Phytoconstituents of *Z. capense*, *R. tridentata*, *R. officinalis*, *X. caffra* and *Z. mucronata* leaf extracts.

Phyto-constituents	Plant species				
	Ximenia caffra	*Zanthoxylum capense*	*Ziziphus mucronata*	*Rosmarinus officinalis*	*Rhoicissus tridentata*
Saponins	-	+	+	+	+
Terpenes	+	+	+	+	+
Phlobatannin	-	+	+	-	-
Tannin	+	-	+	+	+
Cardiac glycosides	+	+	+	+	+
Flavonoids	+	+	+	+	+
Steroids	+	-	-	+	+
Alkaloids	-	-	-	-	-

Key: += present, - = absent

3.3.4. Standard curves used for quantification of phyto-constituents

The total concentrated amount of phenolics, flavonoids and tannins present in the plant extracts was determined using three standard curves. The total phenolic content was determined using the gallic acid standard curve (Figure 3.5), $y = 2.7011x + 0.0216$, total tannin content was determined using the gallic acid standard curve (Figure 3.6), $y = 1.4763x + 0.0026$ and the total flavonoid content was determined using the quercetin standard curve (Figure 3.7) with the equation $y = 0.6371x + 0.0049$. The straight lines of the standard curves indicate a positive relationship between the average absorbance values and the concentration of phytochemicals.

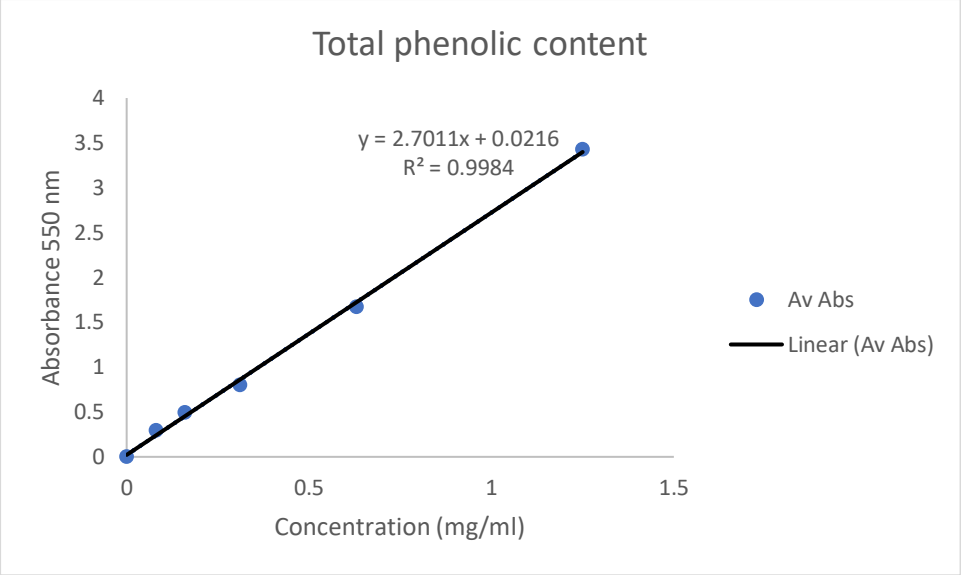

Figure 3. 5: Gallic acid standard curve for the determination of total phenolic content.

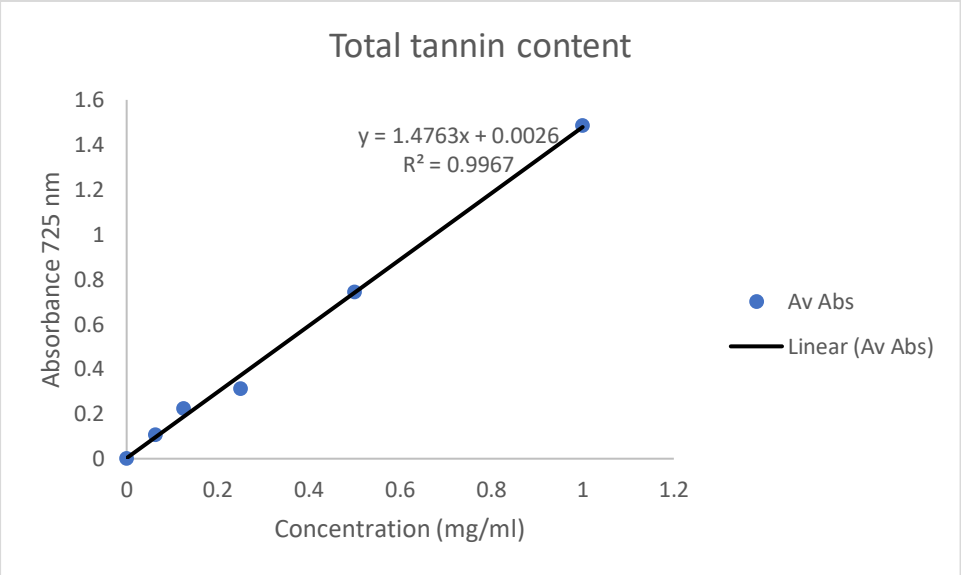

Figure 3. 6: Gallic acid standard curve for the determination of total tannin content.

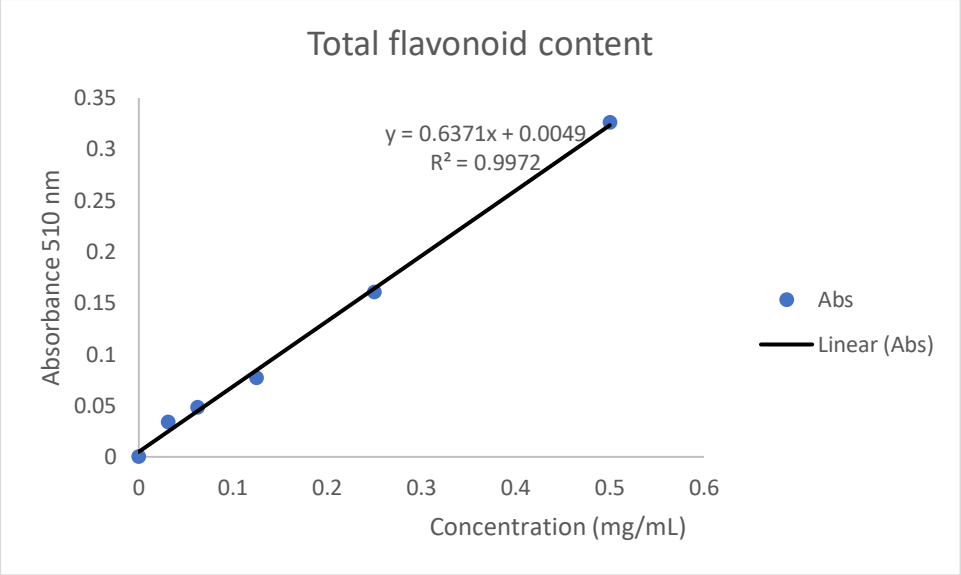

Figure 3. 7: The quercetin standard curve used for the determination of total flavonoid content.

3.3.5. Total quantified tannins, flavonoids, and phenols of different plant extracts

Major phytochemicals were quantified using the three above standard curves and the results are represented as the mean of triplicates ± standard deviation. *R. tridentata* had the highest total phenolic (335.20 ± 8.26 mg GAE/g of extract) and tannin (103.48 ± 7.36 mg GAE/g of extract) content from the water extracts while the highest total flavonoid content was found in *R. officinalis* (45.90 ± 11.04 mg QE/g of extract) from the methanol extract (Table 3.2).

Table 3. 2: Total phenolic, tannin and flavonoid content of *Z. capense*, *R. tridentata*, *R. officinalis*, *X. caffra* and *Z. mucronata* extracts. Data was analysed and recorded as mean ± standard deviation.

Solvents	Total phenolic (mg GAE/g extract)	Total tannin (mg GAE/ g extract)	Total flavonoid (mg QE/g extract)
	Zanthoxylum capense		
n-Hexane	5.19 ± 1.57	5.06 ± 0.81	2.68 ± 0.57
Dichloromethane	20.98 ± 3.72	9.15 ± 1.51	34.60 ± 2.18
Acetone	27.80 ± 2.97	2.69 ± 1.41	17.07 ± 10.41

Methanol	12.74 ± 0.67	0.77 ± 0.18	6.45 ± 1.10
Water	14.54 ± 1.58	13.51 ± 0.34	-4.69 ± 0.57
	Rhoicissus tridentata		
n-Hexane	256.42 ± 15.18	31.66 ± 1.22	8.02 ± 1.40
Dichloromethane	139.80 ± 15.59	23.49 ± 4.26	20.00 ± 2.12
Acetone	139.26 ± 17.07	26.90 ± 2.91	0.64 ± 0.16
Methanol	236.28 ± 20.57	52.52 ± 8.67	6.40 ± 1.00
Water	335.20 ± 8.26	103.48 ± 7.36	6.40 ± 3.44
	Ziziphus mucronata		
n-Hexane	36.34 ± 6.92	9.96 ± 1.22	2.16 ± 1.27
Dichloromethane	66.57 ± 4.96	13.71 ± 2.37	23.82 ± 1.41
Acetone	37.15 ± 2.96	10.07 ± 0.22	9.59 ± 1.81
Methanol	63.58 ± 8.22	6.10 ± 0.45	4.99 ± 0.50
Water	84.76 ± 7.68	7.77 ± 3.72	6.89 ± 0.42
	Rosmarinus officinalis		
n-Hexane	180.80 ± 11.91	50.06 ± 6.99	35.33 ± 0.42
Dichloromethane	126.67 ± 2.26	20.05 ± 6.37	20.68 ± 4.99
Acetone	149.43 ± 3.19	34.37 ± 10.10	35.91 ± 4.18
Methanol	177.71 ± 30.34	22.83 ± 12.50	45.90 ± 11.04
Water	32.71 ± 1.14	10.10 ± 1.51	4.69 ± 0.27
	Ximenia caffra		
n-Hexane	133.78 ± 7.89	9.53 ± 0.58	19.90 ± 2.36
Dichloromethane	147.01 ± 13.94	3.53 ± 0.41	7.45 ± 2.22
Acetone	163.27 ± 9.69	10.17 ± 1.66	35.28 ± 4.40
Methanol	229.76 ± 27.82	11.50 ± 1.74	37.16 ± 3.77
Water	225.62 ± 4.01	41.48 ± 6.85	28.79 ± 3.87

Key: GAE = gallic acid equivalence, QE = quercetin equivalence

3.4. Discussion

Harvesting of leaves is generally reflected as less of a threat compared to that of the bark and roots. Using the bark and roots results in the damage of medical plants and the roots as well as threats of their sustainability (Mengesha, 2016). Plant leaves were

collected and immediately dried under room temperature. This is supported by Lakshmi *et al*. (2019) who reported that herbs require immediate drying after being collected from the farm to avoid microbial activity and to keep their original constituents. After drying, they were ground into fine powder and stored in bottles in the dark before being extracted because some traditional healers considered medicines prepared with plant powders (obtained by drying and milling with a mortar) to be more efficient, as the powder form allows the enhanced extraction of bioactive compounds (Tchicaillat-Landou *et al*., 2018). The extraction was done with five different solvents of varying polarities from non-polar to polar solvents (n-Hexane, dichloromethane, acetone, methanol, and water) to increase the extraction conditions. This was done because varying solvents have a prominent effect on the accuracy of the quantification of antioxidant content. Furthermore, the interaction between bioactive compounds and the solvents depend on their chemical structures and polarities (Thavamoney *et al*., 2018). Results in Figure 3.1 show that methanol extracted the highest plant material in *Z. capense*, *Z. mucronata*, and *R. tridentata*, while water extracted the highest plant material in *R. officinalis* and *X. caffra*.

The extracts were reconstituted with acetone because as reported by Mogashoa *et al*. (2019), acetone has a good volatility, miscibility with polar and non-polar solvents and is relatively low toxic to the test organisms. Qualitative phytochemical analysis was carried out using TLC, where the plates were developed in three different mobile phases EMW (polar), CEF (intermediate) and BEA (non-polar) because West and Lesellier (2008) state that there are a few clear guidelines for the choice of a stationary phase for a particular analyte; as such, more than one phase needs to be examined to obtain the chemistry of compounds within extracts. TLC separates compounds based on size and small compounds travel faster. More fluorescing compounds from the 254 nm (Figure 3.2) were detected in EMW and CEF plates while on the 365 nm plates (Figure 3.3), there were more fluorescing compounds in BEA. This is because UV-Vis spectrophotometry measures the amount of a chemical substance based on the intensity of light absorbed when a beam of light passes through the sample solution (Sulaiman, 2021). The plates were further sprayed with vanillin sulphuric acid and heated at 110 °C until colour development. This helped to visualise separated compounds (Masoko *et al*., 2008). The different colours observed on Figure 3.4 represent separated compounds and their polarities. The highest number of bands

were observed on a TLC plate developed in BEA (no-polar mobile system), which means that the plant extracts had more non-polar compounds. Several compounds were observed on the plate developed in CEF (the intermediate mobile system) and less compounds from the polar mobile system (EMW).

Even though TLC fingerprints assisted with the phytochemical profile of the compounds, it was not enough to specify the types of the phytochemicals present. The screening of major phytochemicals on Table 3.1 revealed that all plants had terpenes, cardiac glycosides, and flavonoids; however, they all lacked alkaloids. Phytochemicals play a huge role in the survival or ecological interactions of plants with competitors, protect them from diseases, pollution, stress, UV rays and contribute to the colour, aroma, and flavour of the plant (Shaikh, 2020). *Z. mucronata*, *R. officinalis* and *R. tridentata* showed to have the highest number of major phytochemicals compared to *X. caffra* and *Z. capense*. *Z. capense* is the only plant species that lacked tannins. Variation in medicinal plants is affected primarily by the cultivation period (Alqethami and Aldhebiani, 2021), temperature, relative humidity, amount of light absorbed by the plant, water content, minerals, and CO_2 concentration in the air, all of which influence the growth of a plant and the production of medicinal metabolites (Sma, 2016). Andrade *et al.* (2018) reported on the phenolics and terpenes found in *R. officinalis*. Alkaloids were absent in all plants, but Manyarara *et al*., (2016), and Nemudzivhadi and Masoko (2015) reported that *Z. mucronata* has alkaloids and that this may be due to seasonal variation because for this research, the plant was collected in winter while they collected in summer. Mukundi *et al*. (2015) also reported that *R. tridentata* has alkaloids, but lacks cardiac glycosides and this may be because the plant was collected in a different country (Kenya).

The quantitative phytochemical analysis was carried out using standard methods because it accounts for the quantity or the concentration of the phytochemicals present in the plant sample (Egbuna *et al*., 2018). Standard curves were used to determine the total phenolic (Figure 3.5), tannin (Figure 3.6), and flavonoid (Figure 3.7) content. For *Z. capense*, the highest total phenolic content was found from the acetone extract and the highest flavonoid content was from the dichloromethane extract. Table 3.2 shows that *R. tridentata* had the highest phenolic and tannin content quantified from the water extract while flavonoid content from the dichloromethane extract. Highest phenolic content was found in the water extract whereas high flavonoid content was

found in the dichloromethane extract for *Z. mucronate*. *R. officinalis* had its highest phenolic and tannin content from the n-hexane extract while its highest flavonoid content was found in the methanol extract. *X. caffra* had both its highest phenolic and flavonoid content from the methanol extract. Overall, *R. tridentata* had the highest total phenolic (335.20 ± 8.26 mg GAE/g of extract) and tannin (103.48 ± 7.36 mg GAE/g of extract) content from the water extracts while the highest total flavonoid content was found in *R. officinalis* (45.90 ± 11.04 mg QE/g of extract) from the methanol extract. This is supported by Mukundi *et al.* (2015) who reported that *R. tridentata* has the highest quantified phenols, alkaloids and saponins and has lower flavonoid content. Phytoconstituents such as alkaloids, phenols, flavonoids, terpenoid, saponins, and carbohydrates have an important role in acting as sources of drugs and improve consumers' health status; thus, they are a vital role for good health (Santhi and Sengottuvel, 2016).

3.5. Conclusion

From the obtained results, extraction was a success. Extracts from the selected medicinal plants have secondary metabolites, and contain different phytoconstituents. The presence of several phytoconstituents is a potential since they act as the main sources of useful drugs, and improve health status. The diversity of phytoconstituents within different plant extracts is a springboard to an investigation of the antioxidant and antimycobacterial activity of the plant extracts.

3.6. References

Alqethami, A. and Aldhebiani, A.Y. 2021. Medicinal plants used in Jeddah, Saudi Arabia: phytochemical screening. *Saudi Journal of Biological Sciences*, **28**(1): 805-812.

Andrade, J.M., Faustino, C., Garcia, C., Ladeiras, D., Reis, C.P. and Rijo, P. 2018. *Rosmarinus officinalis* L.: an update review of its phytochemistry and biological activity. *Future Science OA*, **4**(4): 283.

Balouiri, M., Sadiki, M. and Ibnsouda, S.K. 2016. Methods for *in vitro* evaluating antimicrobial activity: a review. *Journal of Pharmaceutical Analysis*, **6**(2): 71-79.

Barbieri, R., Coppo, E., Marchese, A., Daglia, M., Sobarzo-Sánchez, E., Nabavi, S.F. and Nabavi, S.M. 2017. Phytochemicals for human disease: an update on plant-derived compounds antibacterial activity. *Microbiological Research*, **196**: 44-68.

Bräm, S. and Wolfram, E. 2017. Recent advances in effect-directed enzyme assays based on thin-layer chromatography. *Phytochemical Analysis*, **28**(2): 74-86.

Borokini, T.I. and Omtayo, T.O. 2012. Phytochemical and ethnobotanical study of some selected medicinal plants from Nigeria. *Journal of Medicinal Plants Research*, **6**(7): 1106-1118.

Cheng, S.C., Bhat, S.M., Lee, C.W. and Shiea, J. 2018. Thin layer chromatography combined with electrospray ionization mass spectrometry for characterizing herbal compounds. *International Journal of Mass Spectrometry*, **434**: 264-271.

Egbuna, C., Ifemeje, J.C., Maduako, M.C., Tijjani, H., Udedi, S.C., Nwaka, A.C. and Ifemeje, M.O. 2018. Phytochemical test methods: qualitative, quantitative, and proximate analysis. *Phytochemistry*: 381-426.

Hassan, B.A., Hamed, F.M. and Alyaseen, F.F. 2018. Phytochemical screened, characterization and antibacterial activity of hesperetin and hesperidin extracted and isolated from dried oranges peels. *International Journal of Research in Pharmaceutical Sciences*, **9**(4):1362-1367.

Humadi, S.S. and Istudor, V. 2008. Quantitative analysis of bioactive compound *Hibiscus sabadariffa* L. extracts note 1: quantitative analysis of flavonoids. *Farmácia*, **6**: 699-707.

Jain, C., Khatana, S. and Vijayvergia, R. 2019. Bioactivity of secondary metabolites of various plants: a review. *International Journal of Pharmaceutical Sciences and Research*, **10**(2): 494-498.

Koparde, A.A., Magdum, C.S. and Doijad, R.C. 2017. Phyto active compounds from herbal plant extracts: its extraction, isolation, and characterization. *World Journal of Pharmaceutical Research*, **6**(8): 1186-1205.

Kotze, M. and Eloff, J.N. 2002. Extraction of antibacterial compounds from *Combretum microphylum* (Combretaceae). *South African Journal of Botany*, **68**: 62-67.

Kumari, P., Kumari, C. and Singh, P.S. 2017. Phytochemical screening of selected medicinal plants for secondary metabolites. *International Journal of Life Sciences Scientific Research*, **3**(4): 1151-1157.

Lakshmi, D.V.N., Muthukumar, P., Layek, A. and Nayak, P.K. 2019. Performance analyses of mixed mode forced convection solar dryer for drying of stevia leaves. *Solar Energy*, **188**: 507-518.

Manyarara, T.E., Chifamba, J. and Tarugarira, F.T. 2016. Antifungal activity of *ziziphus mucronata* and *Erythrina abyssinica* bark crude extracts on *Cryptococcus neofomans* and *Candida albicans* species. *British Journal of Pharmaceutical Research*, **10**(3): 1-11.

Masoko, P., Mmushi, T.J., Mogashoa, M.M., Mokgotho, M.P., Mampuru, L.J. and Howard, R.L. 2008. *In vitro* evaluation of the antifungal activity of *Sclerocarya birrea* extracts against pathogenic yeasts. *African Journal of Biotechnology*, **7**(20).

Mengesha, G.G. 2016. Ethnobotanical survey of medicinal plants used in treating human and livestock health problems in *Mandura Woreda* of Benishangul Gumuz, Ethiopia. *Advancement in Medical Plant Research*, **4**(1): 11-26.

Mogashoa, M.M., Masoko, P. and Eloff, J.N. 2019. Different *Combretum molle* (Combretaceae) leaf extracts contain several different antifungal and antibacterial compounds. *South African Journal of Botany*, **126**: 322-327.

Mukundi, M.J., Mwaniki, N.E., Ngugi, M.P., Njagi, J.M., Agyirifo, S.D., Gathumbi, K.P. and Muchugi, N.A. 2015. *In vivo* anti-diabetic effects of aqueous leaf extracts of *Rhoicissus tridentata* in alloxan induced diabetic mice. *Journal of Developing Drugs*, **4**(3): 1-5.

Nemudzivhadi, V. and Masoko, P. 2015. Antioxidant and antibacterial properties of *Ziziphus mucronata* and *Ricinus communis* leaves extracts. *African Journal of Traditional, Complementary and Alternative Medicines*, **12**(1): 81-89.

Odebiyi, O.O. and Sofowora, E.A. 1978. Phytochemical screening of Nigerian medicinal plants, part iii. *Lloydia Journal*, **41**: 234-246.

Rana, A., Negi, P.B. and Sahoo, N.G. 2021. Phytochemical screening and characterization of bioactive compounds from *Juniperus squamata* root extract. *Materials Today: Proceedings*, **48**(3): 672-675.

Santhi, K. and Sengottuvel, R. 2016. Qualitative and quantitative phytochemical analysis of *Moringa concanensis* Nimmo. *International Journal of Current Microbiology and Applied Sciences*, **5**(1): 633-640.

Shaikh, J.R. and Patil, M.K. 2020. Qualitative tests for preliminary phytochemical screening: an overview. *International Journal of Chemical Studies*, **8**(2): 603-608.

Sma, Z. 2016. Medicinal components. *Plant Factory*:187-192.

Sulaiman, R. 2021. *Isolation and characterisation of secondary metabolites with antiplasmodial activity in selected medicinal plants obtained from Niger State*. (Doctoral dissertation, Federal University of Technology, Minna).

Tambe, V.D. and Bhambar, R.S. 2014. Estimation of total phenol, tannin, alkaloid, and flavonoid in *Hibiscus Tiliaceus* Linn. wood extracts. Research and reviews. *Journal of Pharmacognosy and Phytotherapy*, **2**(4): 2321-6182.

Tchicaillat-Landou, M., Petit, J., Gaiani, C., Miabangana, E.S., Kimbonguila, A., Nzikou, J.M., Scher, J. and Matos, L. 2018. Ethnobotanical study of medicinal plants

used by traditional healers for the treatment of oxidative stress-related diseases in the Congo Basin. *Journal of Herbal Medicine*, **13**: 76-90.

Thavamoney, N., Sivanadian, L., Tee, L.H., Khoo, H.E., Prasad, K.N. and Kong, K.W. 2018. Extraction and recovery of phytochemical components and antioxidative properties in fruit parts of *Dacryodes rostrata* influenced by different solvents. *Journal of Food Science and Technology*, **55**(7): 2523-2532.

Velioglu, Y.S., Mazza, G., Gao, L. and Oomah, B.D. 1998. Antioxidant activity and total phenolics in selected fruits, vegetables, and grain products. *Journal of Agricultural and Food Chemistry*, **46**(10): 113-4117.

West, C. and Lesellier, E. 2008. A unified classification of stationary phases for packed column supercritical fluid chromatography. *Journal of Chromatography A*, ***1191***(1-2): 21-39.

Xu, D.P., Li, Y., Meng, X., Zhou, T., Zhou, Y., Zheng, J., Zhang, J.J. and Li, H.B. 2017. Natural antioxidants in foods and medicinal plants: extraction, assessment, and resources. *International Journal of Molecular Sciences*, **18**(1): 96.

Zhang, Q.W., Lin, L.G. and Ye, W.C. 2018. Techniques for extraction and isolation of natural products: a comprehensive review. *Chinese Medicine*, **13**(1): 1-26.

CHAPTER 4

4. Antioxidant activity

4.1. Introduction

Normally, the human body has an antioxidant system that scavenges free radicals, which provides balance between anti-oxidation and oxidation. Being exposed to smoking of cigarettes, radiation, alcohol, or environmental toxins, promotes the production of excess reactive oxygen and nitrogen species. The production of excess reactive oxygen and nitrogen species disrupts the balance between oxidation and anti-oxidation (Santos-Sánchez *et al*., 2019; Xu *et al*., 2017; Apak *et al*., 2016). Reactive oxygen species (ROS) and free radicals are unstable molecules produced in biological systems during cellular metabolism. A high number of free radicals causes oxidative stress, which causes human diseases like cancer, arthritis, diabetes, rheumatoid arthritis, atherosclerosis, hypertension, and chronic inflammatory disorders (Elisha *et al*., 2016; Saha and Verma, 2016).

Antioxidants from both synthetic and natural sources are highly effective in controlling the production of free radicals to prevent its undesirable effects and supporting the mechanisms of antioxidants (Martins *et al*., 2016). There are two types of antioxidants used in medicine and industries, which are synthetic and natural antioxidants. Synthetic antioxidants have harmful side effects on the human body, as such, more attention is given to natural antioxidant compounds found in plants (Olszowy, 2019).

Medicinal herbs are used as an alternative to chemical drugs and the main reason is their low level of side effects compared to chemical drugs, and their antioxidant contribution decreases drug toxicity (Kooti and Daraei, 2017). Bioactive compounds have gained interest in scientific research as they are extracted from natural sources and applied to cure diseases, improve health and increase the value of nutraceuticals and cosmetics (Mosca *et al*., 2018). Phenolic compounds within plants are the most important antioxidant compounds (Salehi *et al.*, 2020; Nirmala *et al*., 2018). However, antioxidant activity is unique for different varieties and morphological parts of natural resources. Adding to that, the antioxidant activity of natural products depends on factors such as soil conditions, climate, or harvest time (Flieger *et al*., 2021).

Inflammation is defined as the process involved with pathogeny and the progression of diseases (Ribeiro *et al*., 2018). Inflammation takes place due to the damage of living tissues by microorganisms such as bacteria. The inflammatory response helps with locating and eliminating harmful agents and to remove damaged tissues so that the healing of damaged organs, system or tissue can take place (Oguntibeju, 2018). Since TB damages the tissues of the host and leads to necrosis and the spread of the disease (Kroesen *et al*., 2017), inflammation reaction takes place through the activation of natural killer cells and macrophages (Aziz *et al*., 2018). An excessively intense inflammatory response can lead to death, tissue damage and organ failure (Marques *et al*., 2019).

Plants and their corresponding botanical preparations have been used for centuries due to their remarkable potential in both the treatment and prevention of oxidative stress-related disorders. They are good sources of exogenous antioxidants, they protect against oxidative stress, which in turn helps in maintaining the balance between oxidants and antioxidants levels (Salehi *et al*., 2020). Three assays used to test for the presence of antioxidants are 2,2-diphenyl-1-picrylhydrazyl radical (DPPH), 2,2′-azino-bis-3-ethylbenzthiazoline-6-sulphonic acid (ABTS), and Ferric Reduction Antioxidant Potential (FRAP) assay (Zhou *et al*., 2019). The aim of this chapter was to determine antioxidant activity using DPPH free radical scavenging assay and ferric reducing antioxidant power assay.

4.2. Method and materials

4.2.1. Qualitative antioxidant activity on TLC plates

The qualitative antioxidant activity of the plant extracts was determined using 2,2-diphenyl-1-picrylhydrazyl radical (DPPH) (Sigma-Aldrich) free radical scavenging assay. From the reconstituted plant extract (10 mg/mL), 10 µL of each extract was loaded in a 1 cm wide line of different TLC plates, which were developed in EMW, CEF, and BEA mobile systems. The plates were air-dried at room temperature to fade excess solvents. After a few minutes (5 to 10 minutes), they were sprayed with 0.2% of DPPH (dissolved in methanol) and colour change was observed (DPPH is purple in colour, but colour change depicts that it is reduced to diphenyl-1-picryl hydrazine, which is yellow) (Braca *et al*., 2002).

4.2.2. Quantitative antioxidant activity assays

4.2.2.1. DPPH free radical scavenging activity assay

The method described by Gyamfi *et al*. (1999) of using 2,2-diphenyl-1-picrylhydrazyl (DPPH) (Sigma-Aldrich) was used to quantify and determine the free radical scavenging activity of the different plant extracts with slight modifications (Chigayo *et al*., 2016). Different concentrations (250-15.63 µg/mL) of plant extracts were prepared up to a volume of 1 mL solutions. The same concentrations used for plant extracts were used to prepare the standard using L-ascorbic acid. To the 1 mL solutions, 2 mL of 0.2 mmol/L of DPPH solution prepared in methanol was added and vortexed thoroughly. Prepared mixtures were then incubated in the dark for 30 minutes. The blank solution was prepared by adding 2 mL of methanol and 1 mL of acetone. The control solution was prepared by adding 2 mL of 0.2 mmol/L DPPH solution to 1 mL of distilled water. After incubation, the solutions were analysed by determining their absorbance readings using the UV/VIS spectrophotometer (Thermo Scientific) at 517 nm and the percentage inhibition was determined using the formula below, where Ac is the absorbance of the control solution whereas As is the absorbance of the plant extract. The experiment was performed in triplicates.

$$\%\ inhibition = \frac{Ac - As}{Ac} \times 100$$

4.2.2.2. Ferric reducing antioxidant power (FRAP) assay

The ferric reducing antioxidant power of different plant extracts was determined using the methods described by Vijayalakshmi and Ruckmani (2016). Different concentrations (625-39 µg/mL) of the plant extracts were prepared by serially diluting a prepared stock solution of 1250 µg/mL. About 2.5 mL of the different concentrations were mixed with 2.5 mL of sodium phosphate buffer (0.2 M, pH 6.6) and 2.5 mL of potassium ferricyanide (1% W/V in distilled water) in a test tube. Then, the mixtures were vortexed thoroughly and incubated for 20 minutes at 50 °C. This was followed by the addition of 2 mL trichloroacetic acid (10% W/V in distilled water) after incubation. The mixtures were then centrifuged for 10 minutes at 3000 rpm and 5 mL of the resulting supernatant was transferred to a new clean test tube. To the 5 mL supernatant, 5 mL of distilled water and 1 mL of ferric chloride (0.1% W/V in distilled

water) were added, and the mixture was vortexed. The mixtures were analysed and their absorbance was read using a UV/VIS spectrophotometer at 700 nm. The blank solution was prepared in the same manner except that the plant extracts were replaced with acetone. Different concentrations (6252-39 µg/mL) of L-ascorbic acid were prepared which was used as the positive control and it was prepared in the same manner as the plant extracts. The experiment was performed in triplicates.

4.2.3. The egg albumin denaturation inhibition assay

The plant acetone extracts were reconstituted to 2 mg/mL using 50% DMSO. The 1.25 mL reaction mixture consisted of 50 µL of egg albumin (from fresh hen's egg), 700 µL of 0.2 M sodium phosphate buffer (pH 6.6) and 500 µL plant extracts (2 mg/mL) and aspirin as the standard drug (2 mg/mL). The negative control of the product solution consisted of 500 µL of the plant extract and 750 µL of the 0.2 M sodium phosphate buffer. This was done to consider the colour of the extracts when using the UV/Vis spectrophotometer. An egg albumin solution (50 µL and 1200 µL of the 0.2 M sodium phosphate buffer) was used as the positive control of the test solution. The positive control represented 100% protein denaturation. The mixtures were incubated at 37 °C in a water bath for 15 minutes and then heated at 70 °C for 5 minutes. After heating, the solutions were allowed to cool at room temperature for 30 minutes. After cooling, their absorbance was measured at 660 nm using the sodium phosphate buffer as a blank (Rahman *et al*., 2015; Uttra and Alamgeer, 2017). The percentage inhibition of protein denaturation was calculated by using the following formula:

$$\%\ Anti\ denaturation\ activity = \frac{(Absorbance\ of\ control - Absorbance\ of\ test\ sample)}{Absorbance\ of\ control} \times 100$$

$$* \text{Absorbance of test sample} = \text{absorbance of test solution} - \text{absorbance of negative}$$

The results were analysed using two-way ANOVA, which was followed by the Tukey multiple comparison post hoc test. The significant difference was considered when $p < 0.05$ and conversely, and non-significant was indicated when $p > 0.05$ values.

4.3. Results

4.3.1. Qualitative antioxidant assay on TLC plates

The qualitative antioxidant activity of the plant extracts was screened using TLC plates developed in different mobile systems, which were then sprayed with 2,2-diphenyl-1-picrylhydrazyl (DPPH) reagent. The TLC plate turns purple in colour when sprayed with DPPH and the presence of antioxidant compounds were detected with yellow bands resulting from the reduction of the purple colour. Figure 4.1 shows that all the plants had antioxidant compounds except *Z. capense*. More prominent antioxidant compounds were detected from *X. caffra*, followed by *R. officinalis*. For *R. tridentata*, the antioxidant compounds did not move.

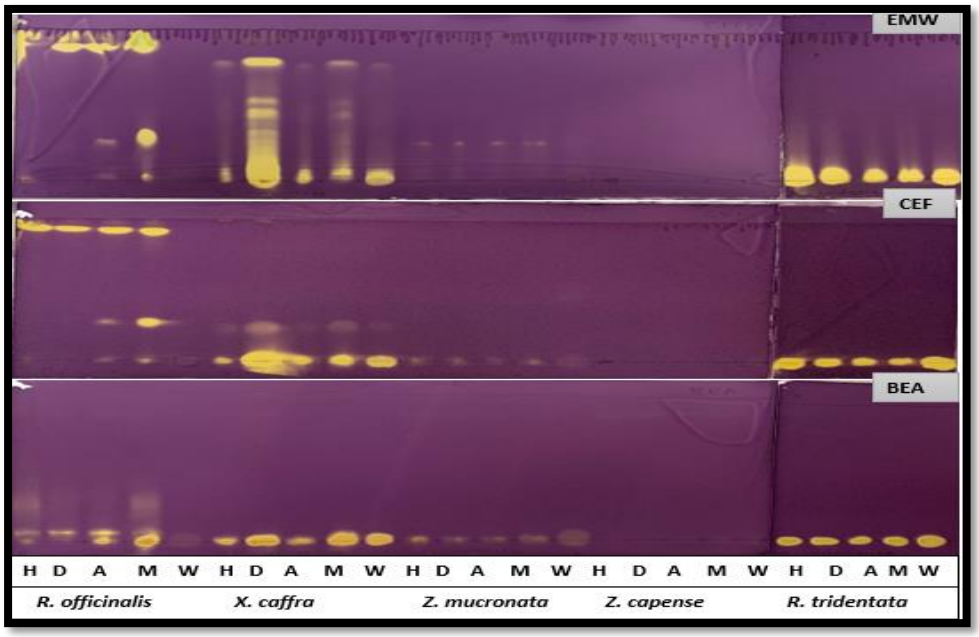

Figure 4. 1: Chromatograms attained after running TLC plates loaded with different plant extracts in three different mobile phases (EMW, CEF, and BEA) and sprayed with 0.2% DPPH. The visualised compounds of different plants which were extracted with: n-hexane (H), dichloromethane (D), acetone (A), methanol (M), and water (W).

4.3.2. Quantitative antioxidant activity

4.3.2.1. DPPH free radical scavenging activity assay

Total antioxidant activity of the plant extracts was quantified using 2,2-diphenyl-1-picrylhydrazyl (DPPH) assay. L-ascorbic acid was used as the standard and the results were expressed in the percentage of inhibition. Figures 4.2 A, B, C, D and E

show that the antioxidant activity of the plant extracts increases with an increase in the plant extracts' concentration. *R. tridentata* (E) had the highest antioxidant while *Z. capense* (A) had the lowest antioxidant activity. Water extracts had high antioxidant activity in C (*Z. mucronata*), E (*R. tridentata*) and lowest in A (*Z. capense*) and D (*R. officinalis*).

A

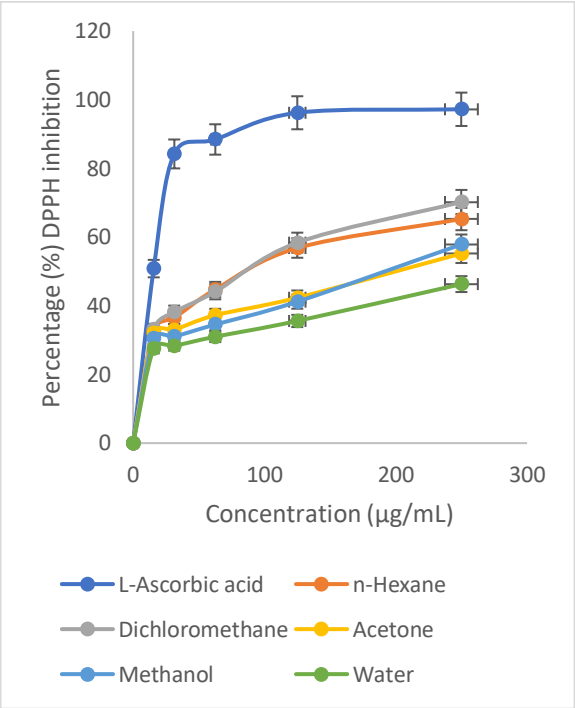

B

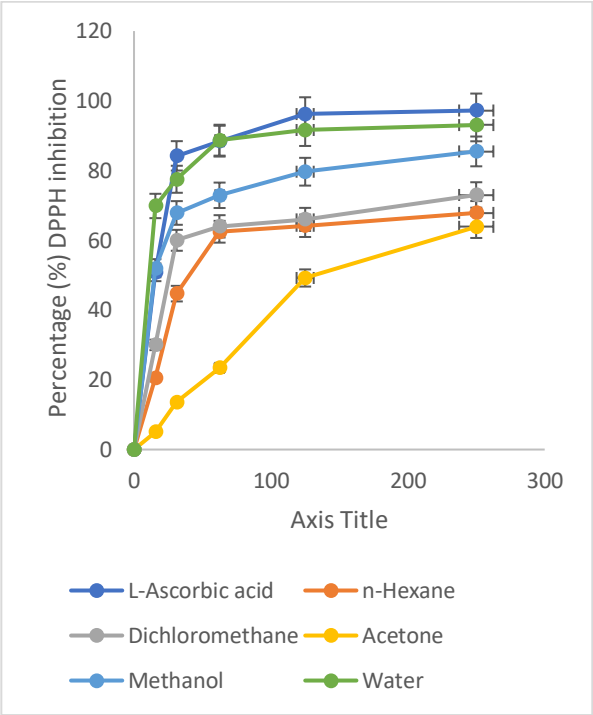

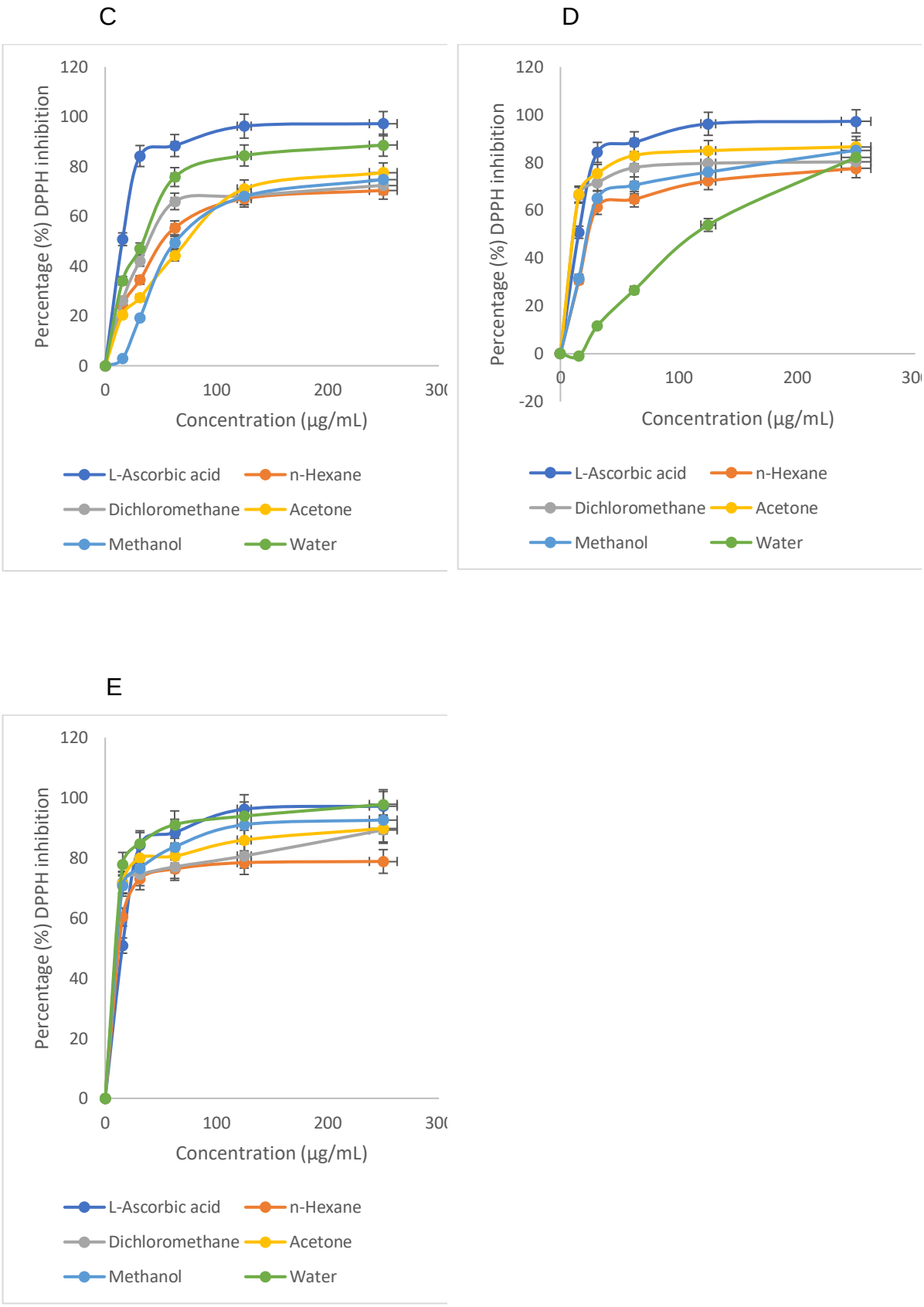

Figure 4. 2: The DPPH free radical scavenging activity of: A (*Z. capense*), B (*X. caffra*), C (*Z. mucronata*), D (*R. officinalis*) and E (*R. tridentata*) compared with L-

ascorbic acid as the standard in percentage inhibition. The results are expressed as the mean of the triplicates ± standard deviation.

4.3.2.2. Ferric Reducing Antioxidant Power (FRAP) assay

The FRAP assay was used to determine the antioxidant activity of the plant extracts, where the L-ascorbic acid was used as the standard to compare the plants' antioxidant activity. The results were expressed on different graphs as absorbance readings at 700 nm. The reducing power of the different plant extracts increased with an increase in concentration. The reducing power of *X. caffra* (B) from the dichloromethane extract had a higher reducing ability than L-ascorbic acid at a concentration of 625 µg/mL (Figure 4.3). The leaf extracts of *Z. capense* (A) had the lowest reducing ability compared to all the plants.

A

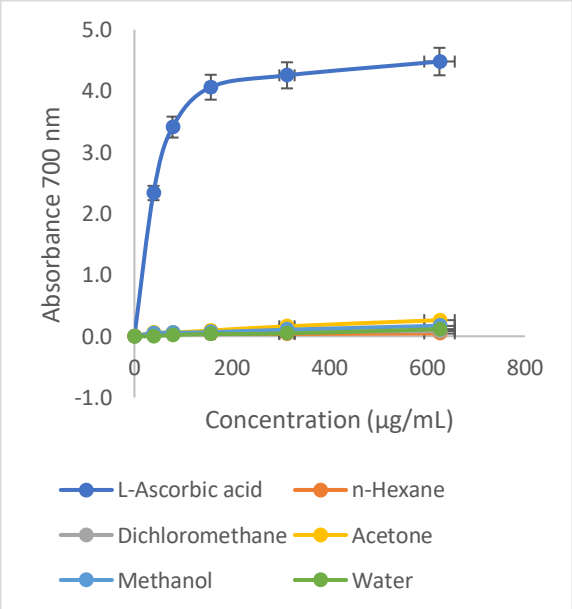

B

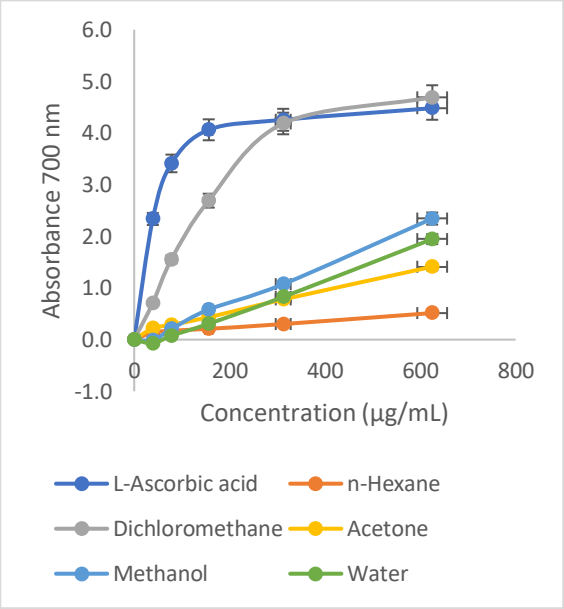

C

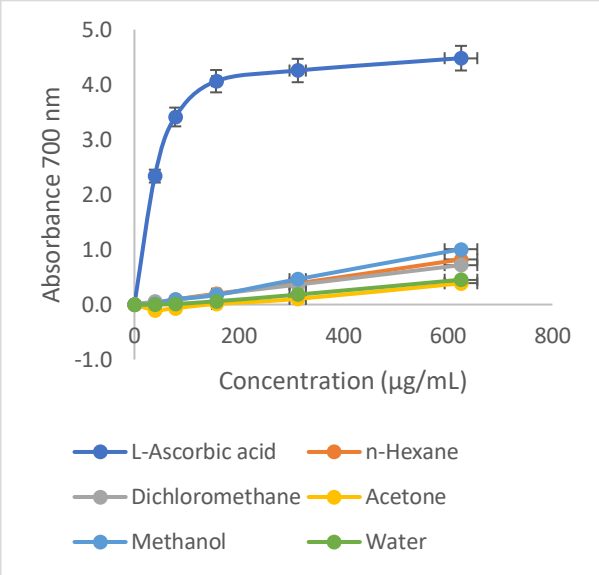

D

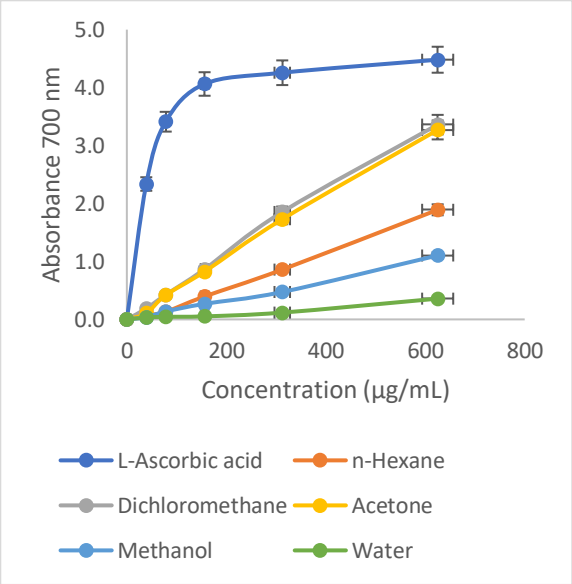

E

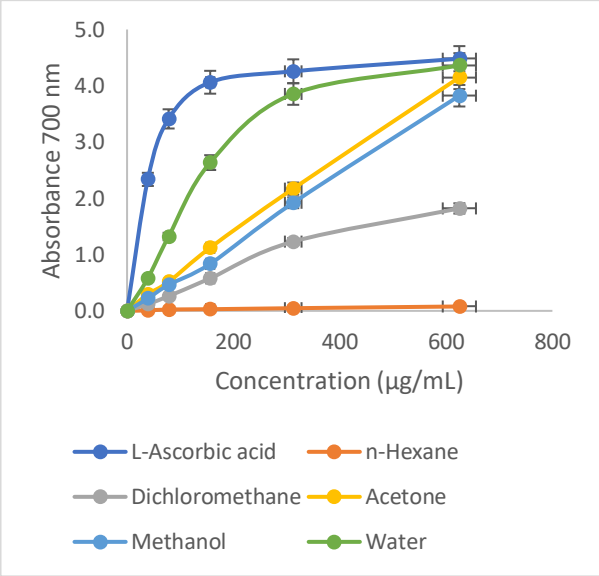

Figure 4. 3: Graphs showing the ferric reducing power activity of: A (*Z. capense*), B (*X. caffra*), C (*Z. mucronata*), D (*R. officinalis*) and E (*R. tridentata*) compared with the L-ascorbic acid as the standard at 700 nm. The results are expressed as the mean of the triplicates ± standard deviation.

4.3.3. The egg albumin denaturation inhibition assay

The anti-inflammatory activity of the plants was tested using an egg albumin denaturation inhibition assay at 2 mg/mL, where an aspirin was used as the positive control. There was a significant difference between the aspirin and all the plant extracts. The percentage inhibition was higher in *R. officinalis* and all the plant acetone

extracts had a promising anti-inflammatory activity except for *Z. capense* which had the percentage (%) inhibition less than 50% (Figure 4.4).

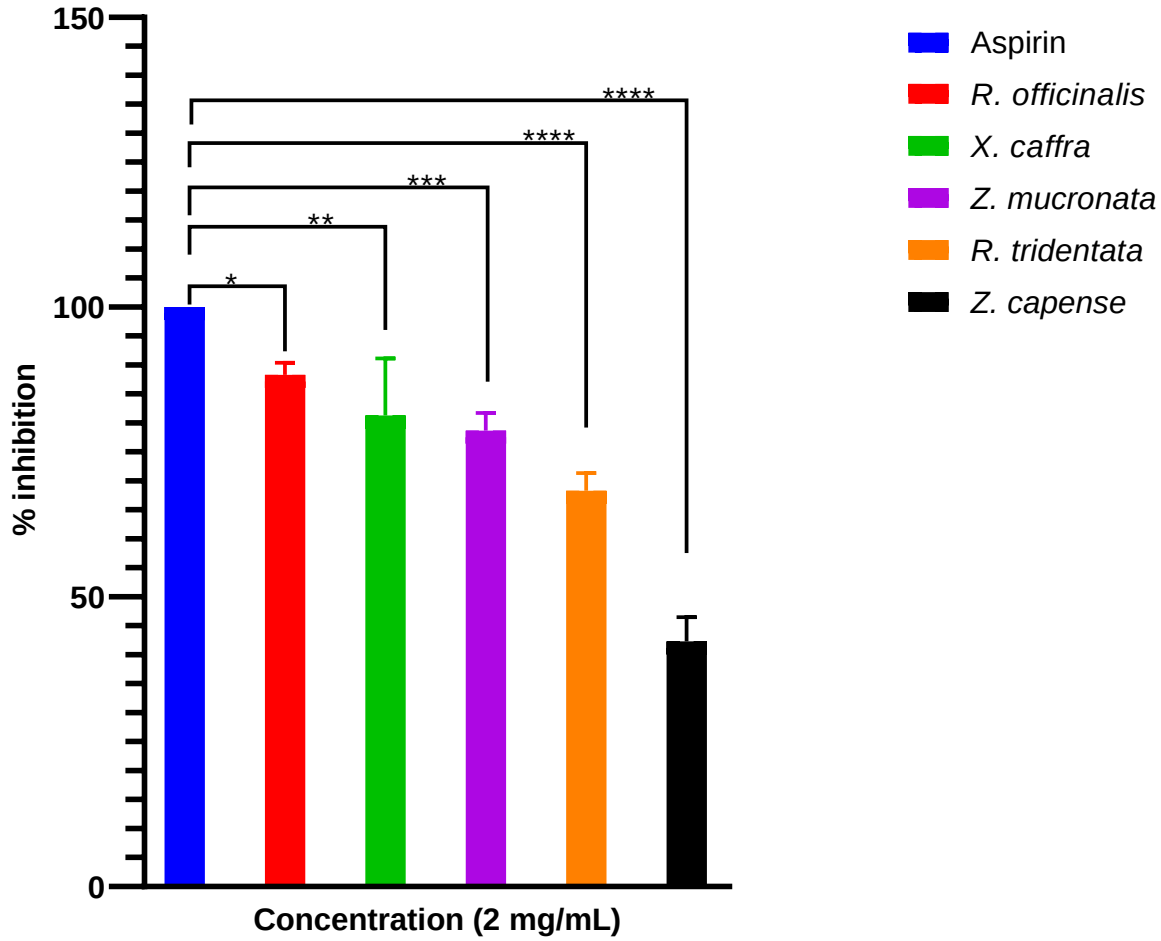

Figure 4. 4: The evaluation of the anti-inflammatory activity of plants acetone extracts using the egg albumin denaturation inhibition assay. The results were analysed using one-way ANOVA, followed by Dunett's multiple comparison test.

Key: * = level of significance compared to positive control (aspirin)

4.4. Discussion

Antioxidants, the scavengers of reactive oxygen species, are substances capable of protecting, scavenging, and repairing oxidative damage by protecting target molecules from oxidative injuries (Sansone and Brunet, 2019). Plant antioxidants are a natural reservoir of bioactive compounds. They play important roles in plants' adaptation to environmental challenges such as climate and play a huge role in human health (Maury *et al*., 2020). The qualitative and quantitative antioxidant activity of the plant extracts was determined using the 2,2-diphenyl-1-picrylhydrazyl (DPPH) reagent.

Qualitative analysis was carried out using TLC developed in different mobile systems (EMW, CEF and BEA), which were then sprayed with DPPH. The TLC plate turned purple in colour and the presence of antioxidant compounds was detected with a yellow colour. The DPPH free radical method is an antioxidant assay based on electron-transfer that produces a violet solution in methanol (Abd-Elghany and Mohamad, 2020). The results obtained are displayed on Figure 4.1. *X. caffra* showed to have the highest number of antioxidant compounds, followed by *R. officinalis* while *Z. capense* did not show any antioxidant compounds on the TLC plate. Antioxidant compounds for *X. caffra* and *R. officinalis* had a good separation on the plates developed in EMW (polar) and CEF (intermediate mobile phase). Antioxidant compounds for *X. caffra*, *Z. mucronata* and *R. tridentata* did not migrate and remained at the bottom of the plate developed in BEA (non-polar).

Total antioxidant activity was quantified using DPPH free radical scavenging activity where an L-ascorbic acid was used as the standard and the results were expressed in the percentage (%) of inhibition. Figure 4.2 (A, B, C, D and E) shows that the antioxidant activity of the plant extracts increases with an increase in the plant extracts' concentration. *R. tridentata* (Figure 4.2 E) showed to have the highest quantified antioxidants while *Z. capense* (Figure 4.2 A) had the lowest antioxidant activity. Naidoo *et al*. (2006) found that *R. tridentata* displayed good free radical scavenging activity when the plates were sprayed with DPPH and less quantity on leaves when using the Trolox Equivalent Antioxidant Capacity assay (TEAC). This is a contradiction that may also be due to the use of different analytical techniques. Even though the antioxidant compounds of *Z. capense* were not visible on the TLC plates, its samples had quantified antioxidant activity ranging between 46.31% to 70.22% inhibition at 250 µg/mL, where the L-ascorbic had the highest DPPH percentage inhibition. This was also observed by Bodebe *et al*. (2017) who reported that all *Z. capense* extracts had antioxidant activity, but their activity was lower than the one of the L-ascorbic acid. Water extracts had high antioxidant activity in *Z. mucronata* (Figure 4.2 C), *R. tridentata* (Figure 4.2 E) and had lowest antioxidant activity in *Z. capense* (Figure 4.2 A) and *R. officinalis* (Figure 4.2 D). A study conducted by Qadir *et al*. (2017) showed that plants are potent sources of antioxidant compounds and also had good antifungal and antimicrobial activity against pathogenic microbes, which suggested that the plants can be used to treat various infections caused by microbes. Several plants such

as *Ziziphus lotus* and *Ziziphus mauritiana* leaf fruit are reported to have a great number of antioxidants and have been successfully used against different bacterial strains. Therefore, they can be formulated for drug discovery in the future for pharmaceutical industries (Kumar *et al*., 2021).

The total antioxidant activity was also quantified using the ferric reducing antioxidant power assay. The FRAP assay is a method that measures the reduction of the complex ferric ions (Fe^{3+}) to ferrous complex (Fe^{2+}) as a signal, indicator, or reaction and this is bound to colour change (Benzie and Devaki, 2018). Antioxidants can either reduce the Fe^{3+} in the solution to Fe^{2+}, which binds the ferricyanide to yield Prussian blue, or reduce the ferricyanide to ferrocyanide, which binds the free Fe^{3+} in the solution and forms Prussian blue (Munteanu and Apetrei, 2021). The ferric reducing ability of the plant extracts was compared with the L-ascorbic as the standard and the reducing power of the different plant extracts increased with an increase in concentration (Figure 4.3). The reducing power of *X. caffra* (Figure 4.3 B) from the dichloromethane extract had a higher reducing ability than the L-ascorbic acid at a concentration of 625 µg/mL. The leaf extracts of *Z. capense* (Figure 4.3 A) had the lowest reducing ability compared to all the plants, followed by the *Z. mucronata* (Figure 4.3 C) plant extracts. Phenolic compounds and flavonoids are well-known antioxidant compounds and many other important bioactive agents that have long been interested in due to their benefits to human health, curing and preventing many diseases (Tungmunnithum *et al*., 2018). The total antioxidant content cannot be evaluated using a single test because of the phytochemicals present in the plants. These assays differ from one another in terms of antioxidant reaction mechanisms, reaction conditions and oxidation initiator, result expression and ease of operation (Gulcin, 2020). The antioxidant activities of the plant extracts were observed to have different activities because the Ferric Reducing Antioxidant Power (FRAP) assay only measures hydrophilic antioxidants while DPPH only applies to hydrophobic systems (Munteanu and Apetrei, 2021).

The anti-inflammatory activity of the plant acetone extracts was tested using the egg albumin denaturation assay at the concentration of 2 mg/mL. Protein denaturation is a well-studied reason for inflammation; so, the ability of plant extracts to inhibit protein denaturation was evaluated. Since inflammation is associated with pain, increase in protein denaturation and altering of the membrane, it was expected that extracts that

can stabilise the membrane must offer protection against injurious substances (Rajesh *et al*., 2019). Aspirin was used as the positive control. Figure 4.4 shows that all the plants had the ability to inhibit protein denaturation, although *Z. capense* had a percentage inhibition of 42%, which is lower than 50% and regarded as poor anti-inflammatory activity. *R. officinalis* had the highest anti-inflammatory activity of 88% and according to Borges *et al*. (2019) and Lorenzo-Leal *et al*., (2019), its essential oils have good anti-inflammatory activity. Macrophages are the main host cells for mycobacteria and are the potential target for regulating improper or extreme production of inflammatory mediators, which contribute to TB pathogenicity, as such, anti-inflammatory therapy is required to prevent excessive inflammation during TB (Araujo *et al*., 2021).

4.5. Conclusion

The antioxidant activity of the plant extracts was screened using the qualitative antioxidant activity (using DPPH). The extensive antioxidants extracted during the extraction process were quantified using DPPH free radical scavenging activity and Ferric Reducing Antioxidant Power (FRAP) assay. The amount of antioxidant compounds present in plant extracts was in relation to the phenolic content. The study also demonstrated the anti-inflammatory activity of the plants and they had promising anti-inflammatory activity except *Z. capense*. Further antimicrobial studies of the antioxidant compounds and isolation of active biological compounds are recommended for them to act as natural compounds for drug discovery.

4.6. References

Abd-Elghany, A.A. and Mohamad, E.A. 2020. *Ex-vivo* transdermal delivery of *Annona squamosa* entrapped in niosomes by electroporation. *Journal of Radiation Research and Applied Sciences*, **13**(1): 164-173.

Apak, R., Ozyurek, M., Guclu, K. and Capanoglu, E. 2016. Antioxidant activity/capacity measurement. 3. Reactive oxygen and nitrogen species (ROS/RNS) scavenging assays, oxidative stress biomarkers, and chromatographic/chemometric assays. *Journal of Agricultural and Food Chemistry*, **64**(5): 1046-1070.

Araujo, M.H.D., Simão, T.L.B.V., Konno, T.U.P., Guimarães, D.O., Leal, I.C.R., Lasunskaia, E. and Muzitano, M.F. 2021. Anti-mycobacterial and anti-inflammatory activity of *restinga* plants: a dual approach in searching for new drugs to treat severe tuberculosis. *Rodriguésia*, **72**: 1-13.

Aziz, N., Kim, M.Y. and Cho, J.Y. 2018. Anti-inflammatory effects of luteolin: a review of *in vitro*, *in vivo*, and in silico studies. *Journal of Ethnopharmacology*, **225**: 342-358.

Benzie, I. and Devaki, M. 2018. The Ferric Reducing Antioxidant Power (FRAP) assay for non-enzymatic antioxidant capacity: concepts, procedures, limitations, and applications. *Measurement of Antioxidant Activity and Capacity*: 77-106.

Bodede, O., Shaik, S., Singh, M. and Moodley, R. 2017. Phytochemical analysis with antioxidant and cytotoxicity studies of the bioactive principles from *Zanthoxylum capense* (Small knobwood). *Anti-Cancer Agents in Medicinal Chemistry (Formerly Current Medicinal Chemistry-Anti-Cancer Agents)*, **17**(4): 627-634.

Borges, R.S., Ortiz, B.L.S., Pereira, A.C.M., Keita, H. and Carvalho, J.C.T. 2019. *Rosmarinus officinalis* essential oil: a review of its phytochemistry, anti-inflammatory activity, and mechanisms of action involved. *Journal of Ethnopharmacology*, **229**: 29-45.

Braca, A., Sortino, C. and Politi, M. 2002. Antioxidant activity of flavonoids from *Licania licaniaeflora*. *Journal of Ethnopharmacology*, **79**(3): 379-381.

Chigayo, K., Mojapelo, P.E.L. and Moleele, S.M. 2016. Phytochemical and antioxidant properties of different solvent extracts of *Kirkia wilmsii* tubers. *Asian Pacific Journal of Tropical Biomedicine*, **6**: 1037–1043.

Elisha, I.L., Dzoyem, J.P., McGaw, L.J., Botha, F.S. and Eloff, J.N. 2016. The anti-arthritic, anti-inflammatory, antioxidant activity and relationships with total phenolics and total flavonoids of nine South African plants used traditionally to treat arthritis. *BMC Complementary and Alternative Medicine*, **16**(1): 1-10.

Gulcin, İ. 2020. Antioxidants and antioxidant methods: an updated overview. *Archives of Toxicology*, **94**(3): 651-715.

Gyamfi, M.A., Yonamine, M. and Aniya, Y. 1999. Free-radical scavenging action of medicinal herbs from Ghana: *Thonningia sanguinea* on experimentally-induced liver injuries. *General Pharmacology*, **32**(6): 661-667.

Kooti, W. and Daraei, N. 2017. A review of the antioxidant activity of celery (*Apium graveolens* L). *Journal of Evidence-Based Complementary and Alternative Medicine*, **22**(4): 1029-1034.

Kroesen, V.M., Gröschel, M.I., Martinson, N., Zumla, A., Maeurer, M., van der Werf, T.S. and Vilaplana, C. 2017. Non-steroidal anti-inflammatory drugs as host-directed therapy for tuberculosis: a systematic review. *Frontiers in Immunology*, **8**: 772.

Kumar, M., Singh, S.K., Singh, P.P., Singh, V.K., Rai, A.C., Srivastava, A.K., Shukla, L., Kesawat, M.S., Kumar Jaiswal, A., Chung, S.M. and Kumar, A. 2021. Potential anti-*mycobacterium tuberculosis* activity of plant secondary metabolites: insight with molecular docking interactions. *Antioxidants*, **10**(12): 1990.

Lorenzo-Leal, A.C., Palou, E., López-Malo, A. and Bach, H. 2019. Antimicrobial, cytotoxic, and anti-inflammatory activities of *Pimenta dioica* and *Rosmarinus officinalis* essential oils. *BioMed Research International*:1-8.

Marques, F.M., Figueira, M.M., Schmitt, E.F.P., Kondratyuk, T.P., Endringer, D.C., Scherer, R. and Fronza, M. 2019. *In vitro* anti-inflammatory activity of terpenes via suppression of superoxide and nitric oxide generation and the NF-κB signalling pathway. *Inflammopharmacology*, **27**(2): 281-289.

Martins, N., Barros, L. and Ferreira, I.C. 2016. *In vivo* antioxidant activity of phenolic compounds: facts and gaps. *Trends in Food Science and Technology*, **48**: 1-12.

Maury, L.G., Rodríguez, M.D., Hendrix, S., Arranz, E.J.C., Boix, F.Y., Pacheco, A.O., Díaz, G.J., Morris-Quevedo, H.J., Dubois, F.A., Aleman, E.I. and Beenaerts, N. 2020. Antioxidants in plants: a valorization potential emphasizing the need for the conservation of plant biodiversity in Cuba. *Antioxidants*, **9**(11): 1048.

Mosca, F., Hidalgo, G.I., Villasante, J. and Almajano, M.P. 2018. Continuous or batch solid-liquid extraction of antioxidant compounds from seeds of *Sterculia apetala* plant and kinetic release study. *Molecules*, **23**(7): 1759.

Munteanu, I.G. and Apetrei, C. 2021. Analytical methods used in determining antioxidant activity: a review. *International Journal of Molecular Sciences*, **22**(7): 3380.

Naidoo, V., Chikoto, H., Bekker, L.C. and Eloff, J.N. 2006. Antioxidant compounds in *Rhoicissus tridentata* extracts may explain their antibabesial activity: research in action. *South African Journal of Science*, **102**(5): 198-200.

Nirmala, C., Bisht, M.S., Bajwa, H.K. and Santosh, O. 2018. Bamboo: a rich source of natural antioxidants and its applications in the food and pharmaceutical industry. *Trends in Food Science and Technology*, **77**: 91-99.

Oguntibeju, O.O. 2018. Medicinal plants with anti-inflammatory activities from selected countries and regions of Africa. *Journal of Inflammation Research*, **11**: 307.

Olszowy, M. 2019. What is responsible for antioxidant properties of polyphenolic compounds from plants? *Plant Physiology and Biochemistry*, **144**: 135-143.

Qadir, A.M., Shahzadi, S.K., Bashir, A., Munir, A. and Shahzad, S. 2017. Evaluation of phenolic compounds and antioxidant and antimicrobial activities of some common herbs. *International Journal of Analytical Chemistry*, ***2017***.

Rahman, H., Eswaraiah, M.C. and Dutta, A.M. 2015. *In-vitro* anti-inflammatory and anti-arthritic activity of *Oryza Sativa* Var. joha rice (an aromatic indigenous rice of Assam). *American-Eurasian Journal of Agricultural and Environmental Sciences*, **15**(1): 115-121.

Rajesh, A., Doss, A., Tresina, P.S. and Mohan, V.R. 2019. *In-vitro* anti-inflammatory activity of ethanol extract of *Crotalaria longipes*. *Journal of Pharmacognosy Phytochemistry*, **8**:1469-1472.

Ribeiro, V.P., Arruda, C., Abd El-Salam, M. and Bastos, J.K. 2018. Brazilian medicinal plants with corroborated anti-inflammatory activities: a review. *Pharmaceutical Biology*, **56**(1): 253-268.

Salehi, B., Azzini, E., Zucca, P., Maria Varoni, E., V Anil Kumar, N., Dini, L., Panzarini, E., Rajkovic, J., Valere Tsouh Fokou, P., Peluso, I. and Prakash Mishra, A. 2020. Plant-derived bioactive and oxidative stress-related disorders: a key trend towards healthy aging and longevity promotion. *Applied Sciences*, **10**(3): 947.

Sansone, C. and Brunet, C. 2019. Promises and challenges of microalgal antioxidant production. *Antioxidants*, **8**(7): 199.

Santos-Sánchez, N.F., Salas-Coronado, R., Villanueva-Cañongo, C. and Hernández-Carlos, B. 2019. *Antioxidant compounds and their antioxidant mechanism. 5th ed*. London, UK, 1-28.

Saha, S. and Verma, R.J. 2016. Antioxidant activity of polyphenolic extract of *Terminalia chebula* Retzius fruits. *Journal of Taibah University for Science*, **10**(6): 805-812.

Tungmunnithum, D., Thongboonyou, A., Pholboon, A. and Yangsabai, A. 2018. Flavonoids and other phenolic compounds from medicinal plants for pharmaceutical and medical aspects: an overview. *Medicines*, **5**(3): 93.

Uttra A.M. and Alamgeer. 2017. Assessment of anti-arthritic potential of *Ephedra gerardiana* by *in vitro* and *in vivo* methods. *Bangladesh Journal of Pharmacology*, **12**: 403-409.

Vijayalakshmi, M. and Ruckmani, K. 2016. Ferric reducing anti-oxidant power assay in plant extract. *Bangladesh Journal of Pharmacology*, **11**(3): 570-572.

Xu, D.P., Li, Y., Meng, X., Zhou, T., Zhou, Y., Zheng, J., Zhang, J.J. and Li, H.B. 2017. Natural antioxidants in foods and medicinal plants: extraction, assessment, and resources. *International Journal of Molecular Sciences*, **18**(1): 96.

Zhou, J.X., Braun, M.S., Wetterauer, P., Wetterauer, B. and Wink, M. 2019. Antioxidant, cytotoxic, and antimicrobial activities of *Glycyrrhiza glabra* L., *Paeonia lactiflora* Pall., and *Eriobotrya japonica* (Thunb.) Lindl. extracts. *Medicines*, **6**(2): 43.

CHAPTER 5

5. Antimycobacterial screening and cytotoxic effects

5.1. Introduction

Antibacterial resistance is the major global health challenge and threat to public health (Elisha *et al*., 2017). The antibacterial resistance mechanisms can be divided into two categories, namely, the innate or intrinsic resistance and acquired resistance. Intrinsic resistance is mainly a feature of a particular bacterium and is based on biological properties of bacteria. The second mechanism of resistance is mainly due to the production of resistance genes by other pathogenic bacteria or chromosomal mutation and a combination of these two mechanisms (Farhadi *et al*., 2019). Antibacterial resistance has a negative impact, especially on vulnerable patients, resulting in prolonged illness and increased mortality (Wikaningtyas and Sukandar, 2016). Therefore, there is a need to search for antibacterial substances derived from natural products, such as phytochemicals that have gained increasing importance alongside the discovery of new synthetic chemical compounds with antibiotic and bacteriophage properties (Barbieri *et al*., 2017).

The production of synthetic drugs is costly, and they produce adverse effects compared to plant-derived drugs (Jouda *et al*., 2016). Plants have medicinal ability and have been used as sources of antimicrobials for a long time by people around the world (Danish *et al*., 2020). They possess a wider range and more efficient biological activity against harmful diseases, such as being rich in secondary metabolites with potential antimicrobial properties. As such, plant derivatives may become a powerful tool against diverse infectious diseases (Shin *et al*., 2018).

The *in vitro* antimicrobial activity of natural extracts or pure compounds involves the use of assays to evaluate their potential to kill or inhibit the microbial growth of microorganisms (Kurhekar *et al*., 2019). The common screening methods for detecting the antimicrobial activity of natural products are divided into three groups: diffusion, bioautographic and dilution methods. The diffusion and bioautographic methods are qualitative techniques due to their giving data on the absence or presence of substances with antimicrobial activity whereas the dilution methods are quantitative, and define the MIC (Massoud *et al*., 2019). Another dilution assay is the minimum

bactericidal concentration (MBC) using the broth microdilution method (Banothu *et al*., 2017).

Thin Layer Chromatography-Bioautography (TLC-B) is an analytical technique used to identify antimicrobial compounds that are separated using a TLC plate, where the antibacterial activity is indicated by zones of inhibition corresponding to spots on eluted TLC plates (Owen *et al*., 2019). These parts are visualised by the use of dehydrogenase activity detecting reagents such as tetrazolium salts (Ncama *et al*., 2019). Bioautography combines TLC with both biological and chemical detection methods by screening the antibacterial and antifungal activity of plant extracts (Balouiri *et al*., 2016). It is the mostly used method because it is effective in studying active compounds from plants and provides information about the activity and location of the antimicrobial activity directly on the TLC absorbent (Armengol *et al*., 2021). One of the advantages when compared to agar diffusion assay is that a very little amount of a sample is needed compared to the well diffusion assay and it is a fast method to detect antimicrobial agents (Murei, 2019).

The MIC and minimum bactericidal concentration (MBC) must be determined to check bacterial activity. MIC is the lowest concentration of an antimicrobial that can inhibit the visible growth of a microorganism after overnight incubation and MBC is the lowest concentration of an antibacterial agent required to kill a particular bacterium (Stankovic *et al*., 2016). On the other side, plant extracts with antimicrobial activity can be combined to check if they can work together. In a combination, the interaction between antimicrobials can result in three different outcomes, which are synergistic, additive, or antagonistic. Synergy is obtained by combining two antimicrobial compounds that produce antibacterial activity greater than the sum of the antibacterial activity of individual components. An additive effect is produced by combining antimicrobials producing an antimicrobial effect that is equal to the sum of the individual compounds. An antagonistic effect results in a decreased antimicrobial activity of two compounds in combination compared to their individual antimicrobial activity (Chouhan *et al*., 2017).

Biofilms are three-dimensionally organised multicellular communities of microorganisms enclosed in a matrix (Richards *et al*., 2019). They can be developed as colonies attached to the surface or pellicles, which ensures the survival of bacteria

in unfavourable environments (Padhi *et al*., 2016). Diseases associated with biofilm formation cause 80% of unmanageable hospital infections. Some pathogenic and non-pathogenic mycobacteria form biofilms to overcome stress (Kumar *et al*., 2019). Methods such as antimicrobial peptides, modification of surfaces to prevent bacterial attachment, nanoparticles with antimicrobial activity, and development of physical biofilm removal technologies are recognised as a good way to overcome biofilms (Schilcher and Horswill, 2020). Since biofilm formation leads to treatment failure (Chakraborty *et al*., 2021), it is necessary to investigate and come up with solutions for bacterial adhesion and biofilm formation (Khelissa *et al*., 2017).

MTT [3-(4,5-dimethylthiazol-2-yl)-2–5-diphenyltetrazolium bromide] assay is one of the most used colorimetric assays to assess cytotoxicity or cell viability. This assay determines cell viability through the determination of the mitochondrial function of cells by measuring the activity of mitochondrial enzymes (Aslantürk, 2018). The MTT assay involves the conversion of the water-soluble yellow dye MTT to an insoluble purple formazan by the action of mitochondrial reductase. Formazan is then solubilised, and the concentration is determined by optical density at 570 nm (Kumar *et al*., 2018). The intensity of purple colour is directly proportional to the cell number, thus indicating the cell viability (Bahuguna *et al*., 2017). It is a vital indicator of the action of cell survival or death in response to drugs or chemical agents. Effects of drugs can either be cytotoxic, which refers to being toxic and killing the cells or cytostatic, which is defined as cell growth inhibition (Adan *et al*., 2016).

5.2. Method and materials

5.2.1. Qualitative antibacterial activity

5.2.1.1. Bioautographic assay

A bioautographic method described by Begue and Kline (1972) was used to analyse the qualitative number of antimicrobial compounds. TLC plates were loaded with 20 µL of plant extracts in a 1 cm wide line on different TLC plates, which were developed in EMW, CEF, and BEA mobile systems. The plates were air-dried at room temperature for seven days to fade excess solvents. In a laminar flow cabinet (Labotec), dried TLC plates were then sprayed with a concentrated suspension of *Mycobacterium smegmatis*, which was grown overnight in a Middlebrook 7H9 broth

base at 37 °C until they were completely moist. The plates were then incubated at 37 °C in 100% humidity for 24 hours. After incubation, the plates were sprayed with 2 mg/mL of p-iodonitrotetrazolium violet (INT) (Sigma-Aldrich) and further incubated for 2-3 hours at 37 °C in 100% relative humidity. The bioautograms were observed for bacterial growth and clear zones against the red-pink background that indicated the inhibition of bacterial growth by the compounds with antibacterial activity.

5.2.1. Quantitative antibacterial activity assay

5.2.2.1. Serial broth dilution assay

The MIC of the plant extracts was determined using the serial broth microdilution assay described by Eloff (1998b). Plant extracts were dissolved in acetone to a concentration of 10 mg/mL. The first stock solution was prepared by inoculating a loopful *Mycobacterium smegmatis* in a 100 mL Middlebrook 7H9 broth and incubated for 24 hours at 37 °C. The second stock culture was prepared by adding 10 mL from the first stock culture into 100 mL Middlebrook 7H9 broth and incubated it for 24 hours at 37 °C. Exactly 100 µL of each plant extract was serially diluted (50%) with sterilised distilled water using a multichannel pipette in 96 well plates. This was followed by the addition of 100 µL of *Mycobacterium smegmatis* in each well of the plate from the second stock solution. Rifampicin was used as the positive control while acetone was used as the negative control. All microtiter plates were covered and incubated for 24 hours at 37 °C. After incubation, 40 µL of 0.2% p-iodonitrotetrazolium violet (INT) (Sigma-Aldrich) dissolved in sterile distilled water was added as the growth indicator. Plates were covered, further incubated at 37 °C for 30 minutes in relative humidity and observed for clear wells (with activity), which resulted from reduction in colour intensity (purple colour). The tests were performed in triplicates and the MIC value was recorded as the lowest concentration of antimicrobial concentration that was able to inhibit the growth of *Mycobacterium smegmatis*. The total activity of the plant extracts was determined by dividing the MIC values with the mass extracted from 1 g of the plant material in mg/mL. The total activity was calculated by dividing the quantity extracted (in mg) from 1 g of plant material by the MIC value (in mg/mL).

5.2.2.2. The antibacterial interaction effects

The 10 mg/mL stock solutions of n-hexane, dichloromethane, acetone, methanol, and water prepared by reconstituting in acetone were used to determine the antibacterial interaction effects. Combinations with the ratio of 1:1 (50 µL of each of the two extracts) were mixed to make the volume up to 100 µL in the first wells of 96-well microtiter plate. The MIC values of each combination were determined to establish any interaction of the plants, as described in section 5.2.2.1. After investigating the independent MIC of the selected plants, the synergistic and antagonistic interactions between the plants were investigated. This was accomplished by determining the MIC of the combinations showing antibacterial activity to establish any interaction effects. The Fractional Inhibitory Concentration (FIC) was calculated for the 1:1 combination of the plants. This was calculated using the equation below, were (i) and (ii) represented the different 1:1 plant combination (Mabona *et al*., 2013). The FIC index was expressed as the sum of FIC (i) and FIC (ii) and this was further used to classify the interaction as either synergistic (≤ 0.50), additive (0.50-1.00), indifferent (> 1.00-4.00) or antagonistic (> 4) (Van Vuuren and Viljoen, 2008).

$$FIC(i) = \frac{MIC\ of\ (a)\ in\ combination\ with\ (b)}{MIC\ of\ (a) independently}$$

$$FIC(ii) = \frac{MIC\ of\ (b)\ in\ combination\ with\ (a)}{MIC\ of\ (b) independently}$$

5.2.2. Antibiofilm activity

A 100 µL aliquot of standardised concentration of culture with OD = 0.02 of 600 *Mycobacterium smegmatis*, was added into individual flat-bottomed 96-well microtiter plates and incubated at 37 °C for 48 hours to allow the mature development of the biofilm. The plates were incubated without shaking. Following the incubation period, 100 µL plant acetone extracts (20 mg/mL) were added into the wells of a 96-well microtiter plates to give a concentration range between 5-0.28 mg/mL. The plates were incubated further at 37 °C for 24 hrs. Rifampicin at the same concentration as the acetone plant extracts served as a positive control while 0.5% DMSO was used as a negative control (Famuyide *et al*., 2019). The biofilm biomass was assayed using the modified crystal violet staining assay. The 96-well microtiter plates were washed three times with sterile distilled water, air-dried and then oven-dried at 60 °C for 45 minutes.

The wells were then stained with 100 µL of 0.5% crystal violet and incubated at room temperature for 15 minutes, and then the plates were washed thrice with sterile distilled water to remove unabsorbed stain. At this point, biofilms were observed as purple rings at the side of the wells. The semi-quantitative assessment of biofilm formation was done by adding 100 µL of Dimethyl sulfoxide (DMSO) to distain the wells. Thereafter, 100 µL of the distaining solution was transferred to a new sterile plate and the absorbance was measured at 595 nm using a microplate reader (Bio-Rad). The mean absorbance of the samples was determined, and the percentage inhibition of biofilm was determined using the equation below (Djordjevic *et al*., 2002).

$$\%\ inhibition = \frac{(OD\ control - OD\ experimental)}{OD\ control} \times 100$$

5.2.3. Cell viability assay

The MTT [3-(4,5-dimethylthiazol-2-yl)-2,5-diphenyltetrazolium bromide] assay described by Mosmann (1983) was performed with a few modifications. A flask with RPMI 1640 medium (Whitehead scientific) was used to maintain the cell culture (THP-1 cell line), which was then supplemented with 10% foetal bovine serum (FBS) (Adcock-Ingram). Cells were dyed with trypan blue and viable cells were quantified with an automatic cell counter (model). Cells were then diluted with Roswell Park Memorial Institute (RPMI) complete media to obtain 5×10^4 cells/mL suspension of cells.

The THP-1 culture was diluted to 2×10^5 cell/mL in a 50 mL vial. In this study, the THP-1 cells were pre-treated with 25 µL of 100 µg/mL phorbol-12-myristate-13-acetate (PMA) to yield a final concentration of 50 ng/µL in the 50 mL vial. The cells were seeded at 2×10^5 cell/mL (in each well) in 5% CO_2 at 37 °C in flat bottom 96 well plates for 72 hrs. This was done to induce the maturation of the monocytes into macrophage-like adherent cells. THP-1 cells from each well were seeded in 96 well plates to a final volume of 100 µL. It is vital to arrest the differentiation of the cell line after a 48-hr treatment with PMA to increase macrophage markers (Chanput *et al*., 2014). After treatment with PMA, the spent media was removed, and the cells were washed with pre-warmed 1X phosphate buffered saline (PBS) and fresh media was added, followed by 24 hours of incubation (Safar *et al*., 2019 THP1). To prepare the stock solutions, the acetone plants extracts were dissolved in dimethyl sulfoxide (DMSO) to a

concentration of 250 mg/mL. The prepared stock solutions were diluted to 1 mg/mL with complete media and 0.25% of DMSO was maintained. Exactly 100 µL of plant extracts with different concentrations (1000, 500, 100 µg/mL) prepared in a different 96 well plate was transferred to the plate containing cell cultures. The microtiter plates were then incubated in a 5% CO_2 incubator at 37 °C for 24 hours.

After incubation, 20 µL of 0.5 mg/mL MTT [3-(4,5-dimethylthiazol-2-yl)-2,5-diphenyltetrazolium bromide] dissolved in 1× PBS was added to each well and the plates were further incubated for four hours. After incubation, 100 µL of DMSO was added to each well and incubated for an hour to allow MTT to dissolve. After incubation, the cytotoxicity of tested samples against the cells was indicated by the lack of a purple formazan colour or clear appearance in the wells. A Promega microtiter plate reader was used to measure the absorbance values of the purple colour at 540 nm. Treated cells (with plant extracts) were compared with untreated cells (without plant extracts).

5.2.4. Statistical analysis

Where appropriate, the results were expressed as the mean ± standard deviation of triplicate determinations. Statistical analysis was performed using GraphPad prism v8.9 by one-way analysis of variance (ANOVA), followed by Dunett's multiple comparison test and two-way ANOVA, which was followed by the Tukey multiple comparison post hoc test. Significant difference was considered when $p < 0.05$ and conversely, and non-significant difference was indicated when $p > 0.05$ values.

5.3. Results

5.3.1. Bioautography assay

The qualitative antimicrobial assay of *Z. capense, R. tridentata, R. officinalis, X. caffra* and *Z. mucronate* against *M. smegmatis* was screened using TLC plates, which were developed in three different mobile phases (EMW, CEF, and BEA) of varying polarities. The clear bands, also called zone of inhibition (inhibition of the microorganism by plant extracts), against the pinkish background indicate the antibacterial activity of the different plant extracts. *R. officinalis* and *Z. mucronata* showed to have activity against *Mycobacterium smegmatis*. *R. officinalis* with Rf values of 0.12 on the BEA plate and 0.81 on the EMW plate, while *Z. mucronata* had the Rf value of 0.06 on the TLC plate developed in BEA and 0.79 on the EMW plate.

Antibacterial activity was not observed on the *X. caffra*, *Z. capense* and *R. tridentata* plant extracts. The CEF (intermediate polarity) plate did not show any activity from all the plant extracts (Figure 5.1).

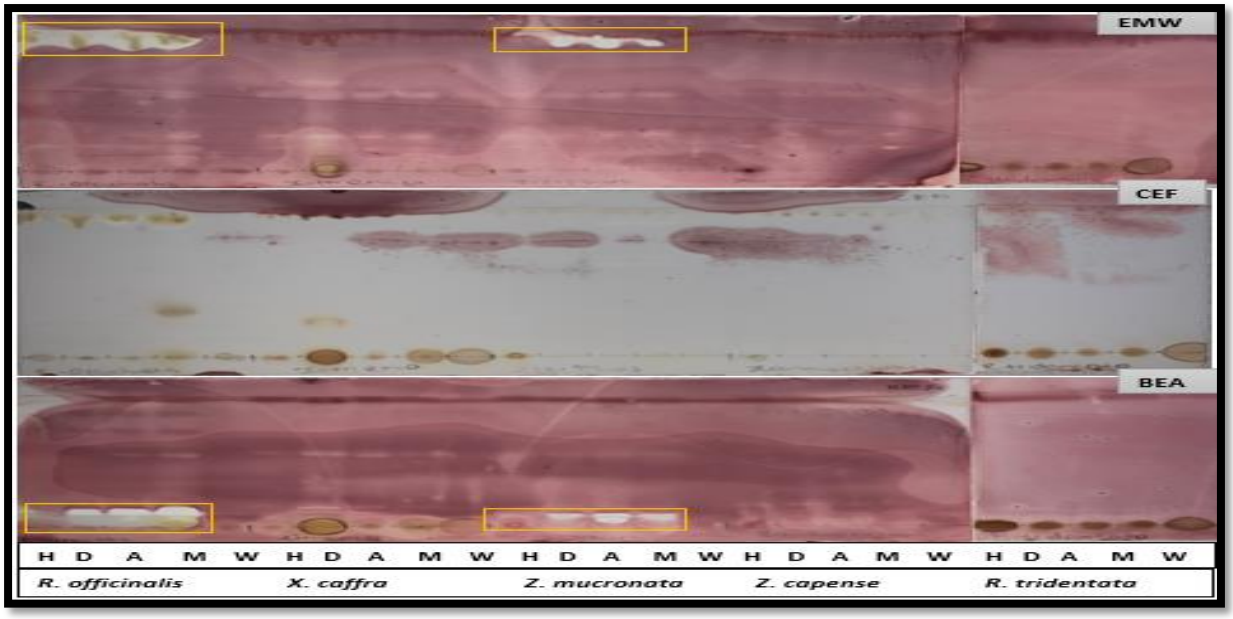

Figure 5. 1: Bioautograms attained after running TLC plates loaded with different plant extracts in three different mobile phases (EMW, CEF, and BEA) and sprayed with *Mycobacterium smegmatis* for overnight. They were then visualised by spraying with 2 mg/mL of INT. Different plants extracts were extracted with: hexane (H), dichloromethane (D), acetone (A), methanol (M), and water (W).

5.3.2. Quantitative antimicrobial assay

5.3.2.1. Serial broth dilution assay

The quantitative microbroth assay determined the antibacterial activity of the plant extracts against *M. smegmatis* as the MIC in mg/mL, where rifampicin was used as the positive control and values ranged from the lowest concentration of 0.08 mg/mL to 2.50 mg/mL. The lowest MIC value of 0.08 mg/mL, same as the positive control was observed from the hexane, dichloromethane, acetone, and methanol extracts of *R. officinalis*. This was followed by 0.16 mg/mL from hexane extract of *R. tridentata*. The dichloromethane extract of *R. tridentata* and hexane extract of *X. caffra* had an MIC value of 0.31 mg/mL while the acetone and methanol extracts of *Z. mucronata* had an

MIC value of 1.25 mg/mL. All other extracts had an MIC value greater than 2.5 mg/mL, same as the negative control (Table 5.1).

Table 5. 1: The MIC values of selected plant extracts in mg/mL against *M. smegmatis*.

Solvent	Plant species					Rifampicin	Acetone
	Z. mucronata	*R. officinalis*	*R. tridentata*	*X. caffra*	*Z. capense*		
Hexane	>2.5	0.08	0.16	0.31	>2.5	0.08	>2.5
Dichloromethane	>2.5	0.08	0.31	>2.5	>2.5		
Acetone	1.25	0.08	>2.5	>2.5	>2.5		
Methanol	1.25	0.08	>2.5	>2.5	>2.5		
Water	>2.5	>2.5	>2.5	>2.5	>2.5		
Average	2.0	0.56	1.59	2.06	2.5		

Total activity

The total activity (mL/g) of the plant extracts obtained by dividing the quantity extracted (in mg) from 1 g of plant material by the MIC value (in mg/mL). The total highest activity of the plant extracts was found from *R. officinalis* methanol (1250 mL/g), dichloromethane (1125 mL/g) and acetone (875 mL/g) extracts, followed by *R. tridentata* hexane extract with a total activity of 769.2 mL/g (Table 5.2). The lowest total activity of 8 mL/g was obtained from the n-hexane and water extracts of *Z. mucronata* (Table 5.2).

Table 5. 2: Total activity of the selected plant extracts (mL/g).

Solvent	Plant species				
	Z. mucronata	*R. officinalis*	*R. tridentata*	*X. caffra*	*Z. capense*
n-Hexane	8	500	769.2	160	12
Dichloromethane	12	1125	384	56	20
Acetone	40	875	60	16	20
Methanol	108.8	1250	96	36	54.4

Water	8	56	72	88	20
Average	35.36	761.2	276.3	71.2	25.28

5.3.2.2. The antibacterial interaction effects

Since the n-hexane and acetone extracts of the plants had the highest activity against *M. smegmatis*. They were then used to check the antibacterial interaction effects. Different n-hexane and acetone plant extracts were mixed together to check their activity using the 1:1 ratio, where 50 µL of a different plant was mixed with 50 µL of the other plant. All n-hexane plant combinations with the *R. officinalis* extract had the lowest MIC value of 0.63 mg/mL while all the other plant combinations had an MIC value of 2.50 mg/mL (Table 5.3). The acetone combination of *R. officinalis* and *R. tridentata* had the lowest MIC value of 0.42 mg/mL (Figure 5.4). The obtained potency of the combinations was then used to calculate the FIC index and check the antagonistic or synergistic effects of the plants. The n-hexane combination of *R. officinalis* and *Z. capense* had a synergistic outcome with the FIC index of 0.06, respectively. The *Z. mucronata and Z. capense* n-hexane combination had an FIC index of 2.00, which is indifferent, while all the other combinations had an antagonistic effect. All acetone combinations of the selected plants with *R. officinalis* had an antagonistic effect and the other acetone plant combinations had an indifferent outcome.

Table 5. 3: The FIC of selected plants using n-hexane extracts.

Combination	MIC (mg/mL)	FIC (i)	FIC (ii)	FIC index	Outcome
RO:RT	0.63	7.81	4.01	11.82	Antagonistic
RO:ZM	0.63	7.81	0.25	8.01	Antagonistic
RO:XC	0.63	7.81	0.20	9.81	Antagonistic
RO:ZC	0.63	7.81	0.25	0.06	Synergistic
RT:ZM	2.50	16.03	1.00	17.03	Antagonistic
RT:XC	2.50	16.03	8.00	24.03	Antagonistic
RT:ZC	2.50	16.03	1.00	17.03	Antagonistic
ZM:XC	2.50	1.00	8.00	9.00	Antagonistic
ZM:ZC	2.50	1.00	1.00	2.00	Indifferent

XC:ZC	2.50	8.00	1.00	9.00	Antagonistic

Key: *R. officinalis* (RO), *R. tridentata* (RT), *X. caffra* (XC), *Z. muconata* (ZM), *Z. capense* (ZC), FIC, and MIC

Table 5. 4: The FIC of selected plants using acetone extracts.

Combination	MIC (mg/mL)	FIC (i)	FIC (ii)	FIC index	Outcome
RO:RT	0.42	5.21	1.17	5.38	Antagonistic
RO:ZM	0.52	6.51	0.42	6.93	Antagonistic
RO:XC	0.52	6.51	0.21	6.72	Antagonistic
RO:ZC	0.63	7.81	0.25	8.06	Antagonistic
RT:ZM	2.50	1.00	2.00	3.00	Indifferent
RT:XC	2.50	1.00	1.00	2.00	Indifferent
RT:ZC	2.50	1.00	1.00	2.00	Indifferent
ZM:XC	2.50	2.00	1.00	3.00	Indifferent
ZM:ZC	2.50	2.00	1.00	3.00	Indifferent

Key: *R. officinalis* (RO), *R. tridentata* (RT), *X. caffra* (XC), *Z. muconata* (ZM), *Z. capense* (ZC), FIC, and MIC

5.3.3. Antibiofilm activity

The antibiofilm activity of the different plant acetone extracts was evaluated by measuring the growth of *M. smegmatis* in the presence of varying concentrations of the plants. Bacterial growth was inhibited by adding 100 µL of different concentrations of the plants, where rifampicin was used as the positive control. There was no significant difference between rifampicin and *X. caffra* (0.28 mg/mL), and rifampicin and *R. officinalis* (0.56 and 1.13 mg/mL). There was an increase in percentage inhibition as the concentration increased (Figure 5.2).

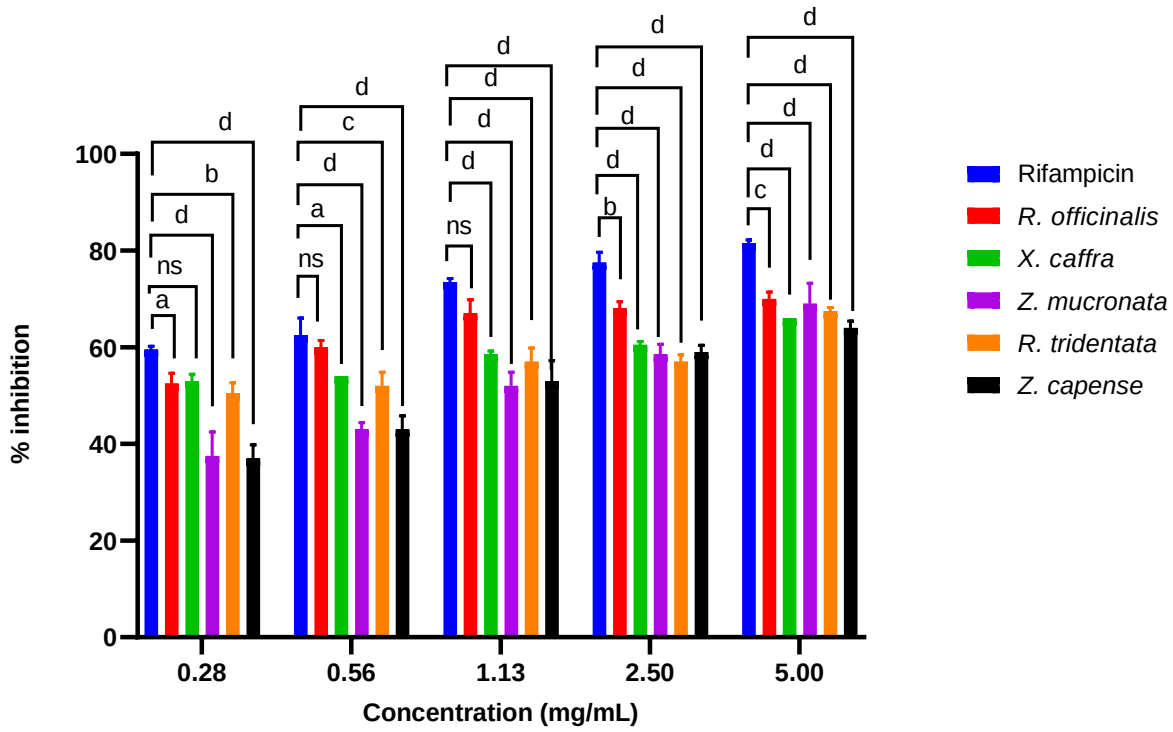

Figure 5. 2: The antibiofilm activity of the plant extracts against *M. smegmatis*. Results were analysed using two-way ANOVA, followed by Tukey multiple comparison post-hoc test.

Key: ns= non-significant, (a, b, c, and d)= level of significance compared to positive control

5.3.4. Cell viability assay

The MTT [3-(4,5-dimethylthiazol-2-yl)-2,5-diphenyltetrazolium bromide] reduction assay was used to test the effects of different plant acetone extracts for cell viability on THP-1 cell line. Varying concentrations (100 µg/mL, 500 µg/mL, and 1000 µg/mL) of plant extracts were prepared and used to treat cells while untreated cells were used as the positive control and DMSO as the negative control. The cell viability of the acetone extracts was determined on THP-1 cells and represented as percentage cell viability in a concentration dependant manner. There was no significant difference between the viability of untreated cells, 0.25% DMSO, *X. caffra* (100 and 500 µg/mL), *R. officinalis* (100 and 500 µg/mL), and R. tridentata (100 and 1000 µg/mL). There was a significant difference between *Z. capense*, *Z. mucronata*, *R. tridentata* (500 µg/mL), *X. caffra* (1000 µg/mL) and *R. officinalis* (1000 µg/mL). The leaves acetone extracts of *R. tridentata* had the highest percentage cell viability while *Z. mucronata* and *Z.*

capense had the lowest percentage cell viability. It shows that the acetone extracts of all plants were not toxic, except for *Z. mucronata* and *Z. capense* at 100 µg/mL, which were toxic to THP-1 cells (Figure 5.3).

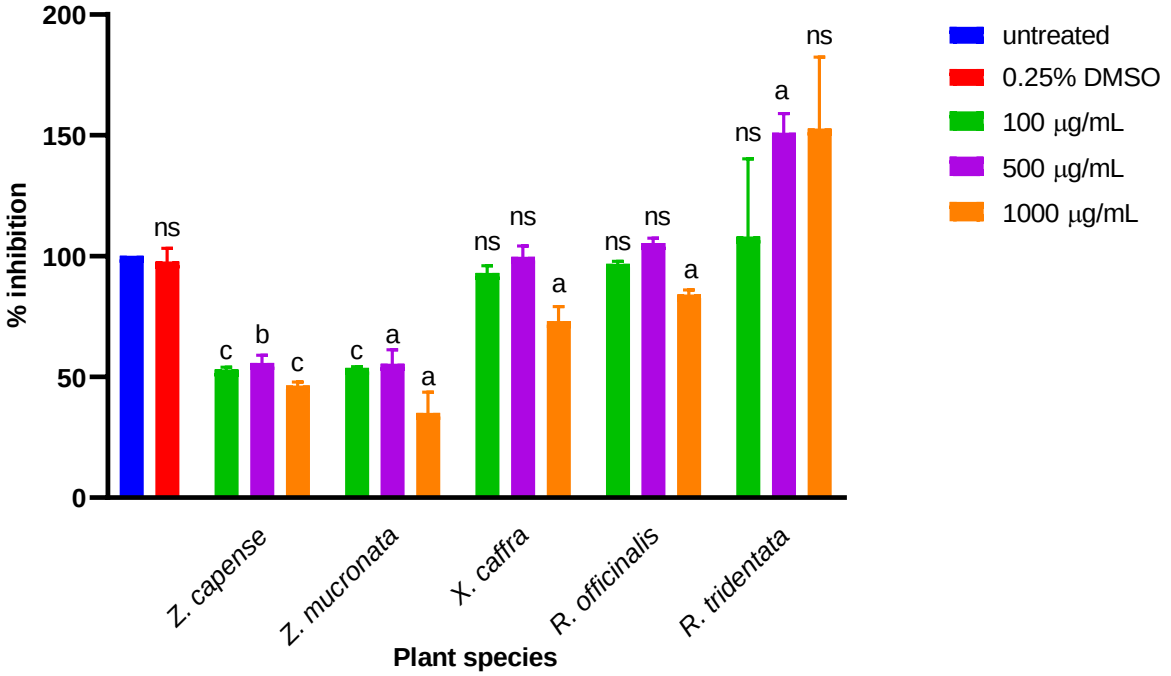

Figure 5. 3: The cytotoxicity effects of *Z. capense*, *Z. muconata*, *X. caffra*, *R. officinalis*, and *R. tridentata* using acetone extracts on THP-1 cells. The results were analysed using two-way ANOVA, followed by the Tukey multiple comparison post hoc test.

Key: ns = non-significant, (a, b, and c) = level of significance compared to untreated cells

5.4. Discussion

Antibacterial resistance to the well-known antibiotics is the major global health challenge now and will still be a challenge in the future (Adamczak *et al*., 2019; Farhadi *et al*., 2019). The antibacterial activity of the selected medicinal plants was screened using TLC in which the plates were developed in three different mobile phases (EMW, CEF and BEA) with varying polarities. TLC helps in revealing compounds that can be targeted for further analysis such as antimicrobial assays and isolation of the respective compounds (Ramese, 2019). The developed plates were sprayed with *Mycobacterium smegmatis* and incubated overnight to allow growth and then spayed with *p*-iodonitrotetrazolium violet (INT) and incubated for two to three hours to visualise

antibacterial activity. INT is used as an indicator of growth when checking the antibacterial activity of plants (Eloff, 2021). Figure 5.1 shows the antibacterial activity of the plants and the clear bands, also called zone of inhibition, against the pinkish background indicates the inhibition of *M. smegmatis* by plant extracts. *R. officinalis* and *Z. mucronata* showed to have activity against *Mycobacterium smegmatis*. *R. officinalis* with Rf values of 0.12 on the BEA plate and 0.81 on the EMW plate, while *Z. mucronata* had Rf value of 0.06 on the TLC plate developed in BEA and 0.79 on the EMW plate. Antibacterial activity was not observed from *X. caffra*, *Z. capense* and *R. tridentata* plant extracts. The CEF (intermediate polarity) plate did not show any activity from all the plant extracts. This does not specify that all plant extracts, which did not show antibacterial activity on the TLC plates, do not have antibacterial activity. Bioautography indicates only the active compounds separated on the TLC plate in an extract but it is not quantitative and it is also possible that other active compounds were present and not separated on the chromatograms; so, they had an antagonistic effect against each other (Famuyide *et al*., 2019).

The antibacterial activity of the plant extracts was quantified by determining the MIC values of the different plant extracts, where rifampicin was used as a positive control and acetone was used as a negative control. Rifampicin is one of the most well-known first anti-TB drugs (Zaw *et al*., 2018). INT was used as an indicator of growth. The colourless tetrazolium dye acts as an electron acceptor and is reduced to a red-coloured formazan product by biologically active organisms. Where microbial growth was inhibited, the solution in the well remained clear after incubation with INT, was taken as its MIC at which no red colour occurred (Omoruyi and Muchenje, 2017). The MIC values in Table 5.1 ranged from the lowest concentration of 0.08 mg/mL to 2.50 mg/mL. The lowest MIC value of 0.08 mg/mL, same as the positive control, was observed from the n-hexane, dichloromethane, acetone, and methanol extracts of *R. officinalis*. This was followed by 0.16 mg/mL from the hexane extract of *R. tridentata*. The dichloromethane extract of *R. tridentata* and the hexane extract of *X. caffra* had an MIC value of 0.31 mg/mL while the acetone and methanol extracts of *Z. mucronata* had an MIC value of 1.25 mg/mL. All other extracts had an MIC value greater than > 2.5 mg/mL, same as the negative control. *R. officinalis* is a good antibacterial plant because as reported by Al Zuhairi *et al*. (2020), it had an antibacterial effect against *S. aureus*, *K. pneumoniae,* and *P. vulgaris* strains with the zone of inhibition and MIC

values with the range 7.00 ± 0.00 - 9.6 ± 0.32 mm and 0.06 ± 0.00 to 0.16 ± 0.07 mg/mL, respectively. *R. tridentata* was reported to have a good antimicrobial activity against *Candida albicans* by Mamba (2017) with an MIC value of 0.8 mg/mL. Obtained MIC values were used to determine total activity (Table 5.2). The total highest activity of the plant extracts was found from *R. officinalis* methanol (1250 mL/g), dichloromethane (1125 mL/g) and acetone (875 mL/g) extracts, followed by *R. tridentata* hexane extract with a total activity of 769.2 mL/g. The lowest total activity of 8 mL/g was obtained from the n-hexane and water extracts of *Z. mucronata.* The active compounds vary from plant to plant due to their biodiversity (Alqethami and Aldhebiani, 2021). The potent antimycobacterial activity of the plant extracts may be due to the presence of phenolics, flavonoids, and tannins, which are reported to have good antimicrobial activity (Carica *et al*., 2020; Oikeh *et al*., 2020). Following the antibacterial activity of different plant extracts, acetone and n-hexane extracts were used for synergistic and antagonistic study. The different n-hexane and acetone plant extracts were combined to determine the MIC value of plant combinations. Combinations of antibacterial drugs are considered as a promising strategy to overcome bacterial resistance mechanisms and re-establish the effectiveness of antibiotics (Caesar and Cech, 2019). This approach involves antibiotic-antibiotic combination or combination of an antibiotic with a compound that when tested alone, is not active, but is able to have antibiotic activity when combined with another compound (Pereira *et al*., 2016). All n-hexane plant combinations with n-hexane *R. officinalis* extract had the lowest MIC value of 0.63 mg/mL while all the other plant combinations had the antibacterial activity of 2.50 mg/mL (Table 5.3). On the other side, using acetone extracts, *R. officinalis* combination with *R. tridentata* had the lowest MIC value of 0.42 mg/mL (Table 5.4). The second lowest MIC was found to be 0.52 mg/mL from the *R. officinalis*: *Z. mucronata* and *R. officinnalis*: *X.caffra*, while the *R.officinalis*: *Z. capense* had a potency of 0.63 mg/mL. Other combinations had an MIC valiue of 2.50 mg/mL.

The obtained MIC values of the plant combinations was used to determine the FIC index of the plants and if they are antagonistic, indifferent, or synergistic. Synergy is when the combined antimicrobial effect is greater than the sum of either treatment alone (Duong *et al*., 2021). An additive effect is used to describe situations where chemicals do not interact, but act together to produce effects without enhancing or

diminishing each other's actions (Rizzati *et al*., 2016), and antagonism is a phenomenon where two or more agents in combination have an overall effect that is less than the sum of their individual effects (Olszowy-Tomczyk, 2020). For n-hexane plant combinations (Table 5.3), *R. officinalis* and *Z. capense* combination had a synergistic outcome with the FIC index of 0.06, respectively. The *Z. mucronata and Z. capense* combination had an FIC index of 2.00, which is indifferent, while all the other combinations had an antagonistic effect. For acetone plant combinations (Table 5.4), the lowest FIC index was found from the *R. tridentata*: *X. caffra* and *R. tridentata*: *Z. capense* combinations, which was 2.00. All acetone combinations of the selected plants with *R. officinalis* had an antagonistic effect and the other acetone plant combinations were indifferent.

The antibiofilm activity of the plant acetone extracts was evaluated against *M. smegmatis*. The antibiofilm activity was measured in microtiter plate using crystal violet. The percentage inhibition of biofilm activity above 50% was considered as good antibiofilm activity and those with percentage inhibition between 0 and 50% were considered as poor antibiofilm activity (Adeyemo *et al*., 2022; Olawuwo *et al*., 2022). Figure 5.2 shows that there was a concentration dependent increase in antibiofilm activity from all the different plants and the positive control (rifampicin). There was no significant difference between rifampicin and *X. caffra* (0.28 mg/mL), and rifampicin and *R. officinalis* (0.56 and 1.13 mg/mL). The lowest antibiofilm activity was observed at 0.28 and 0.56 mg/mL of *Z. mucronata* and *Z. capense*, which is a poor antibiofilm activity.

The toxicity of the plants is a major concern with bioactive compounds and was determined using the cell viability assay. Plant materials and their extracts contain various toxic substances synthesised by plants as a defence against disease, insects, and other organisms (Modarresi *et al*., 2020). It is important to study the toxicological profile of medicinal plants and to provide a database on the toxicity of those plants because many traditional healers and indigenous remedies are not scientifically evaluated and some herbs are harmful (Kharchoufa *et al*., 2018). The MTT [3-(4,5-dimethylthiazol-2-yl)-2,5-diphenyltetrazolium bromide] reduction assay was used to test the effects of different plant acetone extracts for cell viability on THP-1 cell line. MTT assay is based on the mitochondrial nicotinamide adenine dinucleotide phosphate (NADPH)-dependent cellular oxidoreductase enzymes released in living

cells to convert MTT ((3-[4,5-dimethylthiazol-2-yl]-2,5 diphenyl tetrazolium bromide) to insoluble formazan crystals (Adan *et al*., 2016; Kuete *et al*., 2017; Grela *et al*., 2018). Varying concentrations (100 µg/mL, 500 µg/mL, and 1000 µg/mL) of acetone plant extracts were prepared and used to treat the cells while untreated cells were used as the positive control and 0.25% DMSO as the negative control. The metabolically active cells reduce the yellow colour of MTT to formazan, which indicates viable cells and quantified using spectrophotometric means (Ranjan *et al*., 2020). Figure 5.3 shows that there was no significant difference between the viability of untreated cells, 0.25% DMSO, *X. caffra* (100 and 500 µg/mL), *R. tridentata* (100 and 1000 µg/mL), and *R. officinalis* (100 and 500 µg/mL) after incubation. There was a significant difference between *Z. capense*, *Z. mucronata*, *R. tridentata* (500 µg/mL), *X. caffra* (1000 µg/mL) and *R. officinalis* (1000 µg/mL). The leaves acetone extracts of *R. tridentata* had the highest percentage cell viability while *Z. mucronata* and *Z. capense* had the lowest percentage cell viability. It shows that the acetone extracts of all the plants were not toxic except for *Z. mucronata* and *Z. capense* at 100 µg/mL, which were toxic to THP-1 cells.

5.5. Conclusion

Obtained results show that selected plants have medicinal purposes as they have antibacterial activity against *Mycobacterium smegmatis*, especially *R. officinalis* with the lowest MIC. It is recommended that the plant extracts must be tested against the *Mycobacterium tuberculosis* strain H37Rv. Plants had promising antibiofilm activity at different concentrations, except *Z. capense* and *Z mucronata* at 0.28 and 0.56 mg/mL. For toxicity, results obtained suggest that it is good to use the plants (*Z. mucronata* and *Z. capense*) with caution at a lower concentration of 100 µg/mL. Other plant extracts were not toxic to THP-1 cells. Further studies, such as *in vivo* assays, need to be performed to evaluate the reaction of plant extracts in living organisms.

5.6. References

Adamczak, A., Ożarowski, M. and Karpiński, T.M. 2019. Antibacterial activity of some flavonoids and organic acids widely distributed in plants. *Journal of Clinical Medicine*, **9(**1): 109.

Adan, A., Kiraz, Y. and Baran, Y. 2016. Cell proliferation and cytotoxicity assays. *Current Pharmaceutical Biotechnology*, **17**(14): 1213-1221.

Adeyemo, R.O., Famuyide, I.M., Dzoyem, J.P. and Lyndy Joy, M. 2022. Anti-biofilm, antibacterial, and anti-quorum sensing activities of selected South African plants traditionally used to treat diarrhoea. *Evidence-Based Complementary and Alternative Medicine*, **2022**: 1-12.

Alqethami, A. and Aldhebiani, A.Y. 2021. Medicinal plants used in Jeddah, Saudi Arabia: phytochemical screening. *Saudi Journal of Biological Sciences*, **28**(1): 805-812.

Al Zuhairi, J.J.M.J., Kashi, F.J., Rahimi-Moghaddam, A. and Yazdani, M. 2020. Antioxidant, cytotoxic and antibacterial activity of *Rosmarinus officinalis* L. essential oil against bacteria isolated from urinary tract infection. *European Journal of Integrative Medicine*, **38**: 101192.

Armengol, E.S., Harmanci, M. and Laffleur, F. 2021. Current strategies to determine antifungal and antimicrobial activity of natural compounds. *Microbiological Research*, **252**: 126867.

Aslantürk, Ö.S. 2018. *In vitro* cytotoxicity and cell viability assays: principles, advantages, and disadvantages. *Genotoxicity-A Predictable Risk to Our Actual World*, **2**: 64-80.

Bahuguna, A., Khan, I., Bajpai, V.K. and Kang, S.C. 2017. MTT assay to evaluate the cytotoxic potential of a drug. *Bangladesh Journal of Pharmacology*, **12**(2): 115-118.

Balouiri, M., Sadiki, M. and Ibnsouda, S.K. 2016. Methods for in vitro evaluating antimicrobial activity: a review. *Journal of Pharmaceutical Analysis*, **6**(2): 71-79.

Barbieri, R., Coppo, E., Marchese, A., Daglia, M., Sobarzo-Sánchez, E., Nabavi, S.F. and Nabavi, S.M. 2017. Phytochemicals for human disease: an update on plant-derived compounds antibacterial activity. *Microbiological Research*, **196**: 44-68.

Begue, W.J. and Kline, R.M. 1972. The use of tetrazolium salts in bioautographic procedures. *Journal of Chromatography*, **64**(1): 182-184.

Caesar, L.K. and Cech, N.B. 2019. Synergy and antagonism in natural product extracts: when 1+ 1 does not equal 2. *Natural Product Reports*, **36**(6): 869-888.

Dwivedi, M.K., Sonter, S., Mishra, S., Patel, D.K. and Singh, P.K. 2020. Antioxidant, antibacterial activity, and phytochemical characterization of *Carica papaya* flowers. *Beni-Suef University Journal of Basic and Applied Sciences*, **9**(1): 1-11.

Chakraborty, P., Bajeli, S., Kaushal, D., Radotra, B.D. and Kumar, A. 2021. Biofilm formation in the lung contributes to virulence and drug tolerance of *Mycobacterium tuberculosis*. *Nature Communications*, **12**(1): 1-17.

Chanput, W., Mes, J.J. and Wichers, H.J. 2014. THP-1 cell line: an *in vitro* cell model for immune modulation approach. *International Immunopharmacology*, **23**(1): 37-45.

Chouhan, S., Sharma, K. and Guleria, S. 2017. Antimicrobial activity of some essential oils—present status and future perspectives. *Medicines*, **4**(3): 58.

Danish, P., Ali, Q., Hafeez, M.M. and Malik, A. 2020. Antifungal and antibacterial activity of aloe vera plant extract. *Biological and Clinical Sciences Research Journal*, **2020**(1): 1-8.

Djordjevic, D., Wiedmann, M. and McLandsborough, L.A. 2002. Microtiter plate assay for assessment of *Listeria monocytogenes* biofilm formation. *Applied and Environmental Microbiology*, **68**(6): 2950-2958.

Duong, L., Gross, S.P. and Siryaporn, A. 2021. Developing antimicrobial synergy with AMPs. *Frontiers in Medical Technology*, **3**: 9.

Elisha, I.L., Botha, F.S., McGaw, L.J. and Eloff, J.N. 2017. The antibacterial activity of extracts of nine plant species with good activity against *Escherichia coli* against five other bacteria and cytotoxicity of extracts. *BMC Complementary and Alternative Medicine*, **17**(1): 1-10.

Eloff, J.N. 1998. A sensitive and quick microplate method to determine the minimal inhibitory concentration of plant extracts for bacteria. *Journal of Medicinal Plant and Natural Product*, **64**(8): 711-713.

Eloff, J.N. 2021. A proposal towards a rational classification of the antimicrobial activity of acetone tree leaf extracts in a search for new antimicrobials. *Planta Medica*, **87**(10/11): 836-840.

Famuyide, I.M., Aro, A.O., Fasina, F.O., Eloff, J.N. and McGaw, L.J. 2019. Antibacterial activity and mode of action of acetone crude leaf extracts of under-investigated *Syzygium* and *Eugenia* (Myrtaceae) species on multidrug resistant porcine diarrhoeagenic *Escherichia coli*. *BMC Veterinary Research*, **15**(1): 1-14.

Famuyide, I.M., Aro, A.O., Fasina, F.O., Eloff, J.N. and McGaw, L.J. 2019. Antibacterial and antibiofilm activity of acetone leaf extracts of nine under-investigated south African *Eugenia* and *Syzygium* (Myrtaceae) species and their selectivity indices. *BMC Complementary and Alternative Medicine*, **19**(1): 1-13.

Farhadi, F., Khameneh, B., Iranshahi, M. and Iranshahy, M. 2019. Antibacterial activity of flavonoids and their structure–activity relationship: an update review. *Phytotherapy Research*, **33**(1): 13-40.

Grela, E., Kozłowska, J. and Grabowiecka, A. 2018. Current methodology of MTT assay in bacteria– a review. *Acta Histochemica*, **120**(4): 303-311.

Jouda, M.M., Elbashiti, T., Masad, A. and Albayoumi, M. 2016. The antibacterial effect of some medicinal plant extracts and their synergistic effect with antibiotics. *World Journal of Pharmacy and Pharmaceutical Sciences*, **5**(2): 23-33.

Kharchoufa, L., Merrouni, I.A., Yamani, A. and Elachouri, M. 2018. Profile on medicinal plants used by the people of North Eastern Morocco: toxicity concerns. *Toxicon*, **154**: 90-113.

Khelissa, S.O., Abdallah, M., Jama, C., Faille, C. and Chihib, N.E. 2017. Bacterial contamination and biofilm formation on abiotic surfaces and strategies to overcome their persistence. *Journal of Materials and Environmental Science*, **8**(9): 3326-3346.

Kuete, V., Karaosmanoğlu, O. and Sivas, H. 2017. Anticancer activities of African medicinal spices and vegetables. In *Medicinal spices and vegetables from Africa.* 1st Ed. London Hall, London, United Kingdom, pp. 271-297.

Kumar, A., Alam, A., Grover, S., Pandey, S., Tripathi, D., Kumari, M., Rani, M., Singh, A., Akhter, Y., Ehtesham, N.Z. and Hasnain, S.E. 2019. Peptidyl-prolyl isomerase-B is involved in *Mycobacterium tuberculosis* biofilm formation and a generic target for drug repurposing-based intervention. *npj Biofilms and Microbiomes*, **5**(1): 1-11.

Kurhekar, J., Tupas, G.D. and Otero, M.C.B. 2019. *In-vitro* assays for antimicrobial assessment. In *Phytochemistry: An In-silico and In-vitro Update,* pp. 279-298.

Kumar, P., Nagarajan, A. and Uchil, P.D. 2018. Analysis of cell viability by the MTT assay. *Cold Spring Harbor Protocols*, **2018**(6): 95505.

Mamba, P.B. 2017. *Bioactivity of selected medicinal plants used for the treatment of sexually transmitted diseases*. (Doctoral dissertation, University of Pretoria).

Massoud, R., Saffari, H., Massoud, A. and Moteian, M.Y. 2019. Screening methods for assessment of antibacterial activity in nature. *Applied Researchers in Science and Engineering*, **4**:1-9.

Modarresi, C.A., Arsad, H. and Lim, V. 2020. Zebrafish as a successful animal model for screening toxicity of medicinal plants. *Plants*, **9**(10): 1345.

Mosmann, T. 1983. Rapid colorimetric assay for cellular growth and survival: application to proliferation and cytotoxicity assays. *Journal of Immunological Methods*, **65**: 55-63.

Murei, A. 2019. *Synthesis, characterization and evaluation of novel treatment against resistant pathogenic bacteria*. (Doctoral dissertation, University of Venda).

Ncama, K., Mditshwa, A., Tesfay, S.Z., Mbili, N.C. and Magwaza, L.S. 2019. Topical procedures adopted in testing and application of plant-based extracts as bio-fungicides in controlling postharvest decay of fresh produce. *Crop Protection*, **115**: 142-151.

Oikeh, E.I., Oviasogie, F.E. and Omoregie, E.S. 2020. Quantitative phytochemical analysis and antimicrobial activities of fresh and dry ethanol extracts of *Citrus sinensis* (L.) Osbeck (sweet Orange) peels. *Clinical Phytoscience*, **6**(1): 1-6.

Olawuwo, O.S., Famuyide, I.M. and McGaw, L.J. 2022. Antibacterial and antibiofilm activity of selected medicinal plant leaf extracts against pathogens implicated in poultry diseases. *Frontiers in Veterinary Science*, **9**.

Olszowy-Tomczyk, M. 2020. Synergistic, antagonistic, and additive antioxidant effects in the binary mixtures. *Phytochemistry Reviews*, **19**(1): 63-103.

Omoruyi, B.E. and Muchenje, V. 2017. Phytomedical assessment of two *Cymbopogon* species found in Nkonkobe Municipality: toxicological effect on human Chang liver cell line. *BMC Complementary and Alternative Medicine*, **17**(1): 1-12.

Owen, L., White, A.W. and Laird, K. 2019. Characterisation and screening of antimicrobial essential oil components against clinically important antibiotic-resistant bacteria using thin layer chromatography-direct bioautography hyphenated with GC-MS, LC-MS and NMR. *Phytochemical Analysis*, **30**(2): 121-131.

Pereira, F., Madureira, A.M., Sancha, S., Mulhovo, S., Luo, X., Duarte, A. and Ferreira, M.J.U. 2016. *Cleistochlamys kirkii* chemical constituents: antibacterial activity and synergistic effects against resistant *Staphylococcus aureus* strains. *Journal of Ethnopharmacology*, **178**: 180-187.

Padhi, A., Naik, S.K., Sengupta, S., Ganguli, G. and Sonawane, A. 2016. Expression of *Mycobacterium tuberculosis* NLPC/p60 family protein Rv0024 induce biofilm formation and resistance against cell wall acting anti-tuberculosis drugs in *Mycobacterium smegmatis*. *Microbes and Infection*, **18**(4): 224-236.

Ramese, N. 2019. *Identification and characterisation of compounds with antimycobacterial activity from Stomatostemma monteiroae.* (Doctoral dissertation, University of Limpopo).

Ranjan, S., Dasgupta, N., Mishra, D. and Ramalingam, C. 2020. Involvement of Bcl-2 activation and G1 cell cycle arrest in colon cancer cells induced by titanium dioxide nanoparticles synthesized by microwave-assisted hybrid approach. *Frontiers in Bioengineering and Biotechnology*, **8**: 606.

Richards, J.P., Cai, W., Zill, N.A., Zhang, W. and Ojha, A.K. 2019. Adaptation of *Mycobacterium tuberculosis* to biofilm growth is genetically linked to drug tolerance. *Antimicrobial Agents and Chemotherapy*, **63**(11): 19.

Rizzati, V., Briand, O., Guillou, H. and Gamet-Payrastre, L. 2016. Effects of pesticide mixtures in human and animal models: an update of the recent literature. *Chemico-Biological Interactions*, **254**: 231-246.

Safar, R., Doumandji, Z., Saidou, T., Ferrari, L., Nahle, S., Rihn, B.H. and Joubert, O. 2019. Cytotoxicity and global transcriptional responses induced by zinc oxide nanoparticles NM 110 in PMA-differentiated THP-1 cells. *Toxicology Letters*, **308**: 65-73.

Schilcher, K. and Horswill, A.R., 2020. Staphylococcal biofilm development: structure, regulation, and treatment strategies. *Microbiology and Molecular Biology Reviews*, **84**(3): 19.

Stanković, N., Mihajilov-Krstev, T., Zlatković, B., Stankov-Jovanović, V., Mitić, V., Jović, J., Čomić, L., Kocić, B. and Bernstein, N. 2016. Antibacterial and antioxidant activity of traditional medicinal plants from the Balkan Peninsula. *NJAS-Wageningen Journal of Life Sciences*, **78**: 21-28.

van Vuuren, S.F. and Viljoen, A.M. 2008. In vitro evidence of phyto-synergy for plant part combinations of *Croton gratissimus* (Euphorbiaceae) used in African traditional healing. *Journal of Ethnopharmacology*, **119**(3): 700-704.

Wikaningtyas, P. and Sukandar, E.Y. 2016. The antibacterial activity of selected plants towards resistant bacteria isolated from clinical specimens. *Asian Pacific Journal of Tropical Biomedicine*, **6**(1): 16-19.

Zaw, M.T., Emran, N.A. and Lin, Z. 2018. Mutations inside rifampicin-resistance determining region of rpoB gene associated with rifampicin-resistance in *Mycobacterium tuberculosis. Journal of Infection and Public Health*, **11**(5): 605-610.

CHAPTER 6

6. Isolation and purification of antioxidant and antimycobacterial compounds

6.1. Introduction

Since the emergence of multidrug resistance due to inappropriate, irregular, and irrational uses of antibiotics, there has been an increased interest in developing new drugs from medicinal plants (Anand *et al*., 2019). Historically, natural products have proved to be the most prolific and a diverse source of antibiotics, including those used for the treatment of TB (Nguta *et al*., 2016). Medicinal plants have been used for thousands of years and are still used for their health benefits and most modern medicines are produced from them (Dar *et al*., 2017). Plants' secondary metabolites are the most important indicators for evaluating the quality of medicinal plants. Therefore, there is a need to develop new agents that are efficient against drug resistant strains and faster acting mechanisms (Kumar *et al*., 2017).

Due to the effectiveness and less/no side effects of medicinal plants, they are explored for the isolation of plant-derived drugs (Venieraki *et al*., 2017). The most used procedure to isolate a pure biological chemical agent from natural products is the bioassay-guided fractionation. It is a step-by-step process of separating extracted components based on their differences in physiochemical properties and assessing the biological activity, followed by another round of separation and assaying (Malviya and Malviya, 2017). Bioassay is divided into direct and indirect bioassay. During direct bioassay, the concentration or potency of a substance is measured, which is required to obtain a specific response whereas indirect bioassay is determined by comparing responses of the equal concentrations of a sample and the accurate standard to achieve a given response (Indrayanto *et al*., 2021).

Bioactive compounds are synthesised in small quantities in plants and are enclosed within the plant matrix and are sometimes mixed with other compounds; noteworthy, a good extraction method is required for extraction (Omeroglu *et al*., 2019). Extraction is the first crucial procedure in the analysis of medicinal plants, because it is necessary to extract the desired chemical components from the plant materials for further separation and characterisation (Sasidharan *et al*., 2011). Extraction affects active compounds both qualitatively and quantitatively. Serial exhaustive extraction is the

gentlest extraction technique where nonpolar extracts are fractionated with solvents of increasing polarity to ensure maximum extraction (Jha and Sit, 2022).

Discovering new bioactive compounds from natural products as leads for the development of new therapeutics is inspired by ethnopharmacological knowledge or achieved by screening a collection of extracts for bioactivity, using *in vitro*, *in cellulo*, and even *in vivo* assays (Nothias *et al*., 2018). The bioautopgraphy technique is used to determine bioactive compounds with antimicrobial activity from plant extracts and helps with localising the compounds to be isolated from a mixture of compounds (Sasidharan *et al*., 2011).

Chromatography is based on the principle where molecules in a mixture applied onto the surface or into the solid, and fluid stationary phase (stable phase) separate from each other while moving with the aid of a mobile phase. The factors effective on this separation process include molecular characteristics related to adsorption (liquid-solid), partition (liquid-solid), and affinity or differences among their molecular weights (Coskun, 2016). In column chromatography, the stationary phase is a solid adsorbent placed in a vertical glass and the mobile phase is a liquid added to the top and flows down through the column by gravity or external pressure (Ibarra-Rivera *et al*., 2020). The most used adsorbent in column chromatography is silica, which separates compounds based on polarity. It does not have a good surface to separate compounds of the same polarity (Pasban *et al*., 2017; Mostafavi *et al*., 2014).

This chapter focused on extracting bioactive compounds using serial exhaustive extraction, determined the antioxidant and antimicrobial activity of *R. officinalis*, and used silica gel as the stationary phase and solvents of increasing polarities to elute different compounds. The compounds were collected as different fractions and analysed again on TLC plates while checking their biological activity, and further chromatographically fractioned and checked biological activity. Preparative TLC was used to scrab off the active compounds and then NMR was used to analyse the pure compound for structure elucidation. The main aim of this chapter was to isolate the bioactive compounds of *R. officinalis* using bioassay-guided fractionation.

6.2. Method and materials

6.2.1. Serial exhaustive extraction

Serial exhaustive extraction was used to extract bioactive compounds from *Rosmarinus officinalis* plant material since it had promising antibacterial activity. Exactly 1 kg of the plant material was weighed and dissolved in 6 litres of n-hexane in a bottle. The bottle was vigorously shaken overnight at 200 rpm using a shaker (Thermo Scientific MaxQ 3000). Plant material was allowed to settle for 30 minutes, the supernatant was filtered and then the same solvent was added twice, and was vigorously shaken for three hours. The same plant residue was extracted using dichloromethane, acetone and methanol using the same procedure. Extracts were concentrated using rotary evaporator (Buchi R-114) at 50 °C and transferred into pre-weighed labelled 250 mL beakers. The remaining solvents were evaporated from the extracts under a stream of cold air at room temperature and the masses of the crude extracts were determined.

6.2.2. Phytochemical analysis

The chemical profiles of the *R. officinalis* extracts were analysed on aluminium-baked TLC plates using a method described by Kotze and Eloff (2002), as explained in section 3.2.3.

6.2.3. Antioxidant activity on TLC

Qualitative 2, 2-diphenyl-1-picrylhydrazyl radical (DPPH) assay was done using TLC, according to the method described by Braca *et al*. (2002), as explained in section 4.2.1.

6.2.4. Bioautography assay

Bioautography was done according to the method described by Begue and Kline (1972), as described in section 5.2.1.

6.2.5. Serial broth micro-dilution assay

The serial broth micro-dilution method described by Eloff (1998) was used to determine the MIC values of the extracts against *Mycobacterium smegmatis,* as explained in section 5.2.2.

6.2.6. Isolation of antioxidant and antibacterial compounds

6.2.6.1. First open column chromatography

The dichloromethane (D1, D2 and D3) extracts resulting from the serial exhaustive extraction were selected and subjected to open column chromatography because they had the same antibacterial activity. An open column (3 cm radius × 59.5 cm height) was packed with silica gel 60 (particles size 0.063 - 0.200 mm) (Fluka) using 100% n-hexane. The dichloromethane extracts (63.71 g) were mixed with a little amount of silica gel and subjected to column chromatography. The chemical constituents of the extracts were eluted through an open column using 1.6 L of the solvent systems, as illustrated in Table 6.1. The fractions were collected and concentrated using a rotary evaporator (Buchi R-114). The solvents were completely evaporated under a stream of cold air in pre-weighed 100 mL beakers at room temperature and the masses of the crude extracts were determined. The fractions were then phytochemically analysed using TLC, tested for antioxidant activity using TLC-DPPH and antibacterial activity using bioautography and serial broth micro-dilution assay.

Table 6. 1: Solvent systems used in the first column.

Solvent systems	Percentage (%)
n-Hexane	100
n-Hexane: Ethyl acetate	90:10
	80:20
	70:30
	50:50
	30:70
	10:90
Ethyl acetate	100
Ethyl acetate: Methanol	90:10
	80:20
	70:30
	50:50
	30:70
	10:90

Methanol	100

6.2.6.2. Second open column chromatography

The results from the first open column chromatography showed that the compound of interest is present in fractions 7-11 (10% n-hexane: ethyl acetate, 100% ethyl acetate and 90-70% ethyl acetate: methanol) with high antibacterial activity and same chemical profiles. Three different mobile systems were chosen to check the one which separates the compounds best (Table 6.2).

Table 6.2: Mobile phases used to determine the eluent for second open column chromatography.

Mobile phase	Solvent system
First	100% n-hexane
Second	50% n-hexane: 50% ethyl acetate
Third	100% ethyl acetate

It was observed that the compounds were able to separate in the non-polar mobile system (100% n-hexane). This shows that the compound was non-polar and separated better when using the combination of 50% n-hexane: 50% ethyl acetate. Since the compound was non-polar, various non-polar solvent combinations were used as mobile phases (Table 6.3) to determine a solvent combination which can separate the targeted compound from other compounds.

Table 6.3: Non-polar systems for determination of the eluent for second open column chromatography.

Mobile phase	Solvent system
First	70% n-hexane: 30% ethyl acetate
Second	80% n-hexane: 20% ethyl acetate
Third	90% n-hexane: 10% ethyl acetate

The chosen crude extracts were combined making a total mass of 17.46 g for further separation and purification of bioactive solvents. The combined fractions were subjected to open column chromatography (3 cm radius × 68.5 cm height) packed with silica gel using 80% n-hexane: 20% ethyl acetate. The column was eluted with the solvent used when packing into small test tubes and concentrated under a stream of cold air. The phytochemical profile of the fractions was analysed using TLC and those with similar chemical profiles were combined. The combined concentrated fractions were tested for the presence of phytochemicals, and antibacterial activity using bioautography and serial broth micro-dilution assay.

6.2.6.3. Preparative TLC

The sub-fractions [test tubes (121 to 240) and (241 to 300)] from the second open column chromatography were mixed and subjected to separation on TLC silica gel glass plates (Merck Silica gel 60 F254) using 80% n-hexane: 20% ethyl acetate. The compounds were visualised using an ultraviolet light at 254 nm and 365 nm. Thereafter, a pencil was used to circle where the different compounds were visualised. The compounds were then scraped off from the plate using a surgical blade. The compounds were separated from the silica by immersing them in ethyl acetate, vortexed and filtered using cotton wool. The isolated compounds were tested for purity on TLC plates and antibacterial activity against *M. smegmatis* using bioautography and micro broth-dilution assay.

6.3. Results

6.3.1. Serial exhaustive extraction: The quantity of the plant material extracted from *R. officinalis*

Serial exhaustive extraction was used to extract the ground leaves (1 Kg) of *R. officinalis* with solvents of varying polarities (n-hexane, dichloromethane, acetone, and methanol), which resulted with a total mass of 216.44 g. Methanol was the best extractant (71.63 g), followed by dichloromethane (63.71 g) then n-hexane (50.13 g), while acetone extracted the least (30.94 g) (Table 6.4).

Table 6. 4: Masses (g) extracted from *R. officinalis*.

Extracts		Mass residue (g)	
		Mass	Total
n-Hexane	1	24.40	
	2	14.94	50.13
	3	10.79	
Dichloromethane	1	35.40	
	2	18.52	63.71
	3	9.79	
Acetone	1	15.90	
	2	8.31	30.94
	3	6.73	
Methanol	1	40.95	
	2	15.19	71.63
	3	15.49	
	Total		216.44

6.3.2. Phytochemical analysis on TLC

The n-hexane, dichloromethane, acetone, and methanol extracts of *R. officinalis* was separated using TLC plates developed in three mobile systems (BEA, CEF, and EMW). The separated compounds were visualised under an UV light (Figure 6.1) at 254 nm (A) and 365 nm (B). The different colours observed on the chromatograms indicated the different chemical compounds present in the plant material. More fluorescing compounds were observed at 365 nm on a plate developed in the BEA solvent system. The plates were further sprayed with the vanillin-sulphuric acid reagent to visualise non-fluorescing compounds (Figure 6.2). More distinct compounds from n-hexane and dichloromethane extracts were observed on a plate developed in BEA, meaning it contained non-polar compounds. Acetone and methanol showed their distinct compounds in a plate developed in EMW, showing that they contained polar compounds.

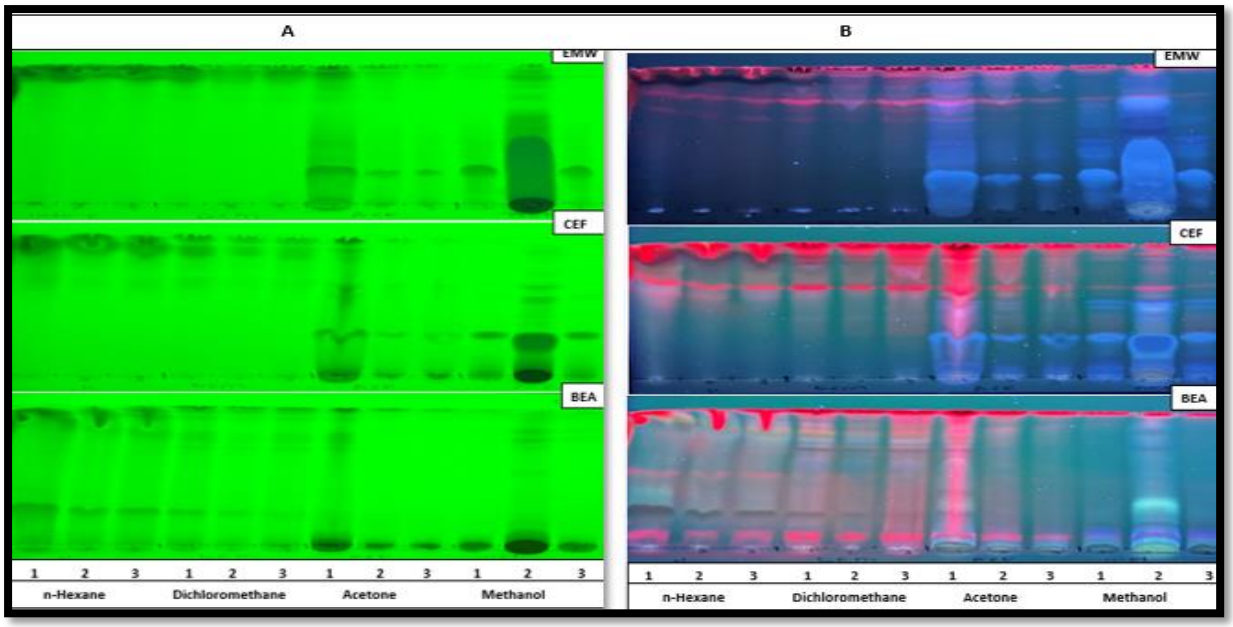

Figure 6. 1: The chromatograms obtained using extracts from serial exhaustive extraction of *R. officinalis* leaves using different solvents and developed in EMW, CEF, and BEA solvent systems and visualised at 254 nm (A) and 365 nm (B).

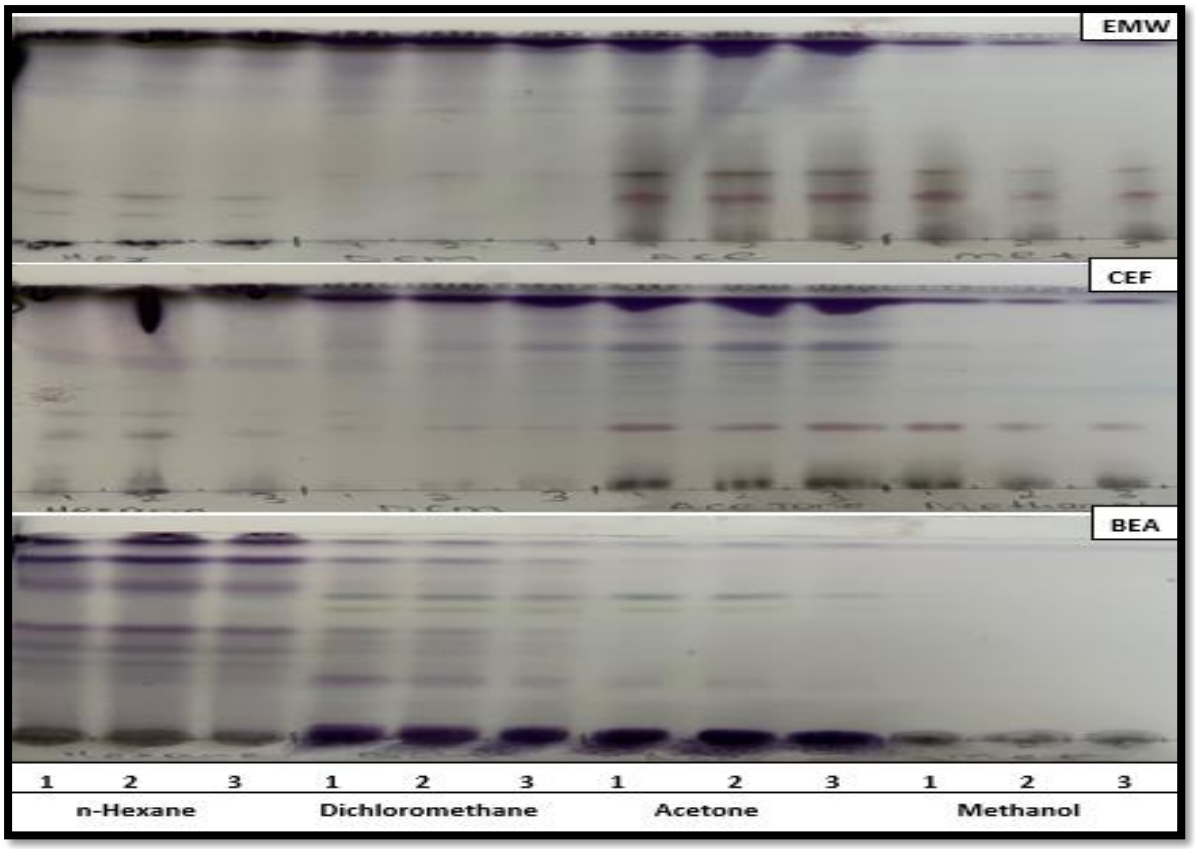

Figure 6. 2: The chromatograms obtained using extracts from a serial exhaustive extraction of *R. officinalis* leaves using different solvents and developed in EMW, CEF, and BEA solvent systems and sprayed with the vanillin sulphuric acid reagent.

6.3.3. DPPH Thin Layer Chromatography assay

The antioxidant activity of the plant extracts was determined by separating the extractants (n-hexane, dichloromethane, acetone, and methanol extracts) of *R. officinalis* using TLC plates developed in three mobile systems (BEA, CEF, and EMW). The plates were sprayed with 0.2% DPPH in methanol. The antioxidant activity of the extracts was indicated by the presence of yellow bands against the purple background. The obtained results show that all extracts had antioxidant compounds (Figure 6.3).

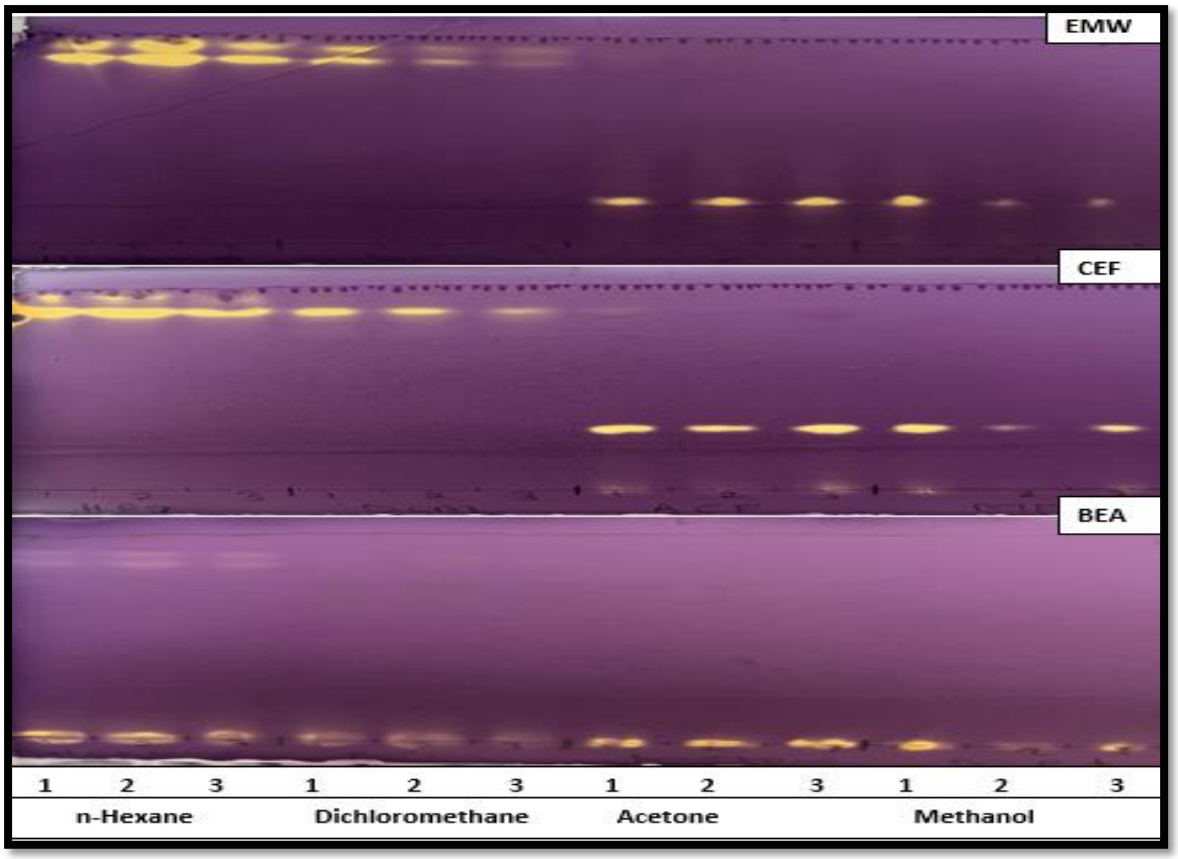

Figure 6. 3: Chromatograms of *R. officinalis* extracts developed in EMW, CEF, and BEA mobile systems and sprayed with 0.2% DPPH dissolved in methanol.

6.3.4. Bioautography assay

The qualitative antibacterial activity assay of the crude extracts was determined using the bioautography assay, where the TLC plates were developed in three mobile phases (BEA, CEF and EMW) and sprayed with *M. smegmatis*. The clear bands against the pinkish background on the chromatograms indicated antibacterial activities of the plant extracts. All plant extracts had antibacterial activity, but the most prominent antibacterial activity bands were observed from dichloromethane and acetone extracts on the BEA mobile system (Figure 6.4).

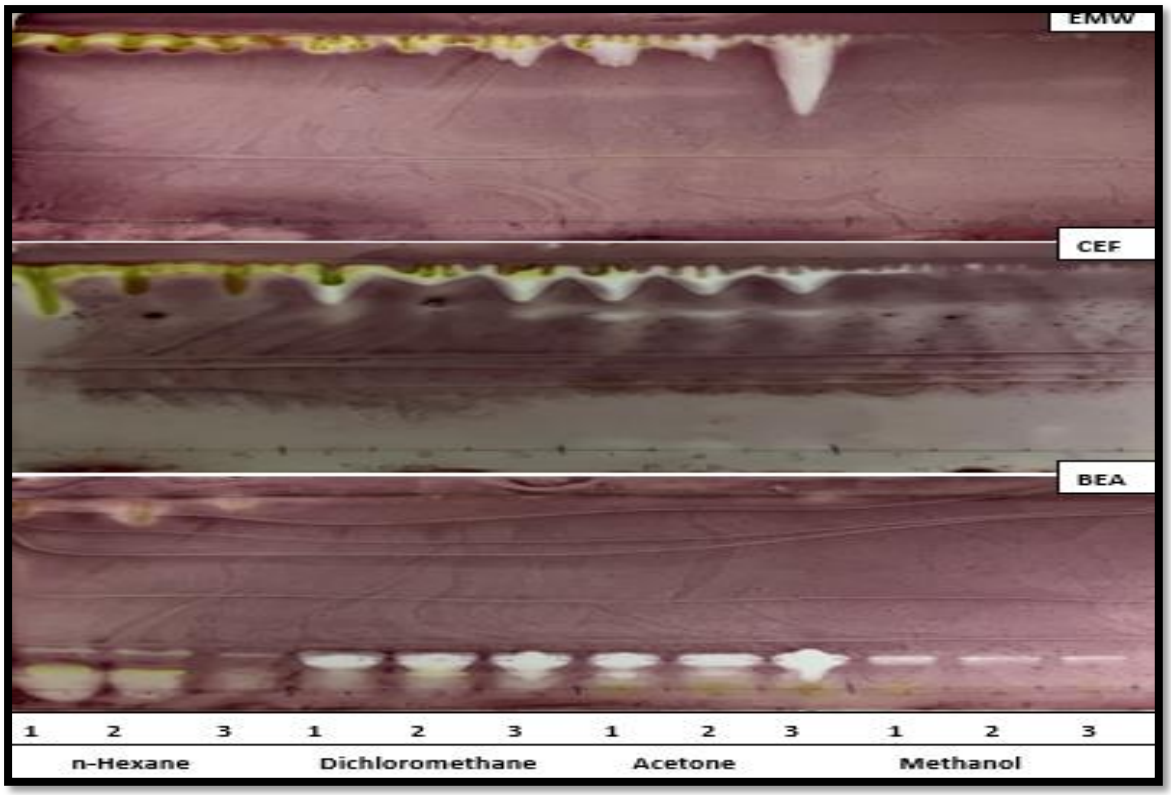

Figure 6. 4: The chromatograms showing antibacterial activity of *R. officinalis* plant extracts developed in EMW, CEF, and BEA and sprayed with *M. smegmatis*.

6.3.5. Serial broth micro-dilution assay

A serial broth micro-dilution assay was used to determine the MIC of the plant extracts against *M. smegmatis*. It was found that the n-hexane extracts (H2 and H3 = 0.156 mg/mL, and H1 = 0.182 mg/mL) (Table 6.5) had the lowest MIC, followed by dichloromethane extracts (0.3125 mg/mL) and then the first acetone extract (A1) (1.125 mg/mL). The methanol extracts had the least activity.

Table 6. 5: The MIC values obtained from serial exhaustive extraction extracts against *Mycobacterium smegmatis*.

Extract	MIC value (mg/mL)
n-Hexane 1	0.182
n-Hexane 2	0.156
n-Hexane 3	0.156
Dichloromethane 1	0.3125
Dichloromethane 2	0.3125
Dichloromethane 3	0.3125

Acetone 1	1.125
Acetone 2	2.5
Acetone 3	2.5
Methanol 1	1.875
Methanol 2	2.5
Methanol 3	2.5

6.3.6. Isolation of bioactive compounds from dichloromethane extracts

6.3.6.1. First open column chromatography

Even though the n-hexane extracts had the lowest MIC, the dichloromethane extracts were chosen for isolation of antibacterial compounds. This is because they had the second same lowest MIC value and the bands on the TLC plate from bioautography were more prominent compared to the n-hexane bands. The combined dichloromethane (63.71 g) extracts were subjected to the first open column chromatography and eluted with solvents of varying polarities. Different fractions were collected into pre-weight beakers, dried, and extracted mass compounds were recorded (Table 6.6). The highest mass was extracted with 70% n-hexane: 30% ethyl acetate (21.25 g), followed by 50% n-hexane: 50% ethyl acetate (9.49 g), and then 30% n-hexane: 70% ethyl acetate (8.96 g), and the least extractant was 100% n-hexane, which extracted 0.10 g.

Table 6. 6: Extracted fraction masses (g) obtained from a combination of dichloromethane extracts using solvents of varying polarities.

Solvent systems	Percentage (%)	Mass extracted (g)
n-Hexane	100	0.10
n-Hexane: Ethyl acetate	90:10	0.57
	80:20	8.65
	70:30	21.25
	50:50	9.49
	30:70	8.96
	10:90	5.21
Ethyl acetate	100	5.38

Ethyl acetate: Methanol	90:10	3.37
	80:20	2.30
	70:30	1.20
	50:50	0.92
	30:70	0.62
	10:90	0.26
Methanol	100	0.14

6.3.6.1.1. Phytochemical analysis of 1st column chromatography fractions

The collected different fractions of first open column chromatography were analysed using TLC plates developed in EMW, CEF, and BEA mobile systems. The plates were visualised under the UV light (Figure 6.5) at 254 nm (A) and 365 nm (B). More fluorescing compounds were observed from 70% n-hexane: 30% ethyl acetate to 10% n-hexane: 90% ethyl acetate. The TLC plates were further sprayed with the vanillin-sulphuric acid reagent to visualise non-fluorescing compounds (Figure 6.6). More compounds were observed on a plate developed in BEA mobile system. Compounds from 10 % n-hexane: 90% ethyl acetate to 70% ethyl acetate: 30% methanol had almost the same chemical compounds on the plate developed in the BEA mobile system.

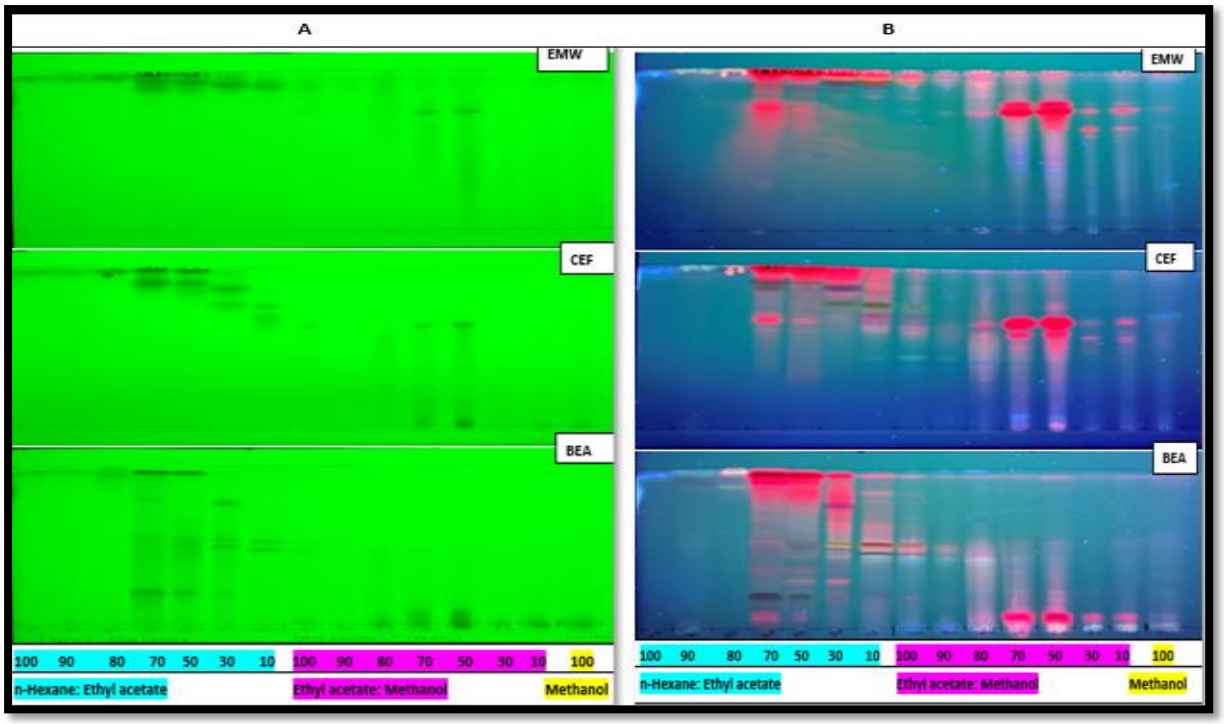

Figure 6. 5: The chromatograms of different fractions obtained from first open column chromatography of *R. officinalis* developed in EMW, CEF, and BEA mobile systems and visualised at 254 nm (A) and 365 nm (B) using an ultraviolet light.

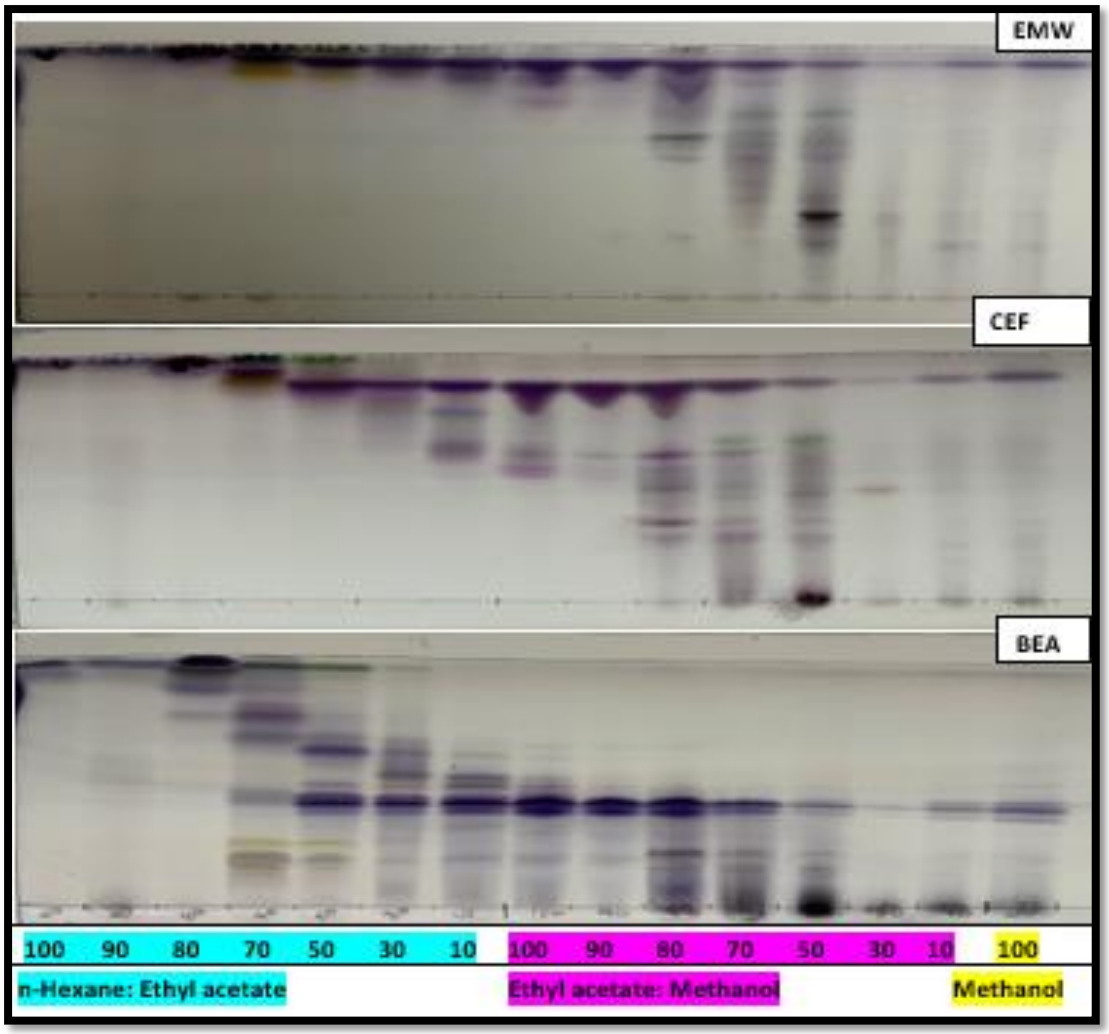

Figure 6. 6: The chromatograms of different fractions obtained from first open column chromatography of *R. officinalis* developed in EMW, CEF, and BEA mobile systems and sprayed with the vanillin-sulphuric acid reagent.

6.3.6.1.2. DPPH TLC of 1st column fractions

The antioxidant activity of *R. officinalis* fractions from first open column chomatography were determined using TLC plates developed in EMW, CEF, and BEA. The TLC plates were then sprayed with 0.2% DPPH in methanol. The yellow bands against the purple background shows the antioxidant compounds. Prominent antioxidant compounds were visible on the 70% n-hexane: 30% ethyl acetate and 50% n-hexane: 50% ethyl acetate (Figure 6.7).

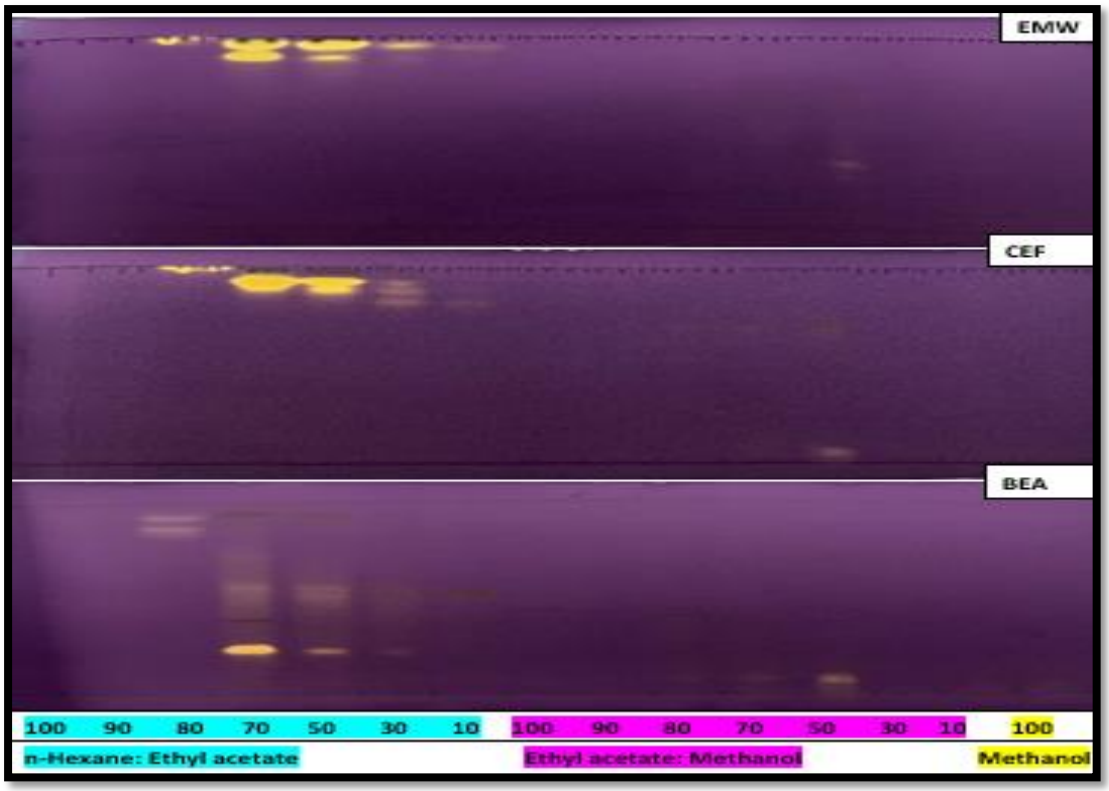

Figure 6. 7: The chromatograms of different fractions obtained from first open column chromatography of *R. officinalis* developed in EMW, CEF, and BEA mobile systems and sprayed with 0.2% DPPH.

6.3.6.1.3. Bioautography assay of 1st column fractions

The antibacterial activity of the eluted fractions was determined using the bioautography assay. The plates were developed in three mobile systems (EMW, CEF, and BEA), then sprayed with *Mycobacterium smegmatis*. Zones of inhibition were observed from 70% n-hexane: 30% ethyl acetate to 70% ethyl acetate: 30% methanol, which indicates antibacterial activity against the tested microorganism (Figure 6.8).

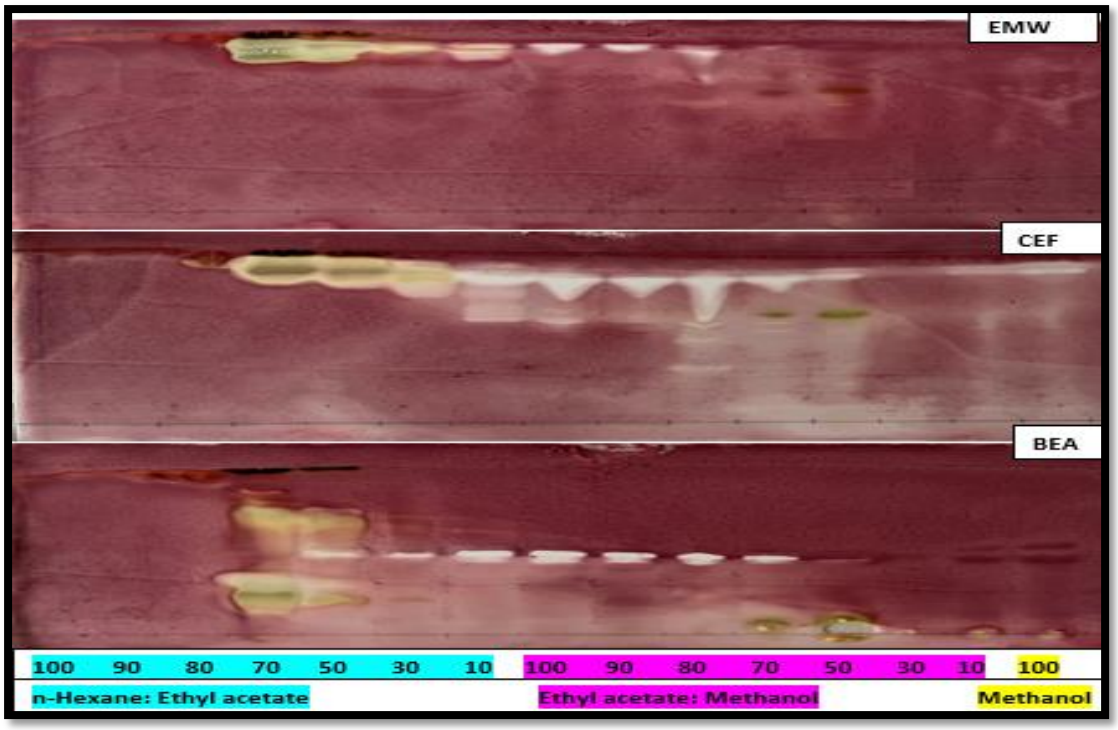

Figure 6.8: The bioautograms of different fractions obtained from first open column chromatography of *R. officinalis* developed in EMW, CEF, and BEA mobile systems against *M. smegmatis*.

6.3.6.1.4. Serial broth micro-dilution assay

The serial broth micro-dilution assay was performed to quantity of antibacterial activity of the fractions. Table 6.7 shows the MICs and the lowest MIC values was found from 70% n-hexane: 30% ethyl acetate (0.08 mg/mL) and 50% n-hexane: 50% ethyl acetate (0.08 mg/mL). This was followed by 30% n-hexane: 70% ethyl acetate with an MIC value of 0.3125 mg/mL.

Table 6. 7: MIC (mg/mL) value of *R. officinalis* fractions from first open column chromatography against *Mycobacterium smegmatis*.

Fractions	MIC value (mg/mL)
1	>2.5
2	>2.5
3	>2.5
4	0.08
5	0.08
6	0.3125

7	1.125
8	0.625
9	1.125
10	1.125
11	0.625
12	1.125
13	>2.5
14	>2.5
15	>2.5

6.3.6.2. Second open column chromatography

Even though fractions 4 and 5 had the lowest MIC value, they were not chosen because they showed to have the highest number of compounds present on the TLC plates developed in the BEA mobile system. Fractions from 10% n-hexane: 90% ethyl acetate to 70% ethyl acetate: 30% methanol were chosen for the second open column chromatography because they had the same active antimicrobial compounds with the same chemical profile as observed from bioautography. The chosen fractions were developed in three mobile phases (in 100% n-hexane, 50% n-hexane: 50% ethyl acetate, and 100% ethyl acetate) and straight bands were observed from 50% n-hexane: 50% ethyl acetate mobile system (Figure 6.9).

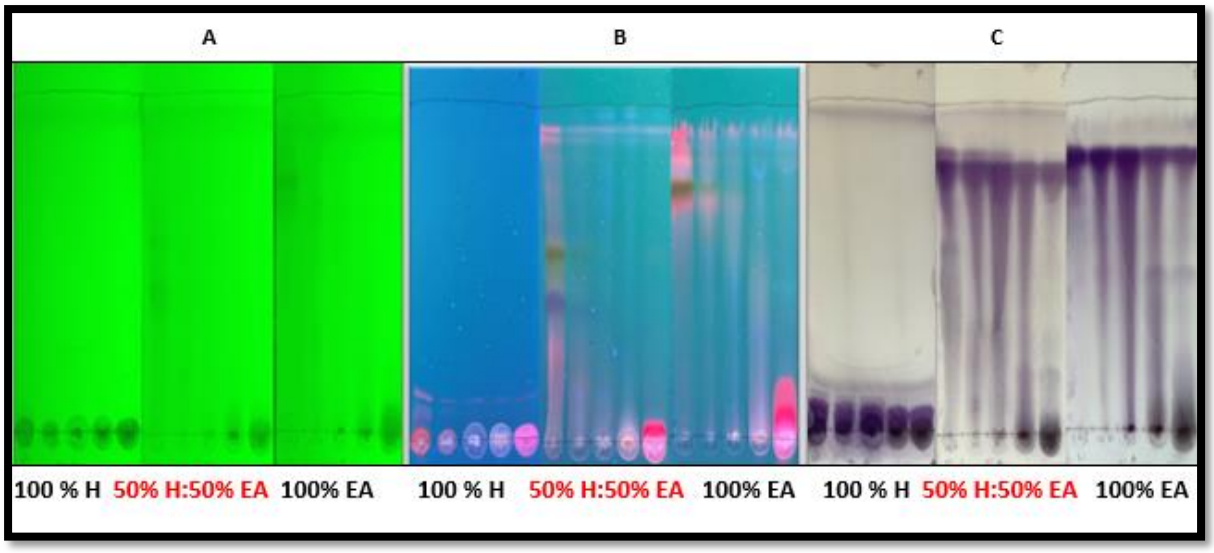

Figure 6. 9: Chromatograms obtained after developing the TLC plates in 100% n-hexane, 50% n-hexane: 50% ethyl acetate, and 100% ethyl acetate, then visualised at 254 nm (A), 365 nm (B) and further spayed with the vanillin sulphuric acid reagent (C).

Key: H- n-Hexane

EA- Ethyl acetate

The chosen fractions were combined and developed in 70% n-hexane in ethyl acetate, 80% n-hexane in ethyl acetate, and 90% n-hexane in ethyl acetate. The plates were visualised under the UV light at 254 nm (A), 365 nm (B), and further sprayed with the vanillin-sulphuric acid reagent (C) to visualise non-fluorescing compounds. The compounds separated well in 80% n-hexane in ethyl acetate, and it was chosen as the solvent system for the second open column chromatography (Figure 6.10).

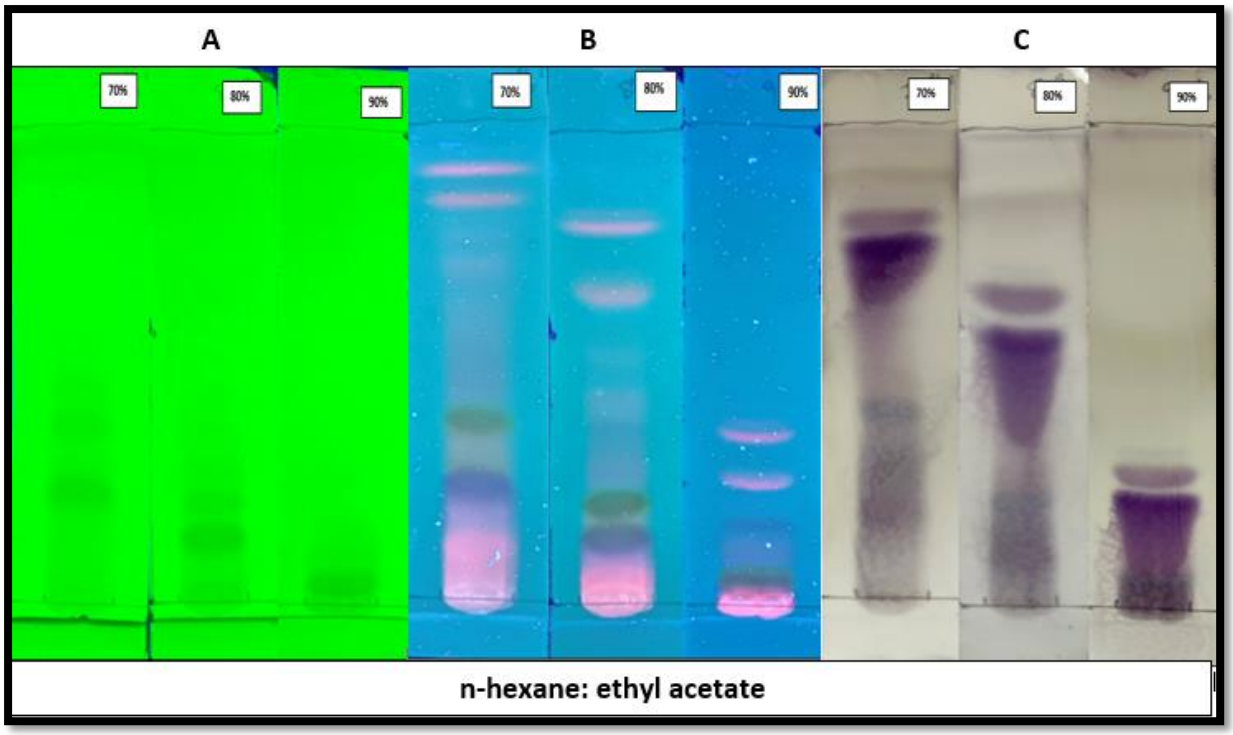

Figure 6.10: Chromatograms of combined chosen *R. officinalis* fractions obtained after developing the TLC plates in 70% n-hexane in ethyl acetate, 80% n-hexane in ethyl acetate, and 90% n-hexane in ethyl acetate mobile systems, then visualised at 254 nm (A), 365 (B), and further sprayed with the vanillin-sulphuric acid reagent (C).

6.3.6.2.1. Phytochemical analysis of the fractions

From the results obtained from the first open chromatography, it was noted that the target compound was from fraction 10% n-hexane: 90% ethyl acetate to fraction 70% ethyl acetate: 30% methanol (with a total mass of 17.46 g). Obtained chromatograms for the determination of the solvent system for the second open column chromatography, which would separate the targeted compounds best was chosen to be 80% hexane: 20% ethyl acetate. The chosen fractions were then subjected to the second open column chromatography using 80% n-hexane in ethyl acetate as the eluent. A total amount of 600 fractions were collected in 8 mL test tubes and spotted on TLC plates to determine their TLC profiles. The TLC plates were visualised under the UV light at 254 nm (Figure 6.11) and 365 nm (Figure 6.12), then sprayed with the vanillin-sulphuric acid reagent (Figure 6.13). Compounds were observed on all the chromatograms.

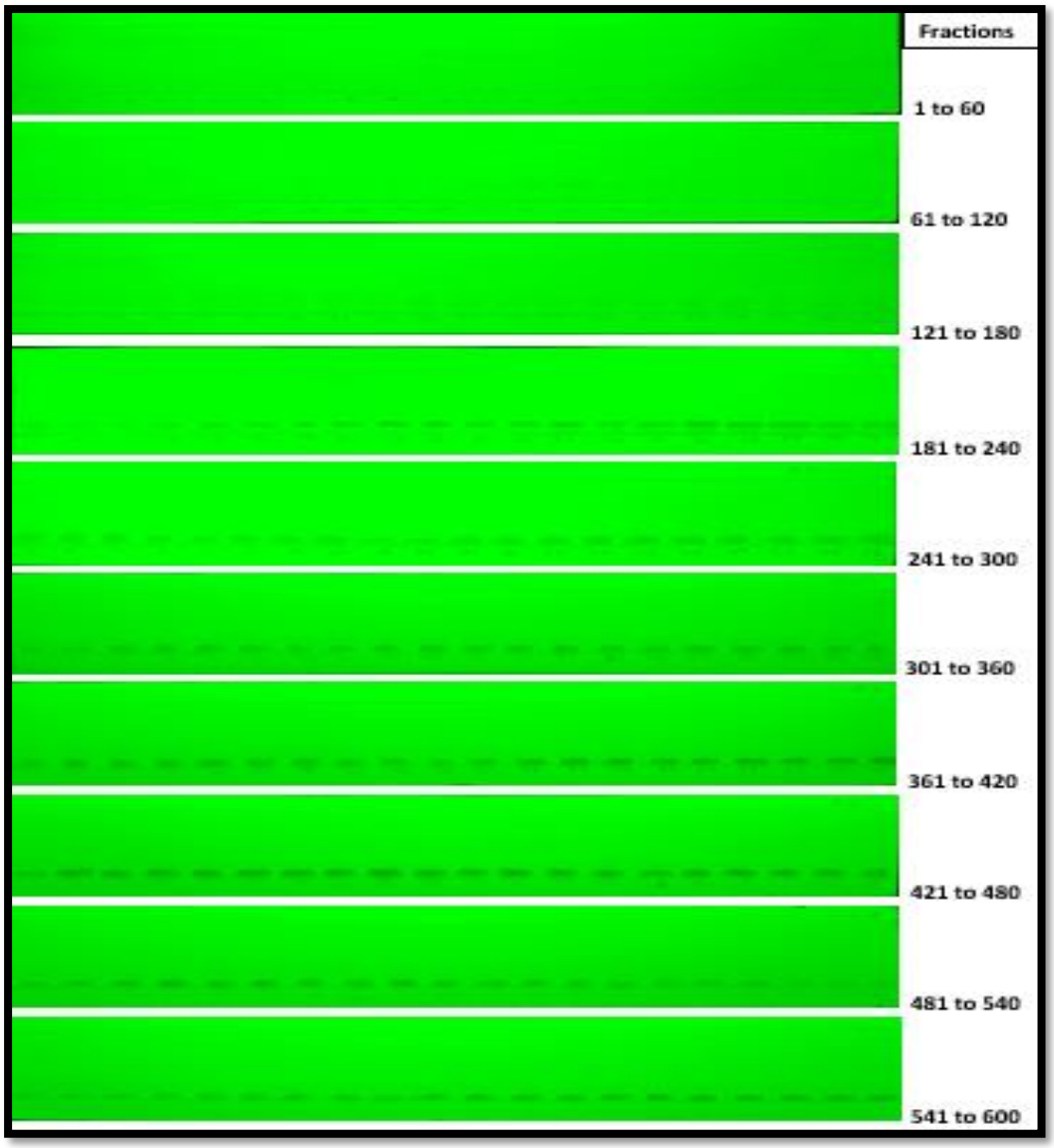

Figure 6. 11: Chromatograms of *R. officinalis* fractions obtained from the second open column chromatography and then developed in 80% n-hexane: 20% ethyl acetate and visualised at 254 nm.

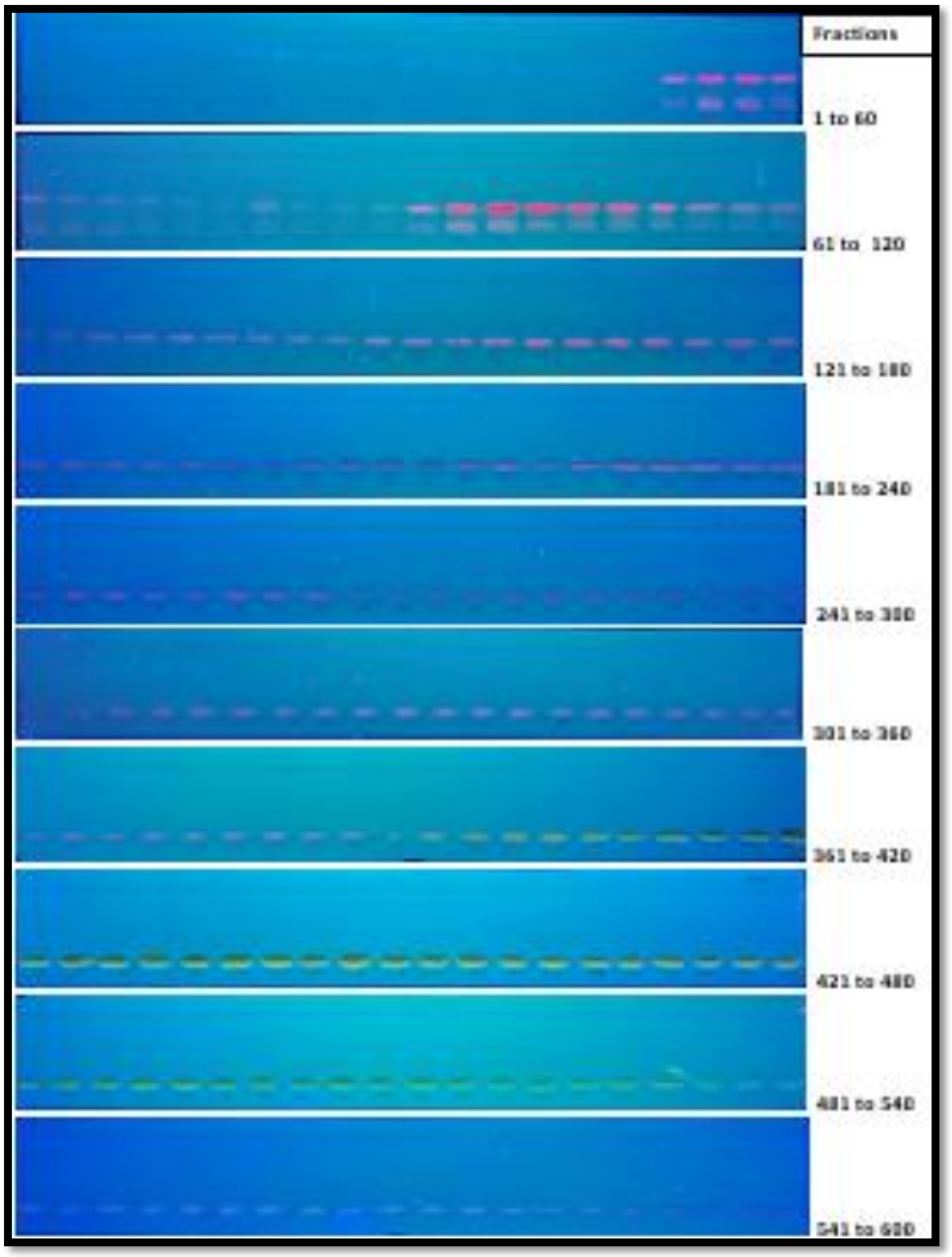

Figure 6. 12: Chromatograms of *R. officinalis* fractions obtained from the second open column chromatography and then developed in 80% n-hexane: 20% ethyl acetate and visualised at 365 nm.

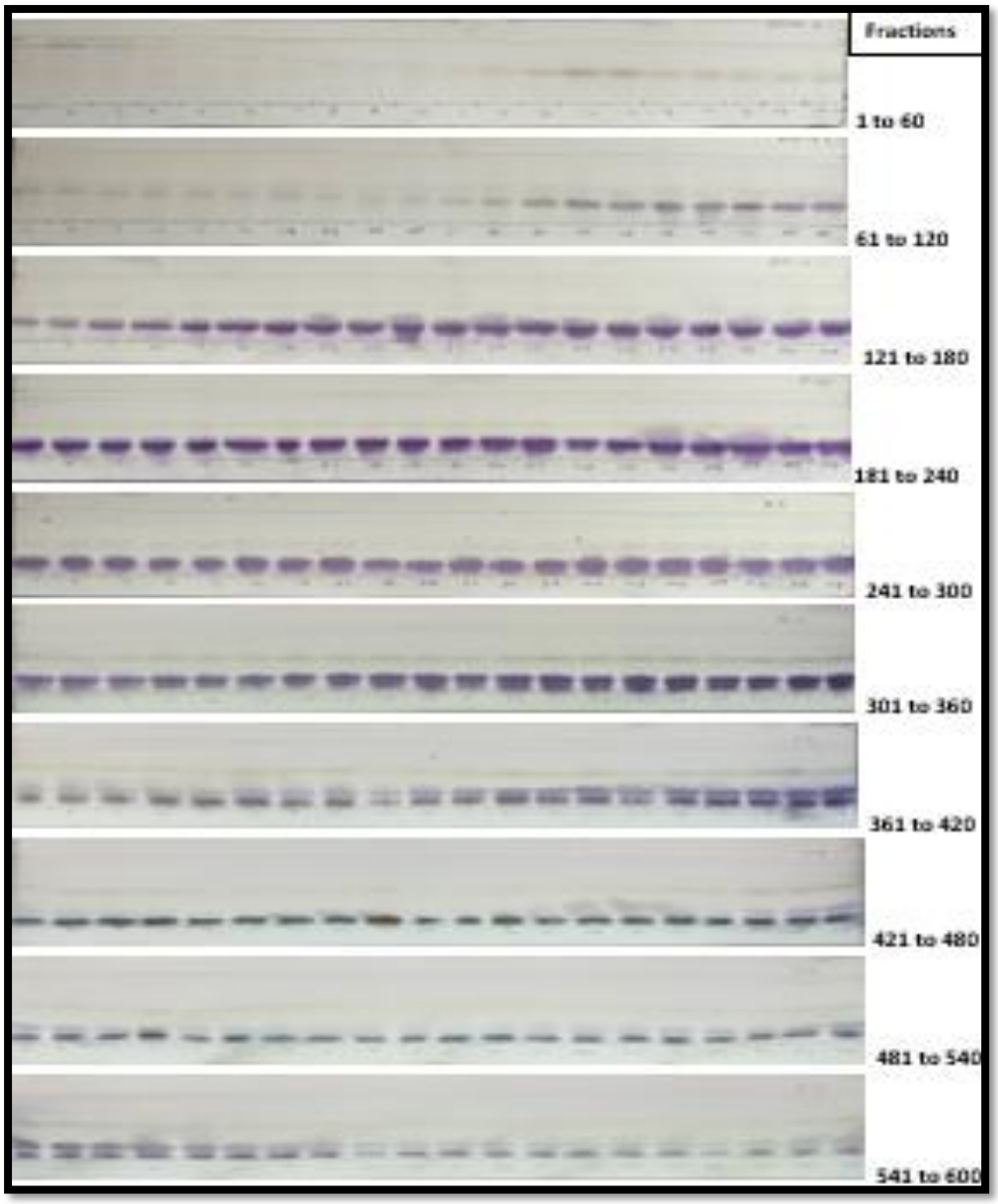

Figure 6. 13: Chromatograms of *R. officinalis* fractions obtained from the second open column chromatography and then developed in 80% n-hexane: 20% ethyl acetate and sprayed with the vanillin-sulphuric acid reagent.

The collected fractions were then combined into groups based on their TLC profile. Test tubes with the same TLC profile were combined into four different groups, namely; group 1 (test tubes 1-120), group 2 (test tubes 121-240), group 3 (test tubes 241-360), and group 4 (test tubes 361- 600). The groups phytochemicals were then analysed using TLC plates. The plates were loaded with the crudes of different groups and developed in 80% n-hexane in ethyl acetate, visualised under the UV light and sprayed with the vanillin-sulphuric acid reagent (Figure 6.14). Most compounds were

observed from the plate visualised at 365 nm (B) and the one sprayed with the vanillin-sulphuric acid reagent (C).

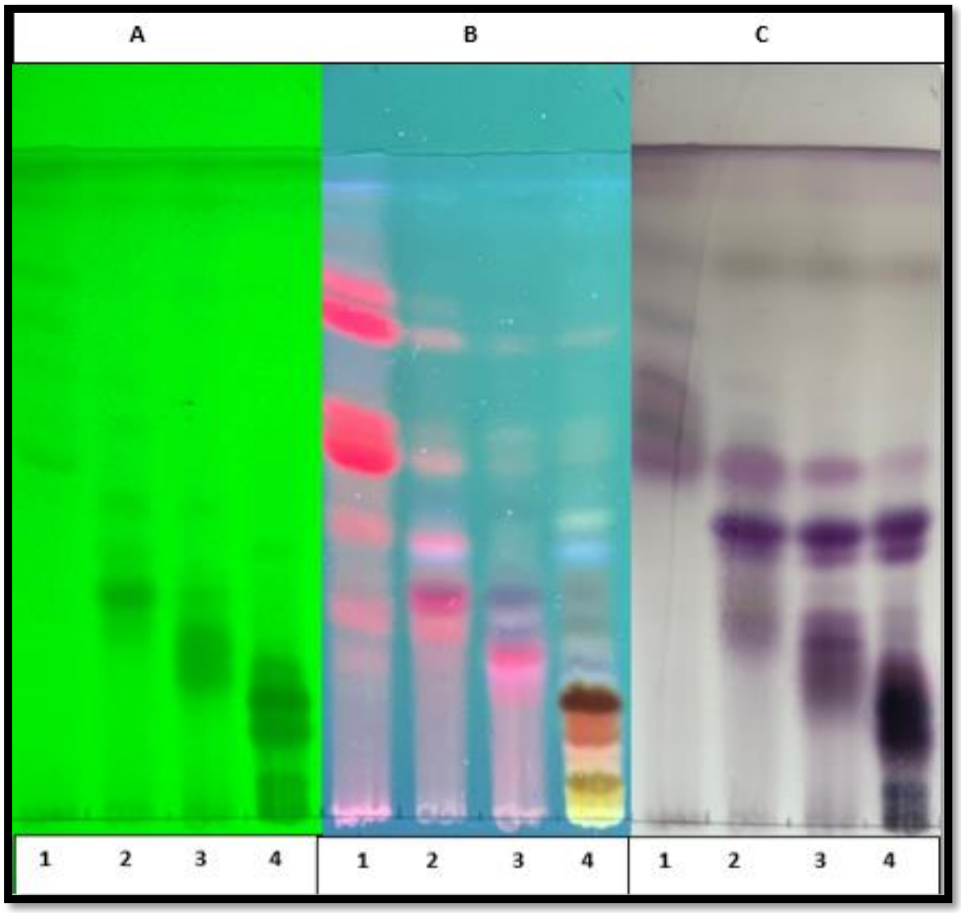

Figure 6. 14: Phytochemical analysis of the grouped fractions developed in 80% hexane: 20% ethyl acetate and then visualised under the UV light at 254 nm (A) and 365 nm (B), and sprayed with the vanillin sulphuric acid reagent (C).

Key: 1 = test tubes 1-120, 2 = test tubes 121-240, 3 = test tubes 241-360, and 4 = test tubes 361- 600

6.3.6.2.2. Bioautography of combined fractions of 2nd column chromatography

Bioautography assay was used to test for antibacterial activity against *Mycobacterium smegmatis* of the different groups. The TLC plate was developed in 80% n-hexane in ethyl acetate to allow the separation of compounds and then sprayed with *M. smegmatis*. Figure 6.15 shows that all four groups had antibacterial activity against *M. smegmatis*.

Figure 6. 15: Bioautogram showing antibacterial activity of groups 1-4 against *M. smegmatis*.

Key: 1 = test tubes 1-120, 2 = test tubes 121-240, 3 = test tubes 241-360, and 4 = test tubes 361- 600

6.3.6.3. Preparative Thin Layer Chromatography (TLC)

All groups had antibacterial activity against *M. smegmatis*. Group 3 and 4 were combined since they showed to have the same TLC profile and preparative TLC was used to isolate the active compounds. The preparative TLC plates were loaded with the combined crude extract of groups 3 and 4, and then developed in 80% n-hexane in ethyl acetate. The plates were visualised under the UV light at 254 and 365 nm. They were circled with a pencil and scraped off into different vials. The compounds were separated from the silica by immersing them in ethyl acetate, vortexed and filtered using cotton wool.

The following flow diagram (Figure 6.16) shows the summary of the isolation process of the active antibacterial compounds of *R. officinalis* ground leaves. The diagram shows masses of collected fractions, combined fractions, and isolated compounds, which were further analysed using the NMR for structural elucidation.

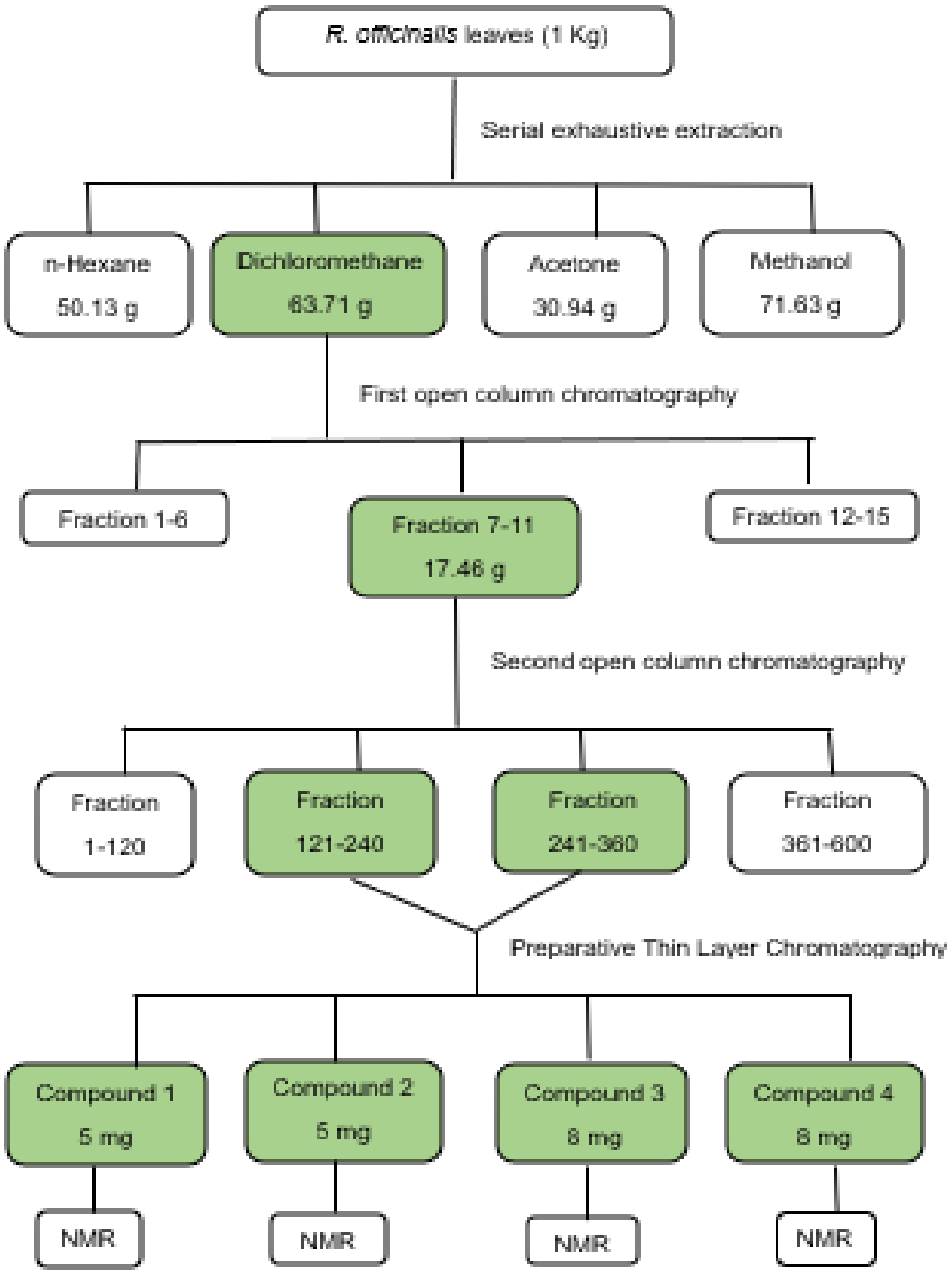

Figure 6. 16: Diagram showing summary of the isolation process.

6.4. Discussion

The leaves of *Rosmarinus officinalis* showed to have promising antibacterial activity against *Mycobacterium smegmatis* using bioautography and micro broth-dilution assay compared to *Z. mucronata*, *Z. capense, X. caffra,* and *R. tridentata*. *R. officinalis* was selected for further analysis to isolate and purify its bioactive compounds using bioassay guided fractionation. A large scale extraction (serial exhaustive extraction) was carried out using solvents of varying polarities from non-polar to a more polar solvent (n-hexane, dichloromethane, acetone, and methanol) to obtain the desired extracts. Extraction is the first and most important step during the isolation and characterisation of plants bioactive compounds. It plays a huge role in the overall success of the qualitative and quantitative analysis of extracted bioactive compounds (Essien *et al*., 2020).

A total mass of 216.44 g (Table 6.4) was extracted from 1 kg of *R. officinalis* leaves with the highest mass being extracted with methanol (71.63 g), followed by dichloromethane (63.71 g), and then n-hexane (50.13 g). The lowest mass was extracted with acetone (30.94 g). The highest extractants were methanol and dichloromethane, which indicated that the *R. officinalis* leaves contain intermediate to polar compounds. Exactly 0.05 g of the obtained extracts were reconstituted with acetone to 10 mg/mL to carry out phytochemical analysis on the TLC plates. The TLC plates were developed in EMW, CEF, and BEA mobile systems, visualised using the UV light (Figure 6.1) at 254 nm (A) and 365 nm (B), and then further sprayed with the vanillin-sulphuric acid reagent (Figure 6.2). More fluorescing compounds were observed on a plate developed in the BEA mobile system at 365 nm. After spraying the plates, the most prominent bands for n-hexane and dichloromethane were observed on a plate developed in BEA and for acetone and methanol on the plates developed in EMW. All the extracts showed to have antioxidant compounds in all the mobile systems, but in BEA, they did not move, although they were able to separate in EMW and CEF. Antioxidant compounds were observed as the yellow bands against the purple background (Figure 6.3).

The qualitative antibacterial activity of the plant extracts was determined using bioautography assay and the plates were developed in EMW, CEF, and BEA. All the extracts showed to have the same chemical profile with antibacterial activity from the BEA plate, but the most prominent bands with antibacterial activity were observed from

dichloromethane and acetone extracts on the plates developed in BEA mobile system (Figure 6.4). Quantitative antibacterial activity was determined using broth micro-dilution assay and the results were recorded as the MIC in Table 6.5. It was found that the n-hexane extracts (H2 and H3 = 0.156 mg/mL, and H1 = 0.182 mg/mL) had the lowest MIC, which indicates the highest activity, followed by dichloromethane extracts (0.3125 mg/mL) and then the first acetone extract (A1) (1.125 mg/mL). The methanol extracts had the least activity.

Even though the n-hexane extracts had the lowest MIC value, the dichloromethane extracts were chosen for the isolation of antibacterial compounds because they had the second same lowest MIC value and the bands on the TLC plate for bioautography were more prominent as compared to the n-hexane bands. The three dichloromethane extracts were combined and subjected to the first open column chromatography and eluted using solvents of varying polarities. Results in Table 6.6 show that the highest mass was extracted with 70% n-hexane in ethyl acetate (21.25 g), followed by 50% n-hexane in ethyl acetate (9.49 g), and then 30% -hexane in ethyl acetate (8.96 g); the least extractant was 100% n-hexane, which extracted 0.10 g.

Phytochemical analysis of the collected fractions was determined using TLC plates developed in EMW, CEF, and BEA mobile systems and visualised at 254 (Figure 6.5 A) nm and 365 nm (Figure 6.5 B). More fluorescing compounds were observed from 70% n-hexane in ethyl acetate to 10% n-hexane in ethyl acetate. The TLC plates were further sprayed with the vanillin-sulphuric acid reagent (Figure 6.6) and more compounds were observed from 70% n-hexane in ethyl acetate to 50% ethyl acetate in methanol. Compounds from 10% n-hexane in ethyl acetate to 70% ethyl acetate in methanol had almost the same chemical compounds on the plate developed in BEA mobile system.

The antioxidant activity of different *R. officinalis* fractions from first open column chromatography was determined using 0.2% DPPH. Figure 6.7 shows that more prominent antioxidant compounds were detected on the three plates developed in EMW, CEF, and BEA from 70% n-hexane in ethyl acetate, and then followed by 50% n-hexane in ethyl acetate. Bioautography assay was used to determine the antibacterial activity of the different fractions against *M. smegmatis*. On Figure 6.8, antibacterial activity was observed from 70% n-hexane in ethyl acetate to 70% ethyl

acetate in methanol from the TLC plate developed in BEA mobile system. Quantitative antibacterial activity against *M. smegmatis* was also determined using broth micro-dilution assay where the lowest MIC value was found from 70% n-hexane in ethyl acetate (0.08 mg/mL) and 50% n-hexane in ethyl acetate (0.08 mg/mL). This was followed by 30% n-hexane in ethyl acetate with an MIC value of 0.3125 mg/mL (Table 6.7).

Obtained chromatograms for the determination of the solvent system for the second open column chromatography, which would separate the targeted compounds best was chosen to be 80% hexane in ethyl acetate (Figure 6.10). The target compound of interest with the best antibacterial activity was from fraction 10% n-hexane in ethyl acetate to 70% ethyl acetate in methanol fractions. They were combined to make a total mass of 17.46 g, which was used for the second open column chromatography. The chosen fractions were then subjected to the second open column chromatography using 80% n-hexane in ethyl acetate as the eluent. A total amount of 8 mL × 600 test tubes were collected and spotted in fractions on the TLC plates to determine their TLC profiles. The TLC plates were visualised under the UV light at 254 nm (Figure 6.11) and 365 nm (Figure 6.12), and then sprayed with the vanillin-sulphuric acid reagent (Figure 6.13). Compounds were observed on all the chromatograms.

Test tubes with the same chemical profiles were combined to make four different groups, namely; group 1 (test tubes 1-120), group 2 (test tubes 121-240), group 3 (test tubes 241-360), and group 4 (test tubes 361- 600). The groups' phytochemicals were then analysed using TLC pates and Figure 6.14 shows the obtained results. The plates were loaded with the crudes of different groups and developed in 80% n-hexane in ethyl acetate, visualised under the UV light and sprayed with the vanillin-sulphuric acid reagent. More fluorescing compounds were observed from the plate visualised at 365 nm (B) and the one sprayed with the vanillin-sulphuric acid reagent (C). Bioautography assay was used to test for the antibacterial activity of the different groups against *Mycobacterium smegmatis*. The TLC plate was developed in 80% n-hexane in ethyl acetate to allow the separation of compounds and then sprayed with *M. smegmatis*. Figure 6.15 shows that all four groups had antibacterial activity against *M. smegmatis*.

Groups 2 and 3 were chosen for further analysis as they had the same chemical profile. Preparative TLC plates were used to load the combination and the plates were

developed in 80% n-hexane in ethyl acetate. The plates were visualised using the UV light at 254 nm and 365 nm, and four compounds were scraped off the preparative TLC plate. The compounds were dissolved in the ethyl acetate and filtered into new vials.

6.5. Conclusions

The active compounds were isolated from the dichloromethane extracts of *R. officinalis,* had potent antibacterial activity against *M. smegmatis,* and were characterised using NMR, as detailed in the following chapter.

6.6. References

Anand, U., Jacobo-Herrera, N., Altemimi, A. and Lakhssassi, N. 2019. A comprehensive review on medicinal plants as antimicrobial therapeutics: potential avenues of biocompatible drug discovery. *Metabolites*, **9**(11): 258.

Coskun, O. 2016. Separation techniques: chromatography. *Northern Clinics of Istanbul*, **3**(2):156.

Dar, R.A., Shahnawaz, M. and Qazi, P.H. 2017. General overview of medicinal plants: a review. *The Journal of Phytopharmacology*, **6**(6): 349-351.

Essien, S.O., Young, B. and Baroutian, S. 2020. Recent advances in subcritical water and supercritical carbon dioxide extraction of bioactive compounds from plant materials. *Trends in Food Science and Technology*, **97**: 156-169.

Ibarra-Rivera, T.R., Delgado-Montemayor, C., Oviedo-Garza, F., Pérez-Meseguer, J., Rivas-Galindo, V.M., Waksman-Minsky, N. and Pérez-López, L.A. 2020. Setting up an educational column chromatography experiment from home. *Journal of Chemical Education*, **97**(9):3055-3059.

Indrayanto, G., Putra, G.S. and Suhud, F. 2021. Validation of in-vitro bioassay methods: application in herbal drug research. *Profiles of Drug Substances, Excipients and Related Methodology*, **46**: 273-307.

Jha, A.K. and Sit, N. 2022. Extraction of bioactive compounds from plant materials using combination of various novel methods. *Trends in Food Science and Technology*, **119**(0924-2244): 579-591.

Kumar, A., Chettiar, S. and Parish, T. 2017. Current challenges in drug discovery for tuberculosis. *Expert Opinion on Drug Discovery*, **12**(1):1-4.

Malviya, N. and Malviya, S. 2017. Bioassay guided fractionation- an emerging technique influence the isolation, identification, and characterization of lead phytomolecules. *Hospital Pharmacy*, **2**(5).

Mostafavi, S.M., Rouhollahi, A., Mohajeri, A. and Piryaei, M. 2014. Separation of aromatic and alcoholic mixtures using novel MWCNT-Silica Gel Nanocomposite as an adsorbent in gas chromatography. *Journal of NanoAnalysis*, **1**(1): 9-16.

Nguta, J.M., Appiah-Opong, R., Nyarko, A.K., Yeboah-Manu, D., Addo, P.G., Otchere, I. and Kissi-Twum, A. 2016. Antimycobacterial and cytotoxic activity of selected medicinal plant extracts. *Journal of Ethnopharmacology*, **182**: 10-15.

Nothias, L.F., Nothias-Esposito, M., Da Silva, R., Wang, M., Protsyuk, I., Zhang, Z., Sarvepalli, A., Leyssen, P., Touboul, D., Costa, J. and Paolini, J. 2018. Bioactivity-based molecular networking for the discovery of drug leads in natural product bioassay-guided fractionation. *Journal of Natural Products*, **81**(4): 758-767.

Omeroglu, P.Y., Acoglu, B., Özdal, T., Tamer, C.E. and Çopur, Ö.U. 2019. Extraction techniques for plant-based bio-active compounds. *Natural Bioactive Compounds,* **2**(5): 465-492.

Pasban, A., Mostafavi, S.M., Malekzadeh, H. and Mohammad Nazari, B. 2017. Quantitative determination of lpg hydrocarbons by modified packed column adsorbent of gas chromatography via full factorial design. *Journal of Nanoanalysis*, **4**(1): 31-40.

Sasidharan, S., Chen, Y., Saravanan, D., Sundram, K.M. and Latha, L.Y. 2011. Extraction, isolation, and characterization of bioactive compounds from plants extracts. *African Journal of Traditional, Complementary, and Alternative Medicines*, **8**(1): 1-10.

Venieraki, A., Dimou, M. and Katinakis, P. 2017. Endophytic fungi residing in medicinal plants have the ability to produce the same or similar pharmacologically active secondary metabolites as their hosts. *Hellenic Plant Protection Journal*, **10**(2): 51-66.

CHAPTER 7

7. Structural elucidation of isolated compounds

7.1. Introduction

Natural products are regarded as chemically complex and differ from synthetic drug molecules (Rodrigues *et al*., 2016). An identification of molecular structures relies on spectroscopic methods that measure the molecular ensembles. The most important tools for structure identification include the NMR, mass spectroscopy, X-ray diffraction and ultraviolet-visible (UV-vis) spectroscopy (Gross *et al*., 2018). Mass spectrometry is a technique that uses ions to measure the mass-to-charge ratio (*m/z*) of molecules when lifted into the gas phase (Kafader *et al*., 2020; Dias *et al*., 2016).

NMR spectroscopy is a powerful tool for the structural analysis of organic compounds and biomolecules which requires macroscopic sample quantities (Lovchinsky *et al*., 2016). The NMR spectroscopy allows the acquisition of qualitative and quantitative information of a mixture of compounds (Rakhmatullin *et al*., 2017). It involves the one-dimensional (1-D) and multidimensional NMR spectroscopy (Simpson *et al*., 2018). The 2-dimensional NMR includes Heteronuclear Single Quantum Correlation (HSQC) to determine interatomic connectivity (Milanowski *et al*., 2018), the Heteronuclear Multiple Bond Correlation (HMBC) method, which provides the two and three bonds correlations, and the 2D-Correlated Spectroscopy (COSY) technique to reveal the identity of coupled protons, and the Total Correlation Spectroscopy (TOCSY), which is a homonuclear NMR technique that creates a correlation between all protons within the system (Ok *et al*., 2019).

The most well-known technique to determine structural formulas, special and electronic structure of synthesised or isolated natural products is the ^{13}C NMR. The quantitative ^{13}C NMR measures the aromaticity (C_{ar}) of the compounds, which is the relative percentage of aromatic carbon atoms in hydrocarbons. The decoupling ^{13}C NMR is used for structure analysis, for obtaining the ^{13}C NMR spectra with all the $^{n}J_{CH}$ coupling constants (n = 1, 2, 3) and signal multiplicity. The Attached Proton Test (APT) is used as a way to assign C–H multiplicities in ^{13}C NMR spectra. It provides information about all sorts of carbons within one experiment. The spin vector evolves differently after the initial pulse depending on the number of hydrocarbons to a carbon atom (C, CH, CH_2, CH_3) (Rakhmatullin *et al*., 2022). The ^{1}H NMR spectrum provides

the identification of the functional groups through chemical shift information, quantification of chemical shift equivalent protons, and connectivity information through homonuclear coupling (Pesek *et al*., 2020). The distortion less enhancement by polarization transfer (DEPT) experiment provides the structural components of the molecule (Soulsby *et al*., 2016). The aim of this chapter was to elucidate the chemical structures of the isolated compounds using NMR and mass spectroscopy.

7.2. Method and materials

7.2.1. Structural elucidation of isolated compound

The four isolated compounds were sent to the Department of Chemistry, University of Limpopo for characterisation under NMR, the 1-dimensional (^{1}H, ^{13}C and DEPT 135) and 2-dimensional NMR (HMBC, HSQC, and COSY). Exactly 40 mg of each compound was dissolved in chloroform. Prepared samples were ran using 400 MHz NMR Spectrometer (Bruker) at 400 MHz, at a temperature of 295.5 K using chloroform as a reference signal solvent to give spectroscopic data. The spectroscopic data was sent to Professor Ofentse Mazimba at the Department of Chemical and Forensic Sciences at Botswana International University of Science and Technology, who assisted with the structural elucidation of the isolated compounds.

7.3. Results

7.3.1. NMR analysis of compound 1

Figure 7.1 to 7.3 show the NMR spectra under ^{1}H Proton, ^{13}C, DEPT 135, and COSY used for the structural elucidation of the isolated compound 1. Table 7.1 shows the summary of the ^{13}C and ^{1}H Proton shift values, which helped with the characterisation of compound 1.

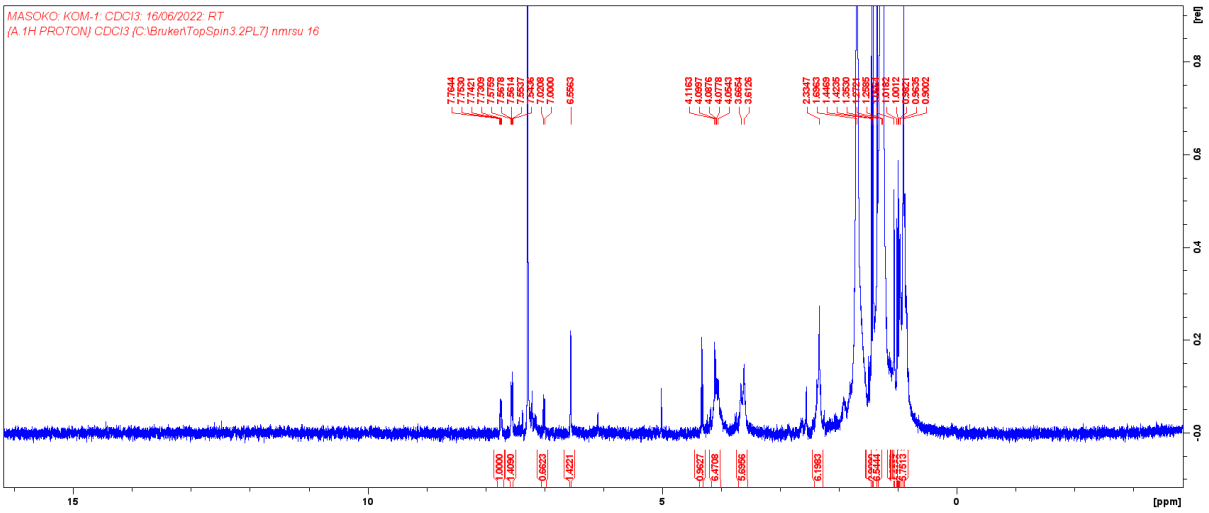

Figure 7. 1: ^{1}H NMR spectrum of isolated compound 1.

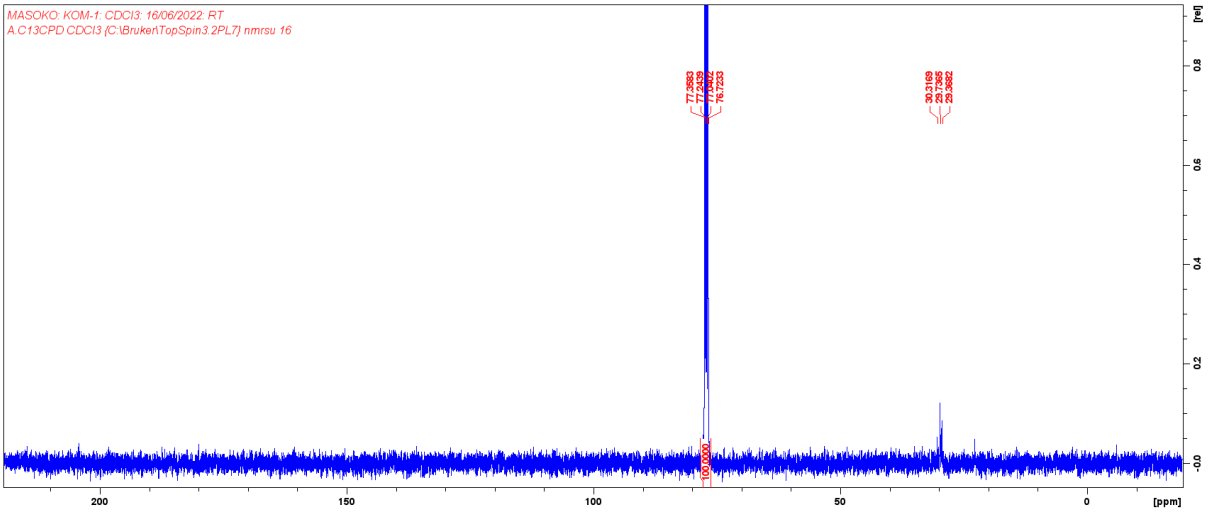

Figure 7. 2: ^{13}C NMR spectrum of isolated compound 1.

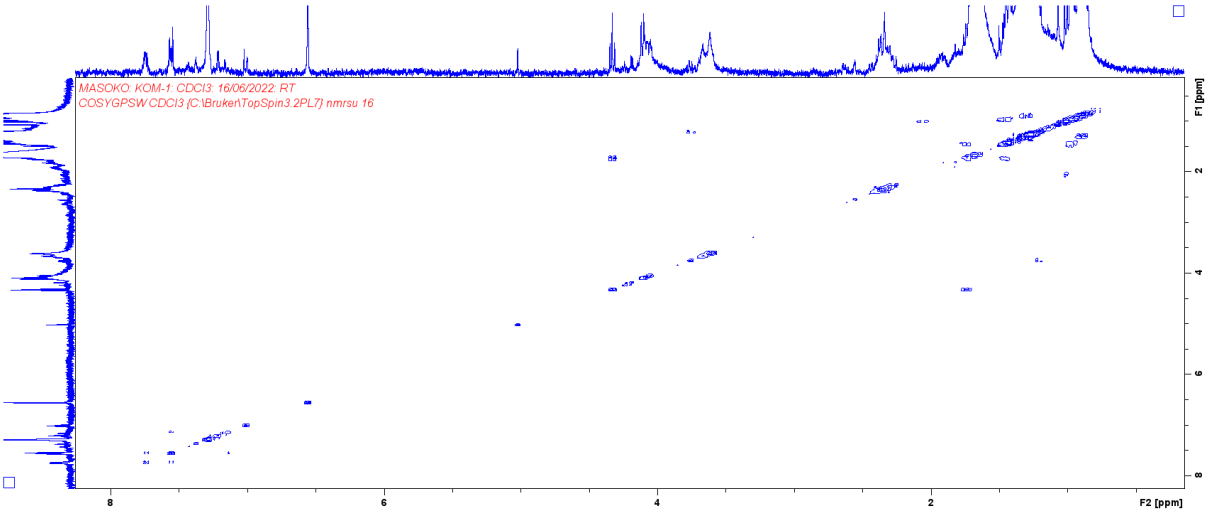

Figure 7. 3: COSY NMR spectrum of isolated compound 1.

7.3.2. Spectroscopic data for compound 1

Table 7. 1: The summary of ^{1}H and ^{13}C spectroscopic data for compound 1.

Positions	δ_H	δ_C
1	-	-
2	-	167.0
3	5.57, *d*, *J*= 5.7 Hz	121.4
4	-	173.0
4a	-	122.0
5	7.74, *d*, *J*= 8.4 Hz	119.0
6	7.12, *dd*, *J*= 2.5, 8.6 Hz	123.9
7	-	141.1
8	7.33, *t*, *J*= 2.0 Hz	124.4
8a	-	147.6
1’	4.00-4.24, *m*	44.0
2’	3.46, *m*	76.4
3’	1.23, *s*	25.4
1’’	4.93, *m*	138.3
2’’	4.91, *dd*, *J*= 1.0, 10.2 Hz	114.0

7.3.3. The structure of compound 1

Figure 7.4 below represents the structure of compound 1 isolated from *R. officinalis* leaves.

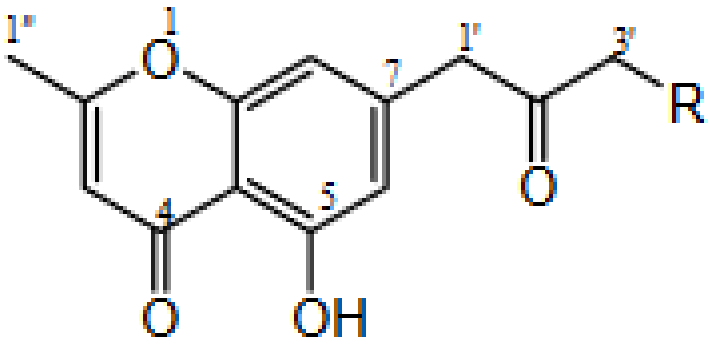

Figure 7. 4: Structure of compound 1.

7.3.4. NMR analysis for compound 2

Figure 7.5 to 7.10 shows the NMR spectra under ^{1}H Proton, ^{13}C, DEPT 135, COSY, HSQC and HMBC used for the structural elucidation of compound 2. Table 7.2 shows the summary of the ^{13}C and ^{1}H Proton shift values, which helped with the characterisation of compound 2.

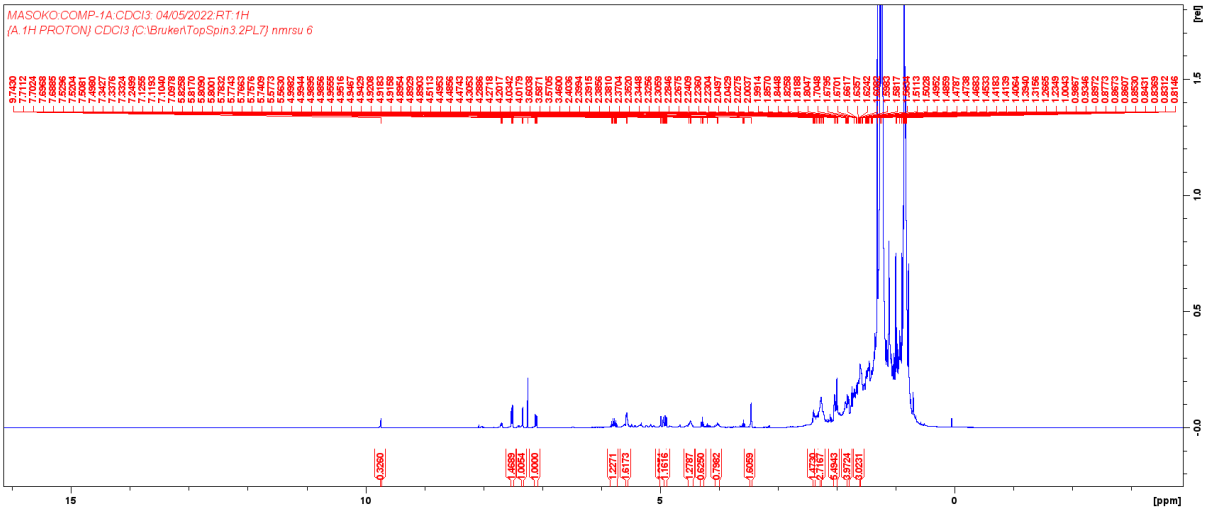

Figure 7. 5: ^{1}H NMR spectrum of isolated compound 2.

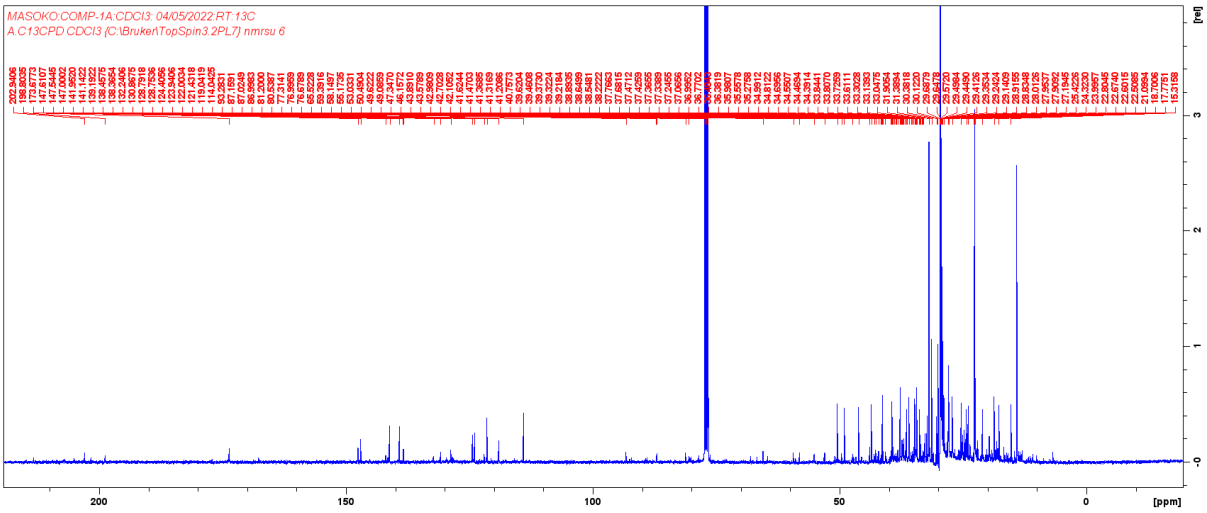

Figure 7. 6: ^{13}C NMR spectrum of compound 2.

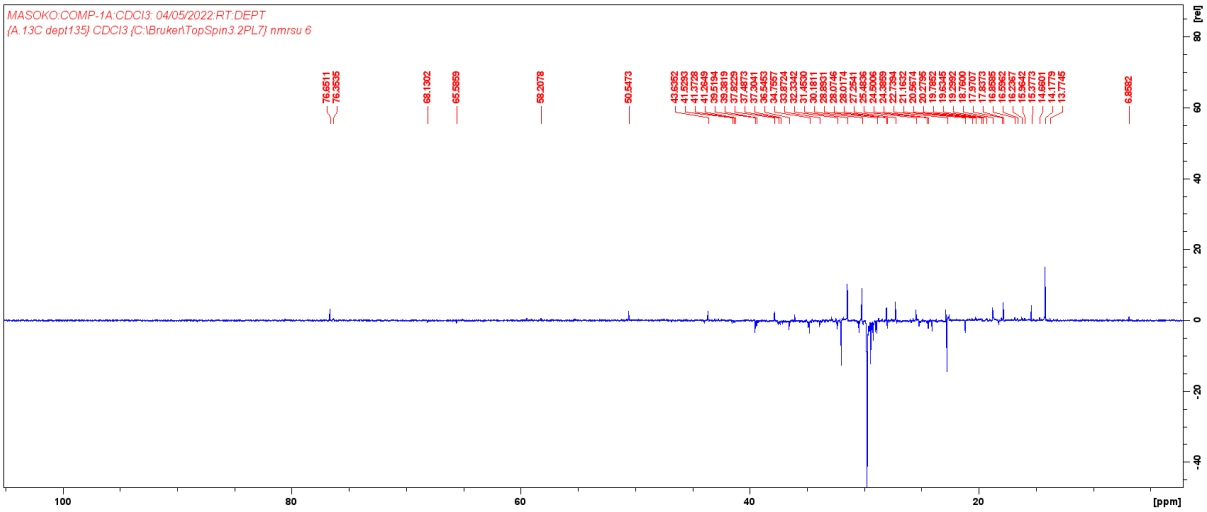

Figure 7. 7: DEPT 135 NMR spectrum of isolated compound 2.

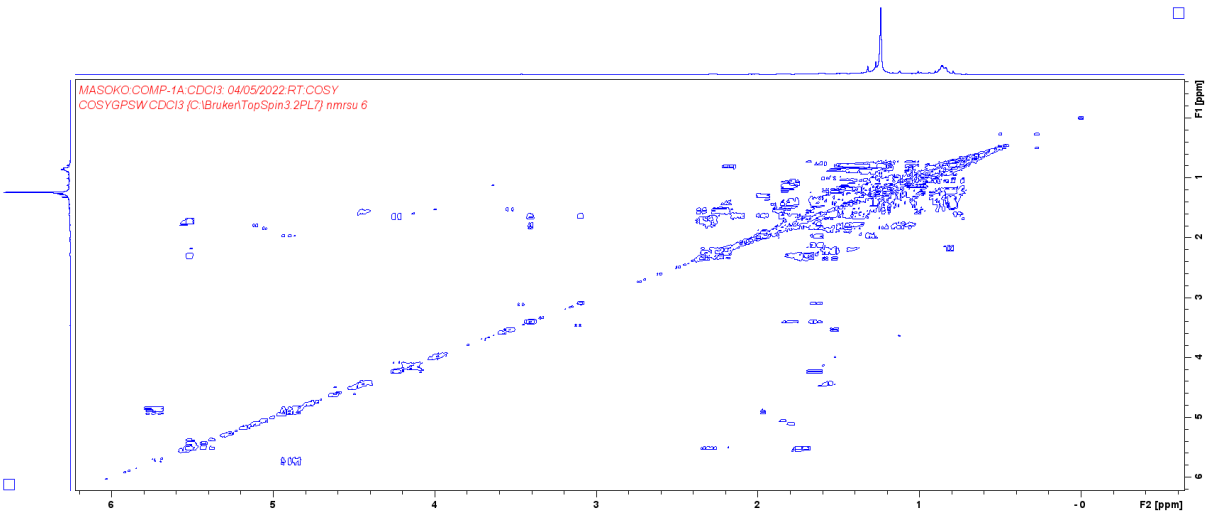

Figure 7. 8: COSY NMR spectrum of compound 2.

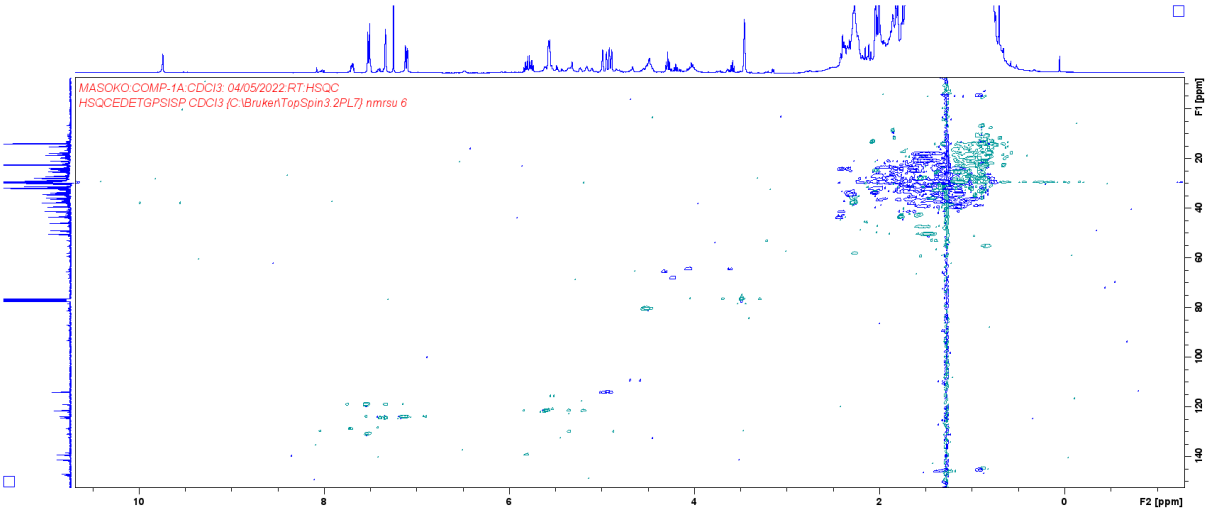

Figure 7. 9: HSQC NMR spectrum of compound 2.

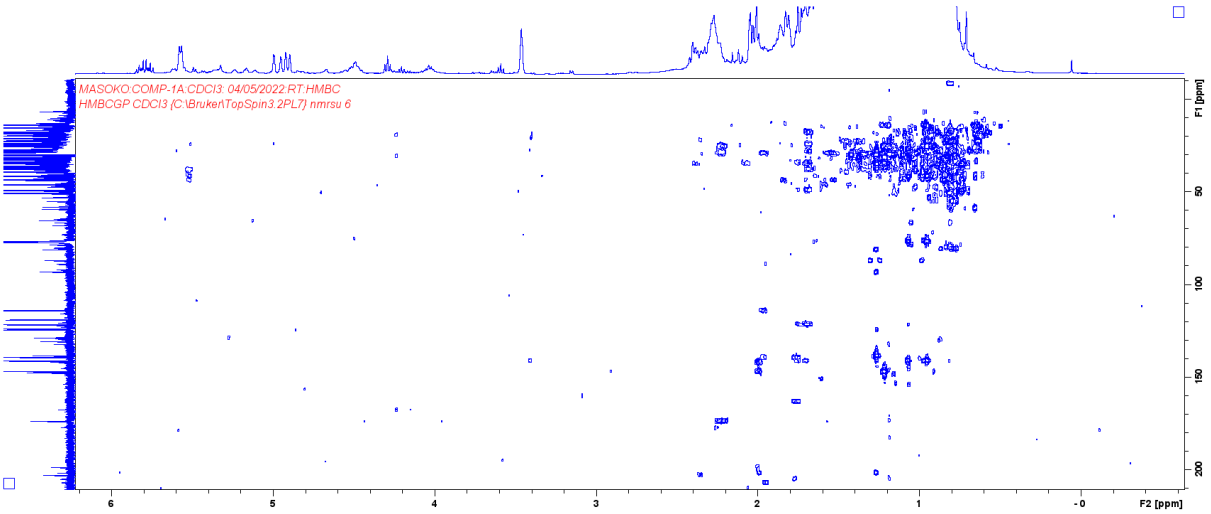

Figure 7. 10: HMBC NMR spectrum of compound 2.

7.3.5. Spectroscopic data for compound 2

Table 7. 2: The summary of ^{1}H and ^{13}C spectroscopic data for compound 2.

Positions	δ_H	δ_C
1	-	-
2	-	167.0
3	5.57, *d*, *J*= 5.7 Hz	121.4
4	-	173.0
4a	-	122.0
5	7.74, *d*, *J*= 8.4 Hz	119.0
6	7.12, *dd*, *J*= 2.5, 8.6 Hz	123.9

7	-	141.1
8	7.33, *t*, *J*= 2.0 Hz	124.4
8a	-	147.6
1’	4.00-4.24, *m*	44.0
2’	3.46, *m*	76.4
3’	1.23, *s*	25.4
1’’	4.93, *m*	138.3
2’’	a) 4.91, *dd*, *J*= 1.0, 10.2 Hz b) 4.99, *dd*, *J*= 2.7, 17.1 Hz	114.0

7.3.6. The structure of compound 2

Figure 7.11 below represents the structure of compound 2 isolated from *R. officinalis* leaves

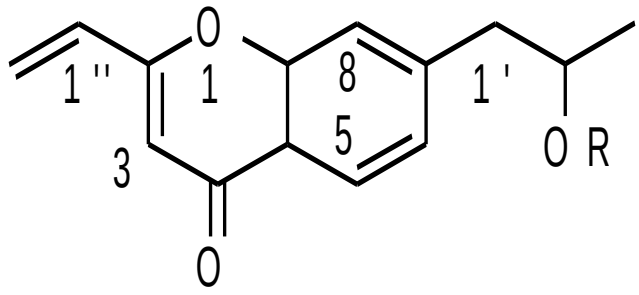

Figure 7. 11: Structure of compound 2.

7.3.7. NMR analysis of compound 3

Figure 7.12 and 7.13 shows the NMR spectra under ^{1}H Proton, and ^{13}C used for the structural elucidation of compound 3. Table 7.3 shows the summary of the ^{13}C and ^{1}H Proton shift values, which helped with the characterisation of compound 3.

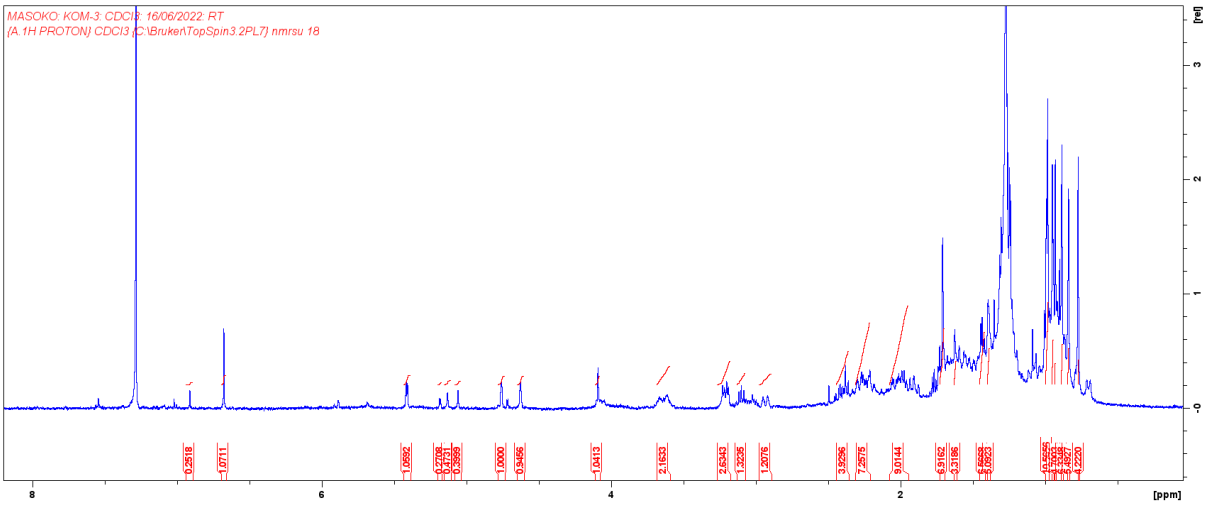

Figure 7. 12: ^{1}H NMR spectrum of isolated compound 3.

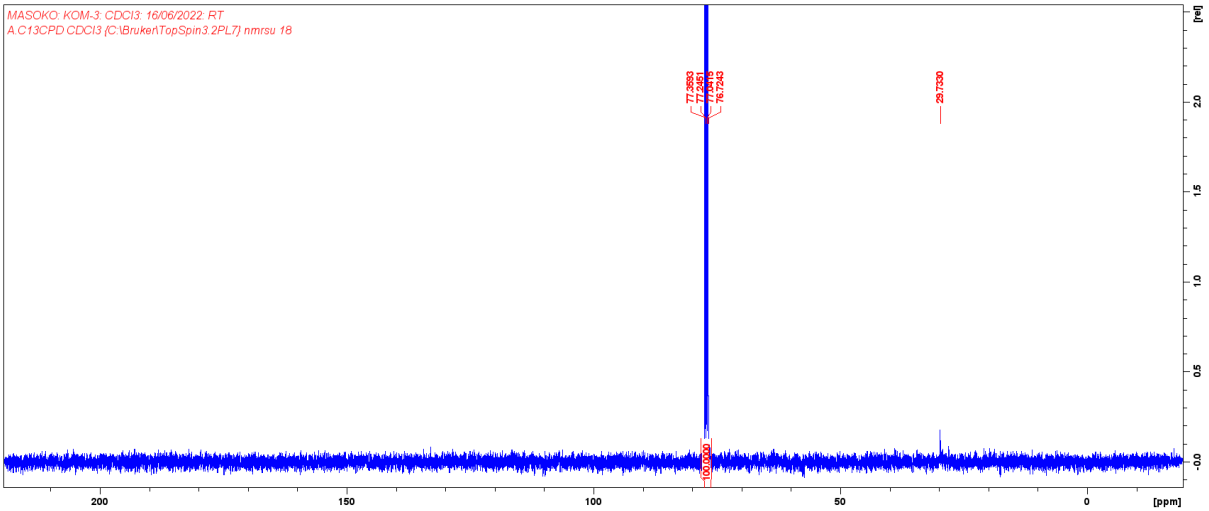

Figure 7. 13: ^{13}C NMR spectrum of isolated compound 3.

7.3.8. Spectroscopic data for compound 3 and 4

Table 7.3 provides the summary of the spectroscopic data of compounds 3 and 4. It gives a comparison of compounds 3 and 4 with the β-sitosterol data from literature.

Table 7. 3: The summary of ^{1}H and ^{13}C spectroscopic data for compounds 3 and 4, and the one from literature.

Positions	Type	Chemical shift, δ (ppm) value			
		Ododo *et al*., 2016		Compound 3 and 4	
		^{13}C	^{1}H	^{13}C	^{1}H
1	CH2	37.2	1.46 (m)	38.77	1.65
2	CH2	31.69	1.56 (m)	30.5	1.85

3	CH(OH)	71.82	3.54 (m)	79.01	3.21
4	CH2	42.33	2.32 (m)	41.92	2.32
5	C	140.77	-	137.87	-
6	CH	121.73	5.37 (overlapping, t)	125.79	5.23, d, J=3.5 Hz
7	CH2	31.93	2.04 (m)	31.91	2.15 (m)
8	CH	31.93	1.69 (m)	31.91	2.12 (m)
9	CH	50.16	1.55 (m)	47.86	1.91
10	C	36.51	-	36.66	-
11	CH2	21.11	1.52 (m)	21.16	1.65
12	CH2	39.80	1.51 (m)	39.41	1.65
13	C	42.34	-	41.57	-
14	CH	56.79	1.50 (m)	55.13	1.65(m)
15	CH2	24.33	1.58 (m)	23.55	1.74 (m)
16	CH2	28.27	1.85 (m)	27.94	1.99 (m)
17	CH	56.08	1.45 (m)	52.87	1.65 (m)
18	CH3	11.89	0.70 (s)	15.29	0.91 (s)
19	CH3	19.42	1.03 (s)	15.44	1.12 (s)
20	CH	36.17	1.60 (m)	36.94	1.74
21	CH3	18.84	0.94 (overlapping, d)	15.57	1.00
22	CH2	33.98	0.93 (m)	32.88	0.89 (m)
23	CH2	26.11	1.15 (m)	27.15	1.52
24	CH	45.86	1.38 (m)	47.40	1.59 (m)
25	CH	29.19	157 (m)	29.35	1.74
26	CH3	19.84	0.84 (overlapping, d)	18.24	0.91 (s)
27	CH3	19.06	0.86 (d)	17.00	0.97 (s)
28	CH2	23.10	1.10 (m)	22.68	1.52

29	CH3	12.01	0.82 (overlapping, t)	14.12	2.86
-	OH	-	1.98 (s)	-	1.98 (s)

7.3.9. The structure of compound 3

Figure 7.14 below represents the structure of compound 3 isolated from *R. officinalis* leaves.

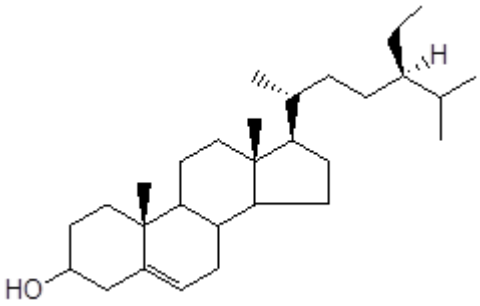

Figure 7. 14: Structure of compound 3.

7.3.10. The analysis of compound 4 using NMR

Figure 7.15 to 7.18 shows the NMR spectra under ^{1}H Proton, ^{13}C, DEPT 135, and HSQC used for structural elucidation of compound 4. Table 7.3 was also used as the summary of the ^{13}C and ^{1}H Proton shift values for the characterisation of compound 4.

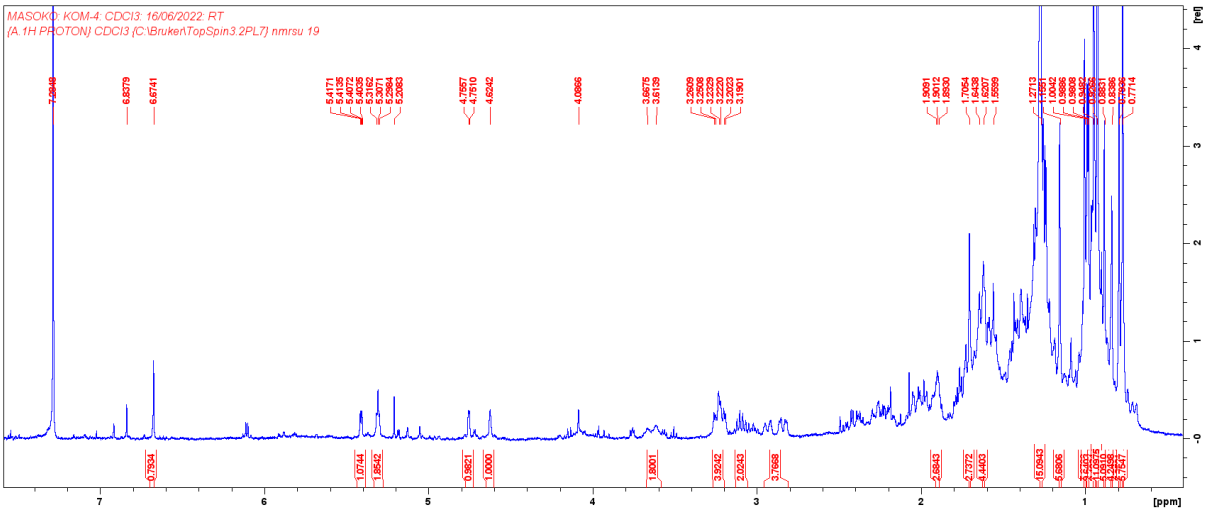

Figure 7. 15: ^{1}H NMR spectrum of isolated compound 4.

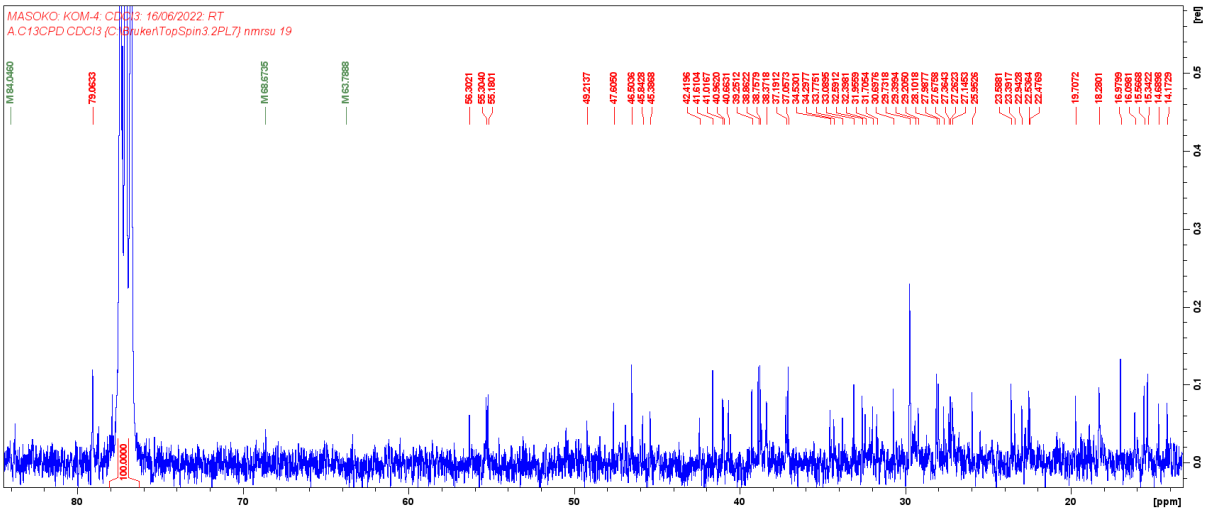

Figure 7. 16: ^{13}C NMR spectrum of isolated compound 4.

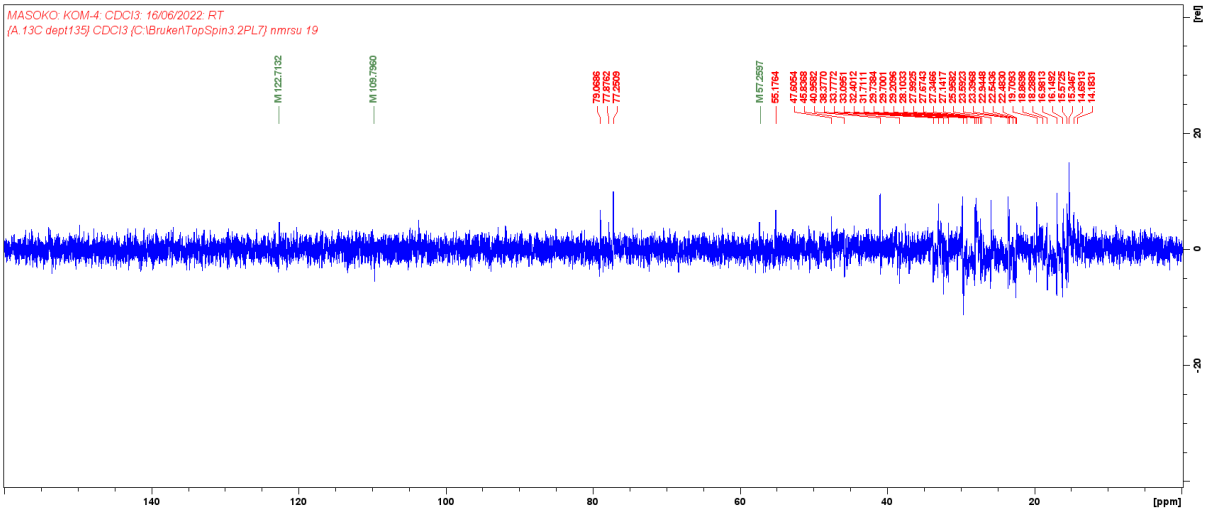

Figure 7. 17: DEPT 135 NMR spectrum of isolated compound 4.

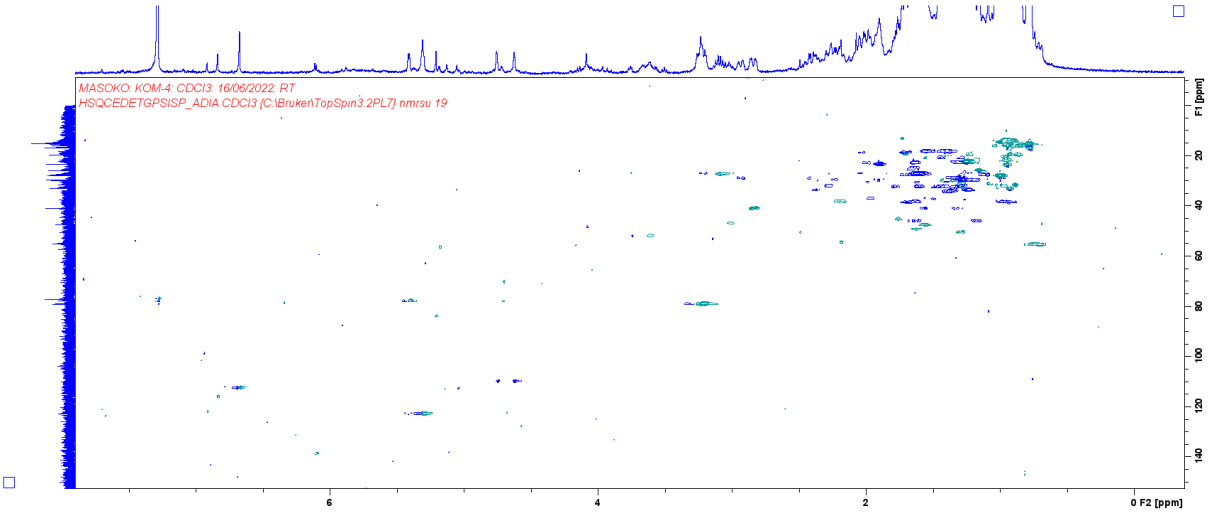

Figure 7. 18: HSQC NMR spectrum of isolated compound 4.

7.3.11. The structure of compound 4

Figure 7.19 below represents the structure of compound 4 isolated from *R. officinalis* leaves.

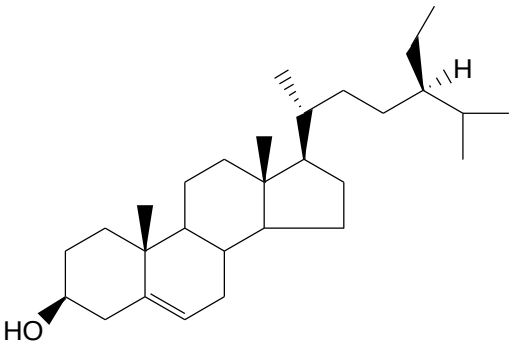

β-sitosterol **8**

Figure 7. 19: Structure of compound 4.

7.4. Discussion

The structural elucidation of *Rosmarinus officinalis* resulted in the isolation of four compounds, which were determined using NMR. The ^{1}H, ^{13}C, HSQC, COSY and HMBC NMR spectrum were used to characterise the isolated compounds. The resulted NMR spectra aided with the structural elucidations of the isolated compounds. Two chromones and two β-sitosterol compounds were elucidated.

Compounds 1 and 2 are chromones with compound 1, which is named 5-hydroxyl-2-methyl-7-(propan-2βol)-chromone and compound 2, which is named 7-acetonyl-5-hydroxy-2-methylchromone. Compound 1 is usually isolated as a yellow powder that does not melt at 300 ˚C. It is deduced to be $C_{13}H_{12}O_4$ based on the molecular ion peak at *m/z* 232.0737. The chromone nature of compound 1 was deduced from the presence of a peak at *m/z* 204 in the EIMS, due to the loss of CO, which is a characteristic of γ-pyrones. The ^{13}C NMR data (experimental) showed thirteen carbon signals, and the HMQC and DEPT 135 led to the assignment of the structure as three carbons attached to oxygen [δ 164.2 (C-2), 158.9 (C-5) and 160.9 (C-8a)] from the ^{13}C NMR spectrum. The ^{1}H NMR spectrum of compound 1 displayed a downfield chelated proton at δ 10.64 (Djemgou *et al*., 2006).

Compound 2 is usually isolated as a yellow powder that does not melt at 300 ˚C. It has the molecular formula $C_{13}H_{14}O_4$ from the positive HREIMS, which revealed a molecular ion peak at m/z 235.0970 [M+H]+ . Fragments on EIMS are found at m/z

233 [M−H], 216 [M−H 2 O], 201 [M−2OH], and 187 [M−2OH−CH 3]. The IR, ^{1}H and ^{13}C NMR spectra (experimental) were very close to those of compound 1. The comparison between compounds 1 and 2 had significant changes, including an additional methine at δ 3.78 instead of a carbonyl, as in compound 1. H-1′ and H-3′(experimental) which were not singlets; (ii) ^{1}H- ^{1}H COSY detected an ABX system at δ 3.48 (H-1′a), 3.39 (H-1′b) and 3.78 (H-2′). Compound 2 was characterised as 5-hydroxyl-2-methyl-7-(propan-2β-ol)-chromone, named petersinone B (Djemgou *et al*., 2006).

Compound 3 and 4 usually form a white crystal with a melting point around 138ºC and have no absorption under the UV-Vis Lamp (254 and 366 nm). Its main IR bands usually appear at 3549 (OH), 2935 (CH2), 2867 (CH), 1637 (C=C) and finally 1063 (C-O), (all absorptions are in cm^{-1}). High-resolution mass spectra of β-sitosterol confirm its molecular mass at m/z to be 414.7, which is related to the molecular formula $C_{29}H_{50}O$. The NMR spectrum of this compound shows the presence of six methyl groups, eleven methylene and three quaternary carbons together with a hydroxyl group. The number of carbons, extracted from ^{13}C NMR reveals the structure of a sterol with 27 carbons (Saeidnia *et al*., 2014). The ^{13}C NMR has shown recognisable signals at 140.943 ppm and 121.132 ppm, which are assigned C5 and C6 double bonds, respectively. The value at 19.064ppm corresponds to an angular carbon atom (C19) 138.404 ppm for C-20 and 129.341ppm for C-21. The alkene carbons appeared at 140.943, 138.404, 129.341 and 121.132 ppm (Pierre and Moses, 2015).

7.5. Conclusion

Four compounds were isolated from the leaves of *R. officinalis*, which are the two chromones and two β-sitosterol compounds. The NMR spectroscopic data obtained and spectroscopic data from literature were used to determine the names of the compounds. This is the first report to account for the presence of chromones and β-sitosterol compounds from *R. officinalis*. The biological activities isolated compounds are covered in the next chapter.

7.6. References

Dias, D.A., Jones, O.A., Beale, D.J., Boughton, B.A., Benheim, D., Kouremenos, K.A., Wolfender, J.L. and Wishart, D.S. 2016. Current and future perspectives on

the structural identification of small molecules in biological systems. *Metabolites*, **6**(4): 46.

Djemgou, P.C., Gatsing, D., Tchuendem, M., Ngadjui, B.T., Tane, P., Ahmed, A.A., Gamal-Eldeen, A.M., Adoga, G.I., Hirata, T. and Mabry, T.J. 2006. Antitumor and immunostimulatory activity of two chromones and other constituents from *Cassia petersiana*. *Natural Product Communications*, **1**(11).

Gross, L., Schuler, B., Pavliček, N., Fatayer, S., Majzik, Z., Moll, N., Peña, D. and Meyer, G. 2018. Atomic force microscopy for molecular structure elucidation. *Angewandte Chemie International Edition*, **57**(15): 3888-3908.

Kafader, J.O., Melani, R.D., Durbin, K.R., Ikwuagwu, B., Early, B.P., Fellers, R.T., Beu, S.C., Zabrouskov, V., Makarov, A.A., Maze, J.T. and Shinholt, D.L. 2020. Multiplexed mass spectrometry of individual ions improves measurement of proteoforms and their complexes. *Nature Methods*, **17**(4): 391-394.

Lovchinsky, I., Sushkov, A.O., Urbach, E., de Leon, N.P., Choi, S., De Greve, K., Evans, R., Gertner, R., Bersin, E., Müller, C. and McGuinness, L. 2016. Nuclear magnetic resonance detection and spectroscopy of single proteins using quantum logic. *Science*, **351**(6275): 836-841.

Milanowski, D.J., Oku, N., Cartner, L.K., Bokesch, H.R., Williamson, R.T., Saurí, J., Liu, Y., Blinov, K.A., Ding, Y., Li, X.C. and Ferreira, D. 2018. Unequivocal determination of caulamidines A and B: application and validation of new tools in the structure elucidation toolbox. *Chemical Science*, **9**(2): 307-314.

Ododo, M.M., Choudhury, M.K. and Dekebo, A.H. 2016. Structure elucidation of β-sitosterol with antibacterial activity from the root bark of *Malva parviflora*. *SpringerPlus*, **5**(1): 1-11.

Ok, S., Mahmoodinia, M., Rajasekaran, N., Sabti, M.A., Lervik, A., van Erp, T.S. and Cabriolu, R. 2019. Molecular structure and solubility determination of asphaltenes. *Energy and Fuels*, **33**(9): 8259-8270.

Pesek, M., Juvan, A., Jakoš, J., Košmrlj, J., Marolt, M. and Gazvoda, M. 2020. Database independent automated structure elucidation of organic molecules based

on IR, ^{1}H NMR, ^{13}C NMR, and MS data. *Journal of Chemical Information and Modeling*, **61**(2): 756-763.

Pierre, L.L. and Moses, M.N. 2015. Isolation and characterisation of stigmasterol and β-sitosterol from *Odontonema strictum* (Acanthaceae). *Journal of Innovations in Pharmaceuticals and Biological Sciences*, **2**(1): 88-95.

Rakhmatullin, I.Z., Efimov, S.V., Margulis, B.Y. and Klochkov, V.V. 2017. Qualitative and quantitative analysis of oil samples extracted from some Bashkortostan and Tatarstan oilfields based on NMR spectroscopy data. *Journal of Petroleum Science and Engineering*, **156**: 12-18.

Rakhmatullin, I.Z., Efimov, S.V., Klochkov, A.V., Gnezdilov, O.I., Varfolomeev, M.A. and Klochkov, V.V. 2022. NMR chemical shifts of carbon atoms and characteristic shift ranges in the oil sample. *Petroleum Research*, **7**(2): 269-274.

Rodrigues, T., Reker, D., Schneider, P. and Schneider, G. 2016. Counting on natural products for drug design. *Nature Chemistry*, **8**(6): 531-541.

Saeidnia, S., Manayi, A., Gohari, A.R. and Abdollahi, M. 2014. The story of beta-sitosterol-a review. *European Journal of Medicinal Plants*, **4**(5): 590.

Simpson, A.J., Simpson, M.J. and Soong, R. 2018. Environmental nuclear magnetic resonance spectroscopy: an overview and a primer. *Analytical Chemistry*, **90**(1): 628-639.

Soulsby, D. and Wallner, A.S. 2016. Introduction to NMR spectroscopy in the undergraduate curriculum. In *NMR Spectroscopy in the undergraduate curriculum: first year and organic chemistry Courses,* **2**: 1-10.

CHAPTER 8

8. Biological activity of the isolated compounds

8.1. Introduction

Rosmarinus officinalis is an evergreen shrub with an aromatic needle like leaves popularly used during cooking, for traditional healing and as an aromatherapy (Satyal *et al*., 2017). Some of the compounds that have been isolated from *R. officinalis* include carnosic acid, carnosol and rosmarinic acid (Gonçalves *et al*., 2022). As reported by Andrade *et al*. (2018), the rosmarinic acid has antiviral, antibacterial, antioxidant and anti-inflammatory properties.

Chromones are compounds derived from a benzopyran skeleton with a substituted keto group on the pyran ring (Nazhand *et al*., 2020). Chromones are widely distributed in the Plant Kingdom, but several fungal species and marine sponges produce chromone derivatives (Semwal *et al*., 2020). It is the backbone of flavones, flavonols, isoflavones and flavonoids. Chromones can scavenge the radical oxygen species and prevents lipid peroxidation. The scavenging of free radicals occurs through a rapid transfer of hydrogen (Lewandowski *et al*., 2020). They perform various biological activities such as antimicrobial, antitumor, antioxidant, anti-inflammatory, antiviral and other activities (Kavitha and Reddy, 2016; Jiang *et al*., 2019).

Beta-sitosterol is a phytosterol with a chemical structure like the one of cholesterol. It has the molecular formula $C_{29}H_{50}O$ (Bin Sayeed *et al*., 2016). It is a white waxy powder with the characteristic aroma. It is found in three different forms depending on the number of water molecules, namely; anhydrous, hemihydrate and monohydrate (Babu and Jayaraman, 2020). This molecule has one functional group, which is a secondary alcohol and one double bond that can be saturated (Novotny *et al*., 2017). Beta-sitosterol is reported to have antimicrobial, antioxidant, antidiabetic, anti-inflammatory, anticancer, angiogenic, immunomodulatory and antinociceptive activities without toxicity (Rashed, 2020).

8.2. Method and materials

8.2.1. Phytochemical analysis of the isolated compounds

The chemical profiles of the isolated compounds were analysed using TLC, relying on the method described in section 3.2.2.

8.2.2. Antibacterial activity

8.2.2.1. Bioautography

The bioautography assay of the isolated compounds was done using the method described in section 5.2.1.

8.2.2.2. Broth micro-dilution assay

Antibacterial activity of the isolated compounds using broth micro-dilution assay was determined, as described in section 5.2.2, to determine the MIC.

8.3. Results

8.3.1. Phytochemical analysis of the isolated compound

Compounds were visible under the UV light and compound 4 was also visible when the TLC plate was sprayed with the vanillin-sulphuric acid reagent (C) (Figure 8.1).

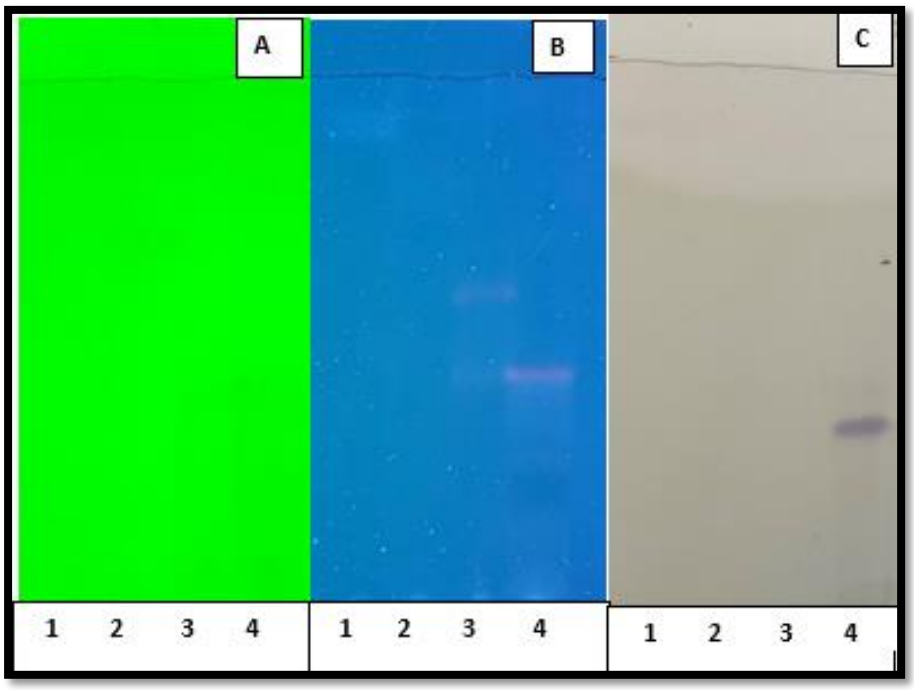

Figure 8.1: The phytochemical analysis of isolated compounds developed in 80% n-hexane: 20% ethyl acetate, visualised at 254 nm (A) and 365 nm (B), and then sprayed with the vanillin-sulphuric acid reagent (C).

8.3.2. Biological activity of the isolated compounds

8.3.2.1. Bioautography

Figure 8.2 shows the antibacterial activity against *M. smegmatis* using the bioautography assay of the isolated compounds. Compound 4 showed a visible zone of inhibition on the TLC plate developed in BEA.

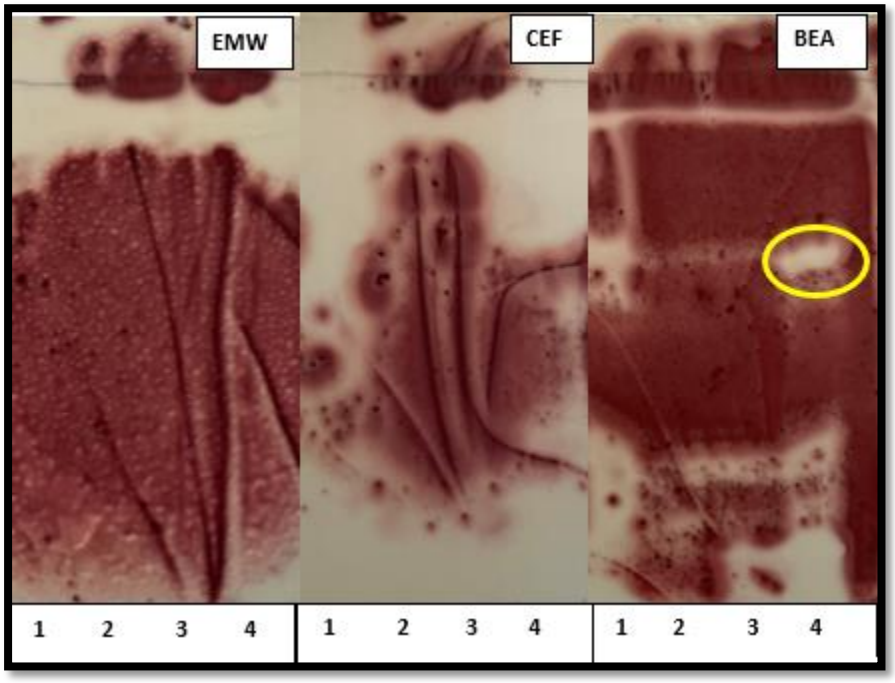

Figure 8. 2: The antibacterial activity of the four isolated compounds against *M. smegmatis* developed in EMW, CEF, and BEA.

8.3.2.2. Broth micro-dilution assay

The antibacterial activity of the isolated compounds was quantified using broth micro-dilution assay, rifampicin was used as the positive control while acetone was used as the negative control. Compound 4 had the lowest MIC value of 0.125 mg/mL compared to the other isolated compounds (Table 8.1).

Table 8.1: MIC values of the isolated compounds against *Mycobacterium smegmatis*.

Isolated compounds	MIC values (mg/mL)
1	0.25
2	0.25
3	0.25
4	0.125
Rifampicin	0.002
Acetone	>0.25

8.4. Discussion

The isolated compounds of *R. officinalis* were analysed using TLC, visualised at 254 nm and 365 nm, and then further sprayed with the vanillin-sulphuric acid reagent. Compound 4 was visible when the plate was sprayed with the vanillin-sulphuric acid (Figure 8.1). Bioautography and broth micro-dilution assay were employed to determine the antibacterial activity of the compounds. There was a visible antibacterial activity of compound 4 on the TLC plate developed in BEA (Figure 8.2). Other compounds did not show any growth inhibition of *M. smegmatis*. The quantified antibacterial activity of the compounds by broth micro-dilution assay, where rifampicin was used as the positive control with an MIC value of 0.002 mg/mL and acetone as the negative control with an MIC value >0.25 mg/mL, showed that compound 4 had the lowest MIC of 0.125 mg/mL compared to the other isolated compounds (Table 8.1). Compounds 1, 2 and 3 had an antibacterial activity of 0.25 mg/mL. As reported by Fadipe *et al*. (2017), β-sitosterol isolated from *Curtisia dentata* had antimycobacterial activity >50 µg/mL when tested against *Mycobacterium tuberculosis* H37Rv (ATCC 27294). Chromone compounds can be attached to other molecules to act actively on microorganisms. Irfan *et al*., (2020) reported that the click chemistry technique was used to attach the chromone to the 1,4-disubstituted [1, 2, 3]-triazole. New hybrid molecules showed *in vitro* antimycobacterial activity and one of the compounds had antimycobacterial activity with an MIC value of 1.56 µg/mL.

8.5. Conclusion

The study evaluated the antibacterial activity of the four isolated compounds from the dichloromethane extracts of *R. officinalis* against *M. smegmatis.* It is recommended

that anti-cancer studies of the isolated compounds be conducted since it is reported that the compounds possess antioxidant, anti-cancer, anti-diabetic, and antimicrobial activities. This can lead to new drug development from the leaves of *R. officinalis* to treat TB.

8.6. References

Andrade, J.M., Faustino, C., Garcia, C., Ladeiras, D., Reis, C.P. and Rijo, P. 2018. *Rosmarinus officinalis* L.: an update review of its phytochemistry and biological activity. *Future Science OA*, **4**(4).

Babu, S. and Jayaraman, S. 2020. An update on β-sitosterol: a potential herbal nutraceutical for diabetic management. *Biomedicine and Pharmacotherapy*, **131**: 110702.

Bin Sayeed, M.S., Karim, S.M.R., Sharmin, T. and Morshed, M.M. 2016. Critical analysis on characterization, systemic effect, and therapeutic potential of beta-sitosterol: a plant-derived orphan phytosterol. *Medicines*, **3**(4): 29.

Fadipe, V.O., Mongalo, N.I., Opoku, A.R., Dikhoba, P.M. and Makhafola, T.J. 2017. Isolation of anti-mycobacterial compounds from *Curtisia dentata* (Burm. f.) CA Sm (Curtisiaceae). *BMC complementary and alternative medicine*, **17**(1): 1-6.

Gonçalves, C., Fernandes, D., Silva, I. and Mateus, V. 2022. Potential anti-inflammatory effect of *Rosmarinus officinalis* in preclinical in vivo models of inflammation. *Molecules*, **27**(3): 609.

Irfan, M. and Saleem, U. 2020. Current strategies in development of new chromone derivatives with diversified pharmacological activities: a review. *Pharmaceutical Chemistry Journal*, **54**(3): 241-257.

Jiang, Y.Y., Guo, F.X., Chen, L.X., Xu, L.L., Zhang, W. and Liu, B. 2019. The antitumor activity of naturally occurring chromones: a review. *Fitoterapia*, **135**: 114-129.

Kavitha, P. and Reddy, K.L. 2016. Pd (II) complexes bearing chromone based Schiff bases: synthesis, characterisation, and biological activity studies. *Arabian Journal of Chemistry*, **9**(5): 640-648.

Lewandowski, W., Lewandowska, H., Golonko, A., Świderski, G., Świsłocka, R. and Kalinowska, M. 2020. Correlations between molecular structure and biological activity in “logical series” of dietary chromone derivatives. *PloS One*, **15**(8).

Nazhand, A., Durazzo, A., Lucarini, M., Romano, R., Mobilia, M.A., Izzo, A.A. and Santini, A. 2020. Human health-related properties of chromones: an overview. *Natural Product Research*, **34**(1): 137-152.

Novotny, L., Abdel-Hamid, M.E. and Hunakova, L. 2017. Anticancer potential of β-sitosterol. *International Journal of Clinical Pharmacology and Pharmacotherapy*, **2**(129):10-15344.

Rashed, K. 2020. Beta-sitosterol medicinal properties: a review article. *International Journal of Science Inventions Today,* **9**(4): 208-212.

Satyal, P., Jones, T.H., Lopez, E.M., McFeeters, R.L., Ali, N.A.A., Mansi, I., Al-Kaf, A.G. and Setzer, W.N. 2017. Chemotypic characterization and biological activity of *Rosmarinus officinalis*. *Foods*, **6**(3): 20.

Semwal, R.B., Semwal, D.K., Combrinck, S. and Viljoen, A. 2020. Health benefits of chromones: common ingredients of our daily diet. *Phytochemistry Reviews*, **19**(4): 761-785.

CHAPTER 9

9. General discussions, conclusions, and recommendations

9.1. General discussion

Healthcare workers are at the highest risk of contracting TB, which is ranked the third common occupational disease in South Africa (Manana *et al*., 2018). It is estimated that one-third of the world's population will be affected by TB and more than 95 % patients died in developing countries due to TB (Singh *et al*., 2018). This is due to the causative agent (*M. tuberculosis*) being resistant to the current available treatment methods. Drug resistance is heritable and usually occurs because of mutation and gene encoding of either the target drug or enzymes that activate the prodrug (Koch *et al*., 2018). It leads to the current available drugs being ineffective against M. TB; hence, there is a need to conduct research and find new effective drugs.

The selection of plants for the study was based on the literature about the ethnopharmacological use of plants to treat respiratory infections and their related symptoms. Plants were collected, dried, and extracted with solvents of varying polarities (non-polar to polar). Different compounds were present in the extract as more different colours were visible on the TLC plates. The total phenolic, tannin and flavonoid content of the extracts were quantified. They are known to exhibit antibacterial, antioxidant and anti-inflammatory activities. *R. tridentata* had the highest phenolics and tannins while *R. officinalis* had the highest flavonoid content.

The antioxidant activity of the plant extracts using TLC and the yellow band against the purple background, indicated the presence of antioxidant compounds. All the plants had antioxidant compounds except *Z. capense*. The DPPH free radical scavenging activity and ferric reducing antioxidant assay to quantify antioxidant compounds revealed that all plants had antioxidant compounds.

The plants' antibacterial activity against *M. smegmatis* was evaluated, and *R. officinalis* had the highest antibacterial activity from the n-hexane, dichloromethane, acetone, and methanol extract. The interaction effects of the plants were determined using broth micro-dilution assay. The n-hexane and acetone extracts were combined using the 1:1 ratio and from the n-hexane extract, and a synergistic outcome was observed when *R. officinalis* was combined with *Z. capense*. This means that the antibacterial effect of the combination is greater than the sum of either treatment alone.

The anti-inflammatory and antibiofilm activities of the plants were determined and *R. officinalis* had good anti-inflammatory and biofilm activities compared to other plants. The MTT assay was used to determine the cell viability of the different acetone plant extracts. The acetone extracts of different plants were not toxic against THP-1 macrophages, except *Z. mucronata* and *Z. capense* at 100 µg/mL.

Since *R officinalis* had the potent antioxidant and antibacterial activity, it was chosen for the isolation of its bioactive compounds and bioassay guided fractionation on column chromatography was employed. Exactly four compounds were isolated and identified as 2 chromones (compound 1 named 5-hydroxyl-2-methyl-7-(propan-2βol)-chromone and compound 2 as 7-acetonyl-5-hydroxy-2-methylchromone) and 2 β-sitosterol compounds. The isolated compounds were tested for antibacterial activity and compound 4 showed potent antimycobacterial activity when using the bioautography assay and broth micro-dilution assay, with the lowest MIC of 0.125 mg/mL.

The bioassays employed during the study determined the potency of the plant extracts against *Mycobacterium smegmatis*. The obtained results were then used to choose extracts with the best antimycobacterial activity. They were fractioned and re-fractioned into different portions using column chromatography and TLC at the end to isolate pure bioactive compounds. Results obtained from the study will contribute towards TB drug discovery and provide scientific contribution and knowledge towards the effective use of medicinal plants.

9.2. Conclusions and recommendations

Findings from the study demonstrated that plants have antioxidants, and antibacterial potentiality due to the presence of the phytochemicals they possess. The anti-inflammatory and antibiofilm activities were analysed and it is recommended that they need to be further investigated in eukaryotic model organisms. The cytotoxic effects of the plants were determined and more cytotoxic assays of the plants using different cell lines are recommended. The bioactive compounds of *R. officinalis* have been isolated and tested for antibacterial activity against *M. smegmatis*. It is recommended that more *in-vitro* and *in-vivo* tests of the isolated compounds be performed.

9.3. References

Koch, A., Cox, H. and Mizrahi, V. 2018. Drug-resistant tuberculosis: challenges and opportunities for diagnosis and treatment. *Current Opinion in pharmacology*, **42**: 7-15.

Manana, P.N., Kuonza, L., Musekiwa, A., Koornhof, H., Nanoo, A. and Ismail, N. 2018. Feasibility of using postal and web-based surveys to estimate the prevalence of tuberculosis among health care workers in South Africa. *PloS one*, **13**(5).

Singh, P., Kant, S., Gaur, P., Tripathi, A. and Pandey, S. 2018. Extra pulmonary tuberculosis: An overview and review of literature. *International Journal of Life Science Scientific Research*, **4**(1): 1539-41.